symmetry

MDPI

Review

The D4/D8 Model and Holographic QCD

Si-Wen Li [1,*] and Xiao-Tong Zhang [2]

[1] Department of Physics, College of Science, Dalian Maritime University, Dalian 116026, China
[2] College of Innovation and Entrepreneurship, Dalian Maritime University, Dalian 116026, China
* Correspondence: siwenli@dlmu.edu.cn

Abstract: As a top-down holographic approach, the D4/D8 model is expected to be a holographic version of QCD, since it almost includes all the elementary features of QCD based on string theory. In this manuscript, we review the fundamental properties of the D4/D8 model with respect to the D4-brane background and the embedding of the flavor branes, holographic quark, gluon, meson, baryon and glueball with various symmetries; then, we take a look at some interesting applications and developments based on this model.

Keywords: gauge-gravity duality; AdS/CFT correspondence; holographic QCD

check for updates

Citation: Li, S.-W.; Zhang, X.-T. The D4/D8 Model and Holographic QCD. *Symmetry* **2023**, *15*, 1213. https://doi.org/10.3390/sym15061213

Academic Editor: Emmanuele Battista

Received: 21 April 2023
Revised: 25 May 2023
Accepted: 29 May 2023
Published: 7 June 2023

1. Introduction

Although it has been about 25 years since the proposal of AdS/CFT and gauge–gravity duality with holography [1–3], it continues to attract great interest today. The most significant part of AdS/CFT and gauge–gravity duality is that people can evaluate strongly coupled quantum field theory (QFT) by quantitatively analyzing its associated gravity theory in the weak coupling region. Thus, it provides a holographic way to study strongly coupled QFT, in which traditional QFT based on the perturbation method is out of reach. Accordingly, a large number of publications on strongly coupled QFT through AdS/CFT and gauge–gravity duality have appeared, for example, on the Wilson loop and quark potential [4–6], the transport coefficient [7–9], the fermionic correlation function [10,11], the Schwinger effect [12], quantum entanglement entropy [13,14] and quantum information on black holes [15], which have become most remarkable works in this field.

On the other hand, QCD (quantum chromodynamics), as the fundamental theory describing the property of strong interaction, is extremely complex in the strong coupling region, especially at a finite temperature with dense matter, due to its asymptotic freedom [16,17]; hence, the holographic version of QCD is naturally becoming an interesting topic. While there are several models and theories attempting to give a holographic version of QCD (e.g., bottom-up approaches [18–20], the D3/D7 approach [21], the D4/D6 approach [22]), one of the most successful achievements in holography is the D4/D8 model (also called the Witten–Sakai–Sugimoto model) [23–25], which includes almost all the elementary features of QCD in a very simple way, e.g., mesons, baryons [26–28], glueballs [29–32], deconfinement transition [33–35], a chiral phase [36,37], a heavy flavor [38–40], a θ term and QCD axion [41–45], and a nucleon interaction [46–52]. The D4/D8 model is based on the holographic duality between the 11-dimensional (11d) M-theory on $AdS_7 \times S^4$ and the $\mathcal{N} = (2,0)$ super conformal field theory (SCFT) on N_c M5-branes [53]. By using the dimensional reduction in [23,54], it reduces to the correspondence of the pure Yang–Mills theory on N_c D4-branes compactified on a circle and 10d IIA supergravity (SUGRA). Flavors as N_f pairs of D8- and anti-D8-branes (D8/$\overline{\text{D8}}$) can be further introduced into the geometric background produced by the N_c D4-branes, so the dual theory includes flavored fundamental quarks, which would be more close to the realistic QCD. Moreover, as the D4/D8 model is a T-dualized version of the D3/D9 system [55], the fundamental quark and meson in the D4/D8 model can therefore be identified to the 4–8 (The 4–8 string refers to the open string connecting the N_c D4-brane and N_f D8-branes; it is similar for, e.g., the 8–8 or 4–$\overline{8}$ string.) and 8–8 strings, respectively, by following the same discussion in the D3/D9 system [55]. Moreover, the baryon vertex is identified as a D4-brane wrapped on S^4 [26], and the glueball is recognized to be the bulk gravitational polarization [29,30]. The chiral phase is determined by the embedding configuration of the D8/$\overline{\text{D8}}$-branes due to the gauge symmetry on their worldvolume [56], while the deconfinement transition is suggested to be the Hawking–Page transition in this model [33–36]. Altogether, this model includes all the fundamental elements of QCD; thus, it can be treated as a holographic version of QCD.

In this review, we revisit the above properties of the D4/D8 model, then take a brief look at some recently relevant developments and holographic approaches with this model. The outline of this review is as follows. In Section 2, we review the relation of 11d M-theory and IIA SUGRA with respect to the case of the M5-brane and D4-brane. Afterwards, we review the embedding configuration of the D8/$\overline{\text{D8}}$-branes to the D4-brane background and the holographic quark, gluon, meson, baryon and glueball with various symmetries, which are all the relevant objects in hadron physics. In Section 3, we review several topics about the developments and holographic approaches of this model, which include deconfinement transition, chiral transition, the Higgs mechanism and heavy–light mesons or baryons, interactions involving glueballs and the QCD θ term in holography. In the Appendixs A, B and C, we give the general form of the black brane solution in type II SUGRA, the relevant dimensional reduction for spinors and discussion about supersymmetric mesons, which are useful to the main content of this paper.

2. The D4/D8 Model

In this section, we revisit the D4-brane background and the embedding of the probe D8/$\overline{\text{D8}}$-branes. Then, we review how to identify quarks, gluons, mesons, baryons and glueballs with various symmetries in this model.

2.1. Eleven-Dimensional Supergravity and D4-Brane Background

The D4-brane background of the D4/D8 model is based on the holographic duality between the type $\mathcal{N} = (2,0)$ super conformal field theory (SCFT) on coincident N_c M5-branes and 11-dimensional (11d) M-theory on AdS$_7 \times S^4$ [53]. In order to obtain a geometric solution, the effective action of the M-theory is necessary, which is known as the 11d supergravity action. In the large-N_c limit, the geometric background can be obtained by solving its bosonic part, which consists of a metric (elfbein) and a three-form C_3: [57],

$$S^{11\text{d}}_{\text{SUGRA}} = \frac{1}{2\kappa_{11}^2}\int d^{11}x\sqrt{-g}\left[\mathcal{R}^{(11)} - \frac{1}{2}|F_4|^2\right] - \frac{1}{12\kappa_{11}^2}\int C_3 \wedge F_4 \wedge F_4, \tag{1}$$

where $F_4 = dC_3$. The convention in (1) is as follows. $\mathcal{R}^{(11)}$ refers to the 11d scalar curvature; κ_{11} is the 11d gravity coupling constant, given by

$$2\kappa_{11}^2 = 16\pi G_{11} = \frac{1}{2\pi}\left(2\pi l_p\right)^9, \tag{2}$$

where G_{11} is 11d Newton's constant and l_p is the Planck length. The quantity $|F_4|^2$ can be obtained by a general notation of an n-form F_n:

$$|F_n|^2 = \frac{1}{n!}g^{A_1B_1}g^{A_2B_2}...g^{A_nB_n}F_{A_1A_2...A_n}F_{B_1B_2...B_n}, \tag{3}$$

where g_{AB} refers to the metric on the manifold. We note that in (1), the last term is a Chern–Simons structure. which is independent on the metric or elfbein, while the first term depends on the metric or elfbein through the metric combination

$$g_{AB} = e^a_A \eta_{ab} e^b_B. \tag{4}$$

The solution for extremal coincident N_c M5-branes is obtained:

$$\begin{aligned} ds^2_{11\text{d}} &= H_5(r)^{-\frac{1}{3}}\eta_{MN}dx^M dx^N + H_5(r)^{\frac{2}{3}}\left(dr^2 + r^2 d\Omega_4^2\right), \\ H_5(r) &= 1 + \frac{r_5^3}{r^3},\ ({}^*F_4)_{r012\ldots5} = -\frac{3r_5^3}{r^4 H_5^2}, \end{aligned} \tag{5}$$

where r denotes the radial coordinate to the M5-branes and M, N run over the M5-branes. Using the BPS condition for M5-brane,

$$2\kappa_{11}^2 T_{\text{M5}} N_c = \int_{S^4} F_4, \tag{6}$$

which leads to

$$r_5^3 = \pi N_c l_p^3, \tag{7}$$

where $T_{\text{M5}} = \frac{1}{(2\pi)^5 l_p^6}$ refers to the tension of the M5-brane. Taking the near-horizon limit $H_5 \to \frac{r_5^3}{r^3}$ and replacing the variables

$$\left\{r, r_5, x^i, \Omega_4\right\} \to \left\{r^2, \frac{L}{2}, \frac{1}{\sqrt{L}}x^i, \frac{1}{\sqrt{L}}\Omega_4\right\}, \tag{8}$$

the metric presented in (5) reduces to

$$ds^2_{11\text{d}} = \frac{r^2}{L^2}\eta_{MN}dx^M dx^N + \frac{L^2}{r^2}\left(dr^2 + \frac{r^2}{4}d\Omega_4^2\right), \tag{9}$$

describing the standard form of $\text{AdS}_7 \times S^4$, where the radius of S^4 is $L/2$. In addition, the action (1) also allows for the near-extremal M5-brane solution, which, after taking near-horizon limit and replacement (8), is

$$\begin{aligned} ds^2_{11\text{d}} &= \frac{r^2}{L^2}\left[-f(r)\left(dx^0\right)^2 + \textstyle\sum_{i=1}^5 dx^i dx^i\right] + \frac{L^2}{r^2}\left[\frac{dr^2}{f(r)} + \frac{r^2}{4}d\Omega_4^2\right], \\ f(r) &= 1 - \frac{r_H^6}{r^6}, \end{aligned} \tag{10}$$

The constant r_H refers to the location of the horizon, which can be determined by omitting the conical singularity,

$$\beta_T = \frac{2\pi L^2}{3r_H}, \tag{11}$$

where β_T is the size of the compactified direction x^0.

In order to obtain a QCD-like low-energy theory in holography, Witten proposed a scheme in [23] based on the above M5-brane solution. Specifically, the first step is to compactify one spacial direction (denoted by x^5) of M5-branes on a circle with periodic condition for fermions, which means the supersymmetry remains. Accordingly, the resultant theory is a supersymmetric gauge theory above the size of the circle. Then, recalling the relation between M-theory and IIA string theory, the 11d metric presented in (9) or (10) reduces to a 10d metric,

$$ds^2_{11\text{d}} = e^{-\frac{2}{3}\phi}ds^2_{10\text{d}} + e^{\frac{4}{3}\phi}\left(dx^5\right)^2, \tag{12}$$

with the nontrivial dilaton $e^\phi = (r/L)^{3/2}$. For later use, let us introduce another radial coordinate, $U \in [U_H, \infty)$, as follows:

$$U = \frac{r^2}{2L}, L = 2R. \tag{13}$$

So, in the large N_c limit, the 11th direction x^5 presented in (12) vanishes due to (7) and (8), which means the coincident N_c M5-branes correspond to coincident N_c D4-branes for

$N_c \to \infty$. In addition, the remaining 10d metric in (12) becomes the near-extremal black D4-brane solution (the extremal D4-brane solution can be obtained by setting $U_H \to 0$):

$$\begin{aligned} ds^2_{10\mathrm{d}} &= \left(\frac{U}{R}\right)^{3/2}\left[-f_T(U)\left(dx^0\right)^2 + \textstyle\sum_{i=1}^4 dx^i dx^i\right] + \left(\frac{R}{U}\right)^{3/2}\left[\frac{dU^2}{f_T(U)} + U^2 d\Omega_4^2\right], \\ f_T(U) &= 1 - \frac{U_H^3}{U^3}, F_4 = 3R^3 g_s^{-1}\epsilon_4, e^\phi = \left(\frac{U}{R}\right)^{3/4}, R^3 = \pi g_s N_c l_s^3 \end{aligned} \tag{14}$$

where ϵ_4 refers to the volume form of a unit S^4. Once the formula (12) is imposed to action (1), the 11d SUGRA action reduces to the 10d type IIA SUGRA action exactly, which is given as follows (there could be a Chern–Simons term to the IIA SUGRA action (15), such as $S_{\mathrm{CS}}^{10\mathrm{d}} = -\frac{1}{4\kappa_{10}^2}\int B_2 \wedge F_4 \wedge F_4$ with $B_{mn} = A_{mn5}$. For the purely black brane solution, the B_2 field can be gauged away by setting $B_2 = 0$, which implies that this CS term could be absent in 10d action [53,57]):

$$S_{\mathrm{IIA}}^{10\mathrm{d}} = \frac{1}{2\kappa_{10}^2}\int d^{10}x\sqrt{-G}e^{-2\phi}\left[\mathcal{R}^{(10)} + 4\partial_\mu\phi\partial\phi\right] - \frac{1}{4\kappa_{10}^2}\int d^{10}x\sqrt{-G}|F_4|^2, \tag{15}$$

where $2\kappa_{10}^2 = 16\pi G_{10} = (2\pi)^7 l_s^8 g_s^2$ is the 10d gravity coupling constant. It would be straightforward to verify that the solution (14) satisfies the equation of motion obtained by varying action (15).

The next step is to perform the double Wick rotation $\{x^0 \to -ix^4, x^4 \to -ix^0\}$ on the metric (14), leading to a bubble D4-brane solution,

$$\begin{aligned} ds^2_{10\mathrm{d}} &= \left(\frac{U}{R}\right)^{3/2}\left[\eta_{\mu\nu}dx^\mu dx^\nu + f(U)\left(dx^4\right)^2\right] + \left(\frac{R}{U}\right)^{3/2}\left[\frac{dU^2}{f(U)} + U^2 d\Omega_4^2\right], \\ f(U) &= 1 - \frac{U_{KK}^3}{U^3}, \end{aligned} \tag{16}$$

which is defined only for $U \in [U_{KK}, \infty)$. We renamed U_H as U_{KK} in (16), since there is not a horizon in the bubble solution, as illustrated in Figure 1.

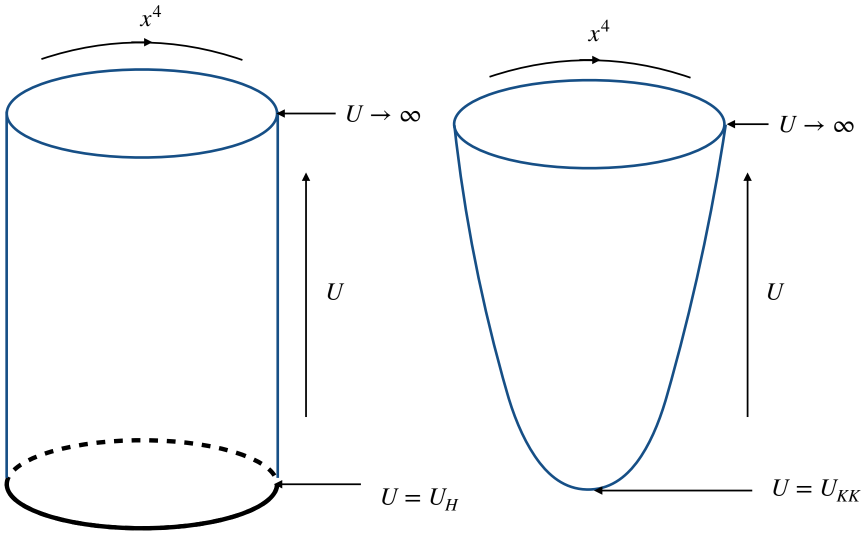

Figure 1. The compactified D4-brane geometry on $U - x^4$ plane. (**Left**) The black D4-brane background geometry. (**Right**) The D4 bubble geometry.

Now, the direction of x^4 is periodic:

$$x^4 \sim x^4 + \delta x^4, \delta x^4 = \frac{2\pi}{M_{KK}} = \frac{4\pi R^{3/2}}{3U_{KK}^{1/2}}, \tag{17}$$

because it is identified as the time direction in the black brane solution (14). M_{KK} refers to the Klein–Kaluza (KK) energy scale, and the supersymmetry on the D4-branes breaks down below M_{KK} by imposing the antiperiodic condition to the supersymmetric fermions along x^4. Accordingly, the low-energy zero modes on the D4-branes are the massless gauge field on the D4-branes and the scalar fields as the transverse modes of the D4-branes. While the scalar fields acquire mass via one-loop corrections, the trace part of the scalars ϕ^i and gauge field along x^4 direction a_4 remain massless. As they give irrelevant coupling terms in the low-energy effective theory on the D4-branes, it means that the dual theory below M_{KK} only contains 4d pure Yang–Mills gauge field, as expected. Note that the three-form C_3 in 11d SUGRA (1) corresponds to the Ramond–Ramond (R-R) three-form in type IIA string theory.

Moreover, as the wrap factor $(U/R)^{3/2}$ in (16) never goes to zero, the dual theory will be able to exhibit confinement according to the behavior of the Wilson loop in this geometry. Since the solution (16) allows for an arbitrarily large period for x^0, it implies that the dual theory on the D4-brane could be defined at a temperature of zero (or very low). Furthermore, in order to obtain a deconfined version of holographic QCD based on (16) at finite temperature, it is also possible to compactify one spacial direction (denoted by x^4) of the D4-branes in the background (14) with the antiperiodic condition for the supersymmetric fermions (there might be an issue if we identify the black brane background (14) to the deconfinement phase exactly since Wilson loop on this background may not match to the deconfinement QCD [58,59]. Nevertheless, we can identify the black brane background (14) to QCD phase at high temperature in which the deconfinement will occur), as is displayed in (17) and Figure 1. In this case, the Hawking temperature T in compactified background (14) is given by (11) as

$$\beta_T = \frac{1}{T} = \frac{4\pi R^{3/2}}{3U_H^{1/2}}, \tag{18}$$

which can, therefore, be identified as the temperature in the dual theory. The variables in terms of the dual theory are summarized as

$$R^3 = \frac{1}{2}\frac{g_{\mathrm{YM}}^2 N_c l_s^2}{M_{KK}},\ U_{KK} = \frac{2}{3} g_{\mathrm{YM}}^2 N_c M_{KK} l_s^2,\ g_s = \frac{1}{2\pi}\frac{g_{\mathrm{YM}}^2}{M_{KK} l_s}, \tag{19}$$

where g_{YM} is the Yang–Mills (YM) coupling constant.

2.2. Embedding the Probe D8/$\overline{\text{D8}}$-Branes

In the D4/D8 model, there is a stack of coincident N_f pairs of D8- and (anti-D8) $\overline{\text{D8}}$-branes as probes embedded into the bulk geometry illustrated in Figure 1. The relevant D-brane configuration is given in Table 1.

Table 1. The D-brane configuration in the D4/D8 model. "-" denotes that the D-brane extends along this direction.

	0	**1**	**2**	**3**	**4**	**5(U)**	**6**	**7**	**8**	**9**
N_c D4-branes	-	-	-	-	-					
N_f D8/$\overline{\text{D8}}$-branes	-	-	-	-		-	-	-	-	-

The embedding configuration of D8/$\overline{\text{D8}}$-branes is determined by solving the bosonic action for D_p-branes, which consists of Dirac–Born–Infeld (DBI) and Wess–Zumino (WZ) terms. The action reads as follows [60]:

$$\begin{aligned} S_{\mathrm{D_p}} &= S_{\mathrm{DBI}} + S_{\mathrm{WZ}}, \\ S_{\mathrm{DBI}} &= -T_{\mathrm{D}_p}\int_{\mathrm{D}_p} d^{p+1}x e^{-\phi}\mathrm{STr}\left[\sqrt{-\det[E_{ab} + E_{aI}(Q^{IJ} - \delta^{IJ})E_{Ib} + 2\pi\alpha' F_{ab}]}\sqrt{\det\left(Q^I{}_J\right)}\right], \\ S_{\mathrm{WZ}} &= g_s T_{\mathrm{D}_p}\int_{\mathrm{D}_p}\textstyle\sum_{n=0,1\ldots} C_{p-2n+1}\wedge\frac{1}{n!}(2\pi\alpha')^n\mathrm{Tr}F^n, \end{aligned} \tag{20}$$

with the D-brane tension $T_{D_p} = g_s^{-1}(2\pi)^{-p} l_s^{-p-1}$ and $e^{\Phi} = g_s e^{\phi}$,

$$\begin{aligned} E_{ab} =& \quad (G_{MN} + B_{MN})\partial_a X^M \partial_b X^N,\ E_{aI} = (G_{MI} + B_{MI})\partial_a X^M, \\ Q^I_{\ J} =& \quad \delta^I_{\ J} + i2\pi\alpha' [\Psi^I, \Psi^J],\ F_{ab} = \partial_a A_b - \partial_b A_a + i[A_a, A_b], \\ a, b =& \quad 0, 1...p,\ M, N = 0, 1...d,\ I, J = p+1, p+2...d. \end{aligned} \tag{21}$$

Here G_{MN}, B_{MN} and Φ refer, respectively, to the metric, the antisymmetric tensor and the dilaton field in the background spacetime. Ψ^I refers to the transverse mode of the D_p-brane under the T-duality. By choosing $p = 8$, the action (20) leads to the action for D8-brane on the N_c D4-brane background as follows (in the D4/D8 approach, the antisymmetric tensor B_{MN} has been gauged away):

$$S_{D8} = -T_{D8} \int_{D8} d^9 x e^{-\phi} \mathrm{STr} \sqrt{-\det[g_{ab} + (2\pi\alpha')F_{ab}]} + \frac{g_s}{3!}(2\pi\alpha')^3 T_{D8} \int_{D8} C_3 \wedge \mathrm{Tr}(F \wedge F \wedge F). \tag{22}$$

Using the induced metric on D8/$\overline{\text{D8}}$-branes with respect to the bubble D4 background (16),

$$ds^2_{D8} = \left(\frac{U}{R}\right)^{3/2} \eta_{\mu\nu} dx^\mu dx^\nu + \left(\frac{U}{R}\right)^{3/2} \left[f(U)\left(x^{4\prime}\right)^2 + \left(\frac{R}{U}\right)^3 \frac{1}{f(U)}\right] dU^2 + R^{3/2} U^{1/2} d\Omega_4^2, \tag{23}$$

and the black D4-brane background (14),

$$\begin{aligned} ds^2_{D8} =& \quad \left(\tfrac{U}{R}\right)^{3/2}\left[-f_T(U)\left(dx^0\right)^2 + \delta_{ij} dx^i dx^j\right] \\ & + \left(\tfrac{U}{R}\right)^{3/2}\left[\left(x^{4\prime}\right)^2 + \left(\tfrac{R}{U}\right)^3 \tfrac{1}{f_T(U)}\right] dU^2 + R^{3/2} U^{1/2} d\Omega_4^2, \end{aligned} \tag{24}$$

the DBI action for D8-branes becomes, respectively,

$$S_{DBI} = -g_s T_{D8} V_3 \beta_4 \Omega_4 \int_{U_{KK}}^{\infty} dU U^4 \left[f(U)\left(x^{4\prime}\right)^2 + \left(\frac{R}{U}\right)^3 \frac{1}{f(U)}\right]^{1/2}, \tag{25}$$

and

$$S_{DBI} = -g_s T_{D8} V_3 \beta_T \Omega_4 \int_{U_H}^{\infty} dU U^4 \left[\left(x^{4\prime}\right)^2 f_T(U) + \left(\frac{R}{U}\right)^3\right]^{1/2}. \tag{26}$$

Here, we use $\Omega_4 = 8\pi^2/3$ to refer to the volume of a unit S^4. Note that the WZ action is independent on the metric or elfbein. Varying actions (25) and (26) with respect to x^4, the associated equations of motion are, respectively, obtained as

$$\frac{d}{dU}\left[\frac{U^4 f(U) x^{4\prime}}{\sqrt{f(U)\left(x^{4\prime}\right)^2 + \left(\frac{R}{U}\right)^3 \frac{1}{f(U)}}}\right] = 0, \tag{27}$$

and

$$\frac{d}{dU}\left[\frac{U^4 f_T(U) x^{4\prime}}{\sqrt{\left(x^{4\prime}\right)^2 f_T(U) + \left(\frac{R}{U}\right)^3}}\right] = 0. \tag{28}$$

As the D8- and $\overline{\text{D8}}$-branes are the only probe branes, they could be connected smoothly at the location $U = U_0$, which means $x^4|_{U=U_0} \to \infty$. With this boundary condition, (27) and (28) reduce, respectively, to the following solutions:

$$\left(x^{4\prime}\right)^2 = \frac{U_0^8 f(U_0)}{U^3 f(U)^2} \frac{R^3}{U^8 f(U) - U_0^8 f(U_0)}, \tag{29}$$

and

$$\left(x^{4'}\right)^2 = \frac{U_0^8 f_T(U_0)}{U^3 f_T(U)} \frac{R^3}{U^8 f_T(U) - U_0^8 f_T(U_0)}. \tag{30}$$

In particular, in the bubble D4-brane background, solution (29) implies $x^4|_{U\to\infty, U_0\to U_{KK}} = \beta_4/4$ and $x^{4'}|_{U_0=U_{KK}} = 0$. Thus, $x^4 = \beta_4/4$ is a solution to (29) representing D8- and $\overline{\text{D8}}$-branes located at the antipodal points of S^1, while they are connected at $U = U_{KK}$, because the size of x^4 shrinks to zero at $U = U_{KK}$. On the other hand, in the black D4-brane background, if $U_0 = U_H$, (30) also implies a constant solution for x^4, while the separation of the D8- and $\overline{\text{D8}}$-branes could be arbitrary, but no more than $\beta_4/2$. For $U_0 > U_{KK}, U_H$, solutions (28) and (29) represent D8- and $\overline{\text{D8}}$-branes joined into a single brane at $U = U_0$. The configuration of the D8- and $\overline{\text{D8}}$-branes in bubble and black D4-brane backgrounds is illustrated in Figures 2 and 3.

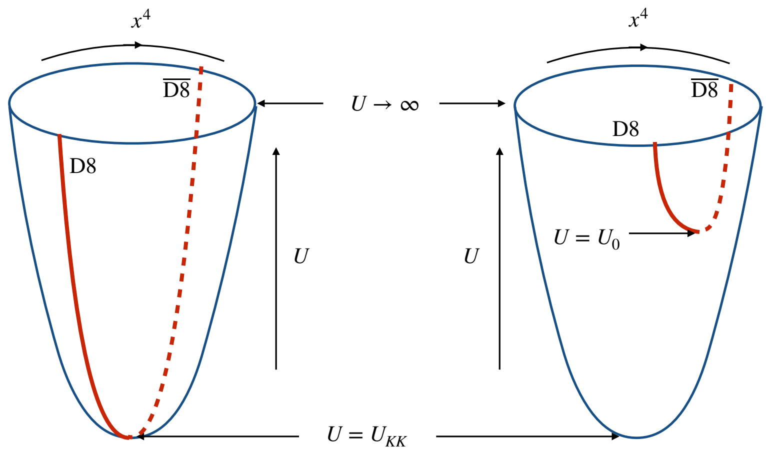

Figure 2. The D8-brane configuration in the bubble D4-brane background. (**Left**) D8- and $\overline{\text{D8}}$-branes are located at the antipodal points of x^4. (**Right**) D8- and $\overline{\text{D8}}$-branes are located at the nonantipodal points of x^4.

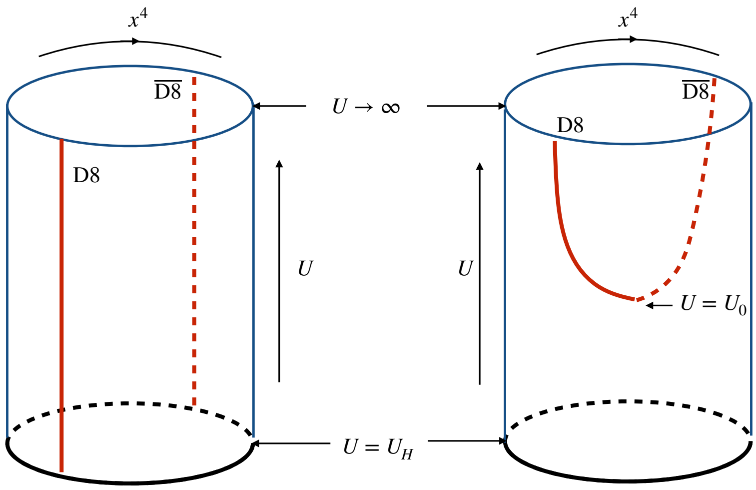

Figure 3. The D8-brane configuration in the black D4-brane background. (**Left**) D8- and $\overline{\text{D8}}$-branes are parallelly located. (**Right**) D8- and $\overline{\text{D8}}$-branes are connected at $U = U_0$.

2.3. Gluon, Quark and Symmetries

As the dual theory in the D4/D8 model is expected to be QCD in the large N_c limit, it is natural to identify the effective theory on N_c D4-branes below M_{KK} to the color sector in QCD, which implies that the gauge field $A_\mu^{(\text{D4})}$ on the D4-branes can be interpreted as gluon in holography. The reason is that the low-energy theory on N_c D4-branes is $U(N_c)$ pure Yang–Mills theory, and it has a SUGRA duality in the strong coupling region in the large N_c limit, as discussed in Section 2.1. We note that the Lorentz symmetry of the 10d spacetime breaks down to $SO(1+4)\times SO(5)$ when a stack of D4-branes is introduced. However, the worldvolume symmetry of the D4-branes becomes $SO(1+3)$, since the D4-branes are compactified on a circle in the D4/D8 model. Furthermore, when the flavors, as D8- and $\overline{\text{D8}}$-branes, are introduced, it is possible to create chiral fermions in the low-energy theory, which can be obtained by analyzing the spectrum of 4–8 or 4–$\overline{8}$ strings in R-sector (Ramond-sector). Both the spectra of 4–8 and 4–$\overline{8}$ strings in R-sector contain spinors with positive and negative chirality as the representations of the Lorentz group $SO(1,3)$. Since the GSO (Gliozzi–Scherk–Olive) projection removes the spinor with one of the chiralities in string theory, we can choose the spinor with positive and negative chirality as the massless fermionic modes (denoted by $q_{L,R}$) of 4–8 and 4–$\overline{8}$ strings, respectively, which accordingly can be identified as the fundamental chiral quarks in the dual theory. We note that these chirally fermionic fields are complex spinors since the 4–8 and 4–$\overline{8}$ strings have two orientations. They are also the fundamental representation of $U(N_c)$ and $U\left(N_f\right)$. The massless modes and symmetries in the D4/D8 system are collected in Table 2.

Table 2. The fields in the D4/D8 model. Here $\mathbf{2}_+$, $\mathbf{2}_-$ denote the positive and negative chirality spinor representations of $SO(1,3)$. a_4 and ϕ^i are the trace parts of the gauge field along x^4 direction on the N_c D4-branes and the transverse modes of the N_c D4-branes, which are decoupled to the gluon and fundamental quarks in the low-energy theory.

Fields	$U(N_c)$	$SO(1,3)$	$SO(5)$	$U(N_f)_L\times U(N_f)_R$
$A_\mu^{(\mathrm{D4})}$	adj.	4	1	(1, 1)
q_L	fund.	$\mathbf{2}_+$	1	(fund., 1)
q_R	fund.	$\mathbf{2}_-$	1	(1, fund.)
a_4	1	1	1	(1, 1)
ϕ^i	1	1	5	(1, 1)

Due to the above holographic correspondence, the chirally symmetric and broken phase in the dual theory can be identified, respectively, to the disconnected and connected configuration of the D8/$\overline{\text{D8}}$-branes. This would be clear if we employed the configuration presented in Figure 2, for example. The effective action for the gauge fields $A_\mu^{(\mathrm{D4})}$ and fundamental fermions $q_{L,R}$ on the N_c D4-branes with N_f D8/$\overline{\text{D8}}$-branes can be evaluated by expanding the DBI action, which leads to

$$S = \begin{array}{l}\int_{\mathrm{D4}} d^5x\sqrt{-g}\left[\delta\left(x^4-X_L\right)q_L^\dagger\bar{\sigma}^\mu\left(i\nabla_\mu+A_\mu\right)q_L+\delta\left(x^4-X_R\right)q_R^\dagger\bar{\sigma}^\mu\left(i\nabla_\mu+A_\mu\right)q_R\right]\\ -\frac{1}{4g_{\mathrm{YM}}^2}\int_{\mathrm{D4}} d^5x\sqrt{-g}\mathrm{Tr}F_{MN},\ M,N=0,1\ldots4,\end{array} \tag{31}$$

where $X_{L,R}$ denotes the intersection of the D4- and D8-branes as well as the D4- and $\overline{\text{D8}}$-branes, and we omit the notation "D4" in A_μ. As all the fields depend on $\{x^\mu,x^4\}$, q_L is identified to be q_R if $X_L=X_R$, which leads to an action with single flavor symmetry $U\left(N_f\right)$. For the connected configurations, we can therefore see that the D8- and $\overline{\text{D8}}$-branes are separated at high energy ($U\to\infty$, $X_L\neq X_R$) according to the solutions (29) and (30), which leads to an approximated $U\left(N_f\right)_L\times U\left(N_f\right)_R$ chiral symmetry. However, at low energy ($U\to U_0, X_L\to X_R$), D8- and $\overline{\text{D8}}$-branes are joined into a single pair of D8-branes at $U=U_0$ ($X_L=X_R$) which implies that the $U\left(N_f\right)_L\times U\left(N_f\right)_R$ symmetry breaks down to a single $U\left(N_f\right)$. This configuration of D8/$\overline{\text{D8}}$-branes provides a geometric interpretation of chiral symmetry in this model [56].

2.4. Mesons on the Flavor Brane

As meson is the bound state in the adjoint representation of the chiral symmetry group, it is identified as the gauge field on the flavor branes, which is the massless mode excited by 8–8 string (massless mode excited by $\overline{8}$–$\overline{8}$ string is therefore identified as antimeson.). The reason is that the gauge field is excited by 8–8 (and $\overline{8}$–$\overline{8}$) is the generator of $U\left(N_f\right)_L$ (and $U\left(N_f\right)_R$). Hence, we consider the gauge field on the flavor branes with nonzero components as $A_M = \left\{A_\mu(x,z), A_z(x,z)\right\}, \mu = 0, 1...3$ in the bubble D4-brane background (16). We note that while the supersymmetry on N_c D4-branes breaks down by compactifying x^4 on a circle, there is no mechanism to break down the supersymmetry on D8/$\overline{\text{D8}}$-branes, since D8/$\overline{\text{D8}}$-branes are vertical to x^4. Therefore, the 8–8 string is supersymmetric, leading to a super partner fermion Ψ of the gauge field A_M in the low-energy theory. As we see in Appendix **??**, this supersymmetric fermion is Majorana spinor, which leads to the fermionic meson (mesino), while they are absent in the realistic QCD.

Nonetheless, let us assume that the supersymmetry on the flavor branes somehow breaks down and the supersymmetric meson can be turned off in order to continue the discussion about the QCD sector of this model. Since the D8-branes are probes, the worldvolume gauge field is fluctuation. Thus, the effective action for A_M can be obtained by expanding (22), which for Abelian case $N_f = 1$ is

$$\begin{aligned} S_{\text{D8}} = & -T_{\text{D8}} \int_{\text{D8}} d^9 x e^{-\phi} \sqrt{-\det[g_{ab} + (2\pi\alpha')F_{ab}]} \\ = & -T_{\text{D8}} \int_{\text{D8}} d^9 x \sqrt{-g} e^{-\phi} \left[1 + \tfrac{1}{4}(2\pi\alpha')^2 F_{MN}F^{MN} + \mathcal{O}\left(F^4\right)\right], \end{aligned} \tag{32}$$

leading to the Yang–Mills (YM) action

$$\begin{aligned} S_{\text{YM}} = & -T_{\text{D8}} \int_{\text{D8}} d^9 x \sqrt{-g} e^{-\phi} \tfrac{1}{4} (2\pi\alpha')^2 F_{MN}F^{MN} \\ = & -\tfrac{2}{3} R^{3/2} U_{KK}^{1/2} (2\pi\alpha')^2 T_{\text{D8}} \Omega_4 \int d^4 x dz \left(\tfrac{R^3}{4U} \eta^{\mu\rho}\eta^{\nu\sigma} F_{\mu\nu}F_{\rho\sigma} + \tfrac{9U^3}{8U_{KK}} \eta^{\mu\nu} F_{\mu z}F_{\nu z}\right) \\ = & -\kappa \int d^4 x dZ \left(\tfrac{1}{2} K^{-1/3} \eta^{\mu\rho}\eta^{\nu\sigma} F_{\mu\nu}F_{\rho\sigma} + K M_{KK}^2 \eta^{\mu\nu} F_{\mu Z}F_{\nu Z}\right), \end{aligned} \tag{33}$$

where we use the Cartesian coordinates z and dimensionless Z, defined as

$$U^3 = U_{KK}^3 + U_{KK} z^2, Z = \frac{z}{U_{KK}}, K(Z) = 1 + Z^2 = \frac{U^3}{U_{KK}^3}, \tag{34}$$

and

$$\kappa = \frac{1}{3} R^{9/2} U_{KK}^{1/2} (2\pi\alpha')^2 T_{\text{D8}} \Omega_4 = \frac{\lambda N_c}{216\pi^3}, \lambda = g_{\text{YM}}^2 N_c, \tag{35}$$

with the induced metric on the D8-branes,

$$ds_{\text{D8}}^2 = \left(\frac{U}{R}\right)^{3/2} \eta_{\mu\nu} dx^\mu dx^\nu + \frac{4R^{3/2} U_{KK}}{9U^{5/2}} dz^2 + R^{3/2} U^{1/2} d\Omega_4^2. \tag{36}$$

We employ the configuration that D8/$\overline{\text{D8}}$-branes are located at the antipodal points of S^1. Then, in order to obtain a 4d mesonic action, let us assume that $A_\mu(x,z), A_z(x,z)$ can be expanded in terms of complete sets $\{\psi_n(z), \phi_n(z)\}$:

$$A_\mu(x,z) = \sum_n B_\mu^{(n)}(x) \psi_n(z), A_z(x,z) = \sum_n \varphi^{(n)}(x) \phi_n(z), \tag{37}$$

where $B_\mu^{(n)}(x), \varphi^{(n)}(x)$ refers to the 4d meson field. To obtain a finite action, the normalization condition for $\psi_n(z)$ is chosen as

$$2\kappa \int dZ K^{-1/3} \psi_n \psi_m = \delta_{mn}, \tag{38}$$

with the eigen equation ($n \geq 1$),

$$-K^{1/3}\partial_Z(K\partial_Z\psi_n) = \lambda_n\psi_n, \tag{39}$$

where λ_n is the associated eigenvalue. In this sense, the basic function $\phi_n(z)$ can be chosen as ($n \geq 1$):

$$\phi_0 = \frac{1}{\sqrt{2\pi\kappa}}\frac{1}{U_{KK}M_{KK}}\frac{1}{K}, \phi_n = m_n^{-1}\partial_Z\psi_n, m_n = \lambda_n M_{KK}. \tag{40}$$

Keeping these in hand, imposing (38)–(40) into (33), then defining the vector field $V_\mu^{(n)}(x)$ by a gauge transformation,

$$V_\mu^{(n)} = B_\mu^{(n)} - m_n^{-1}\partial_\mu\varphi^{(n)}, \tag{41}$$

the Yang–Mills action (33) reduces to a 4d effective action for mesons:

$$S_{\mathrm{YM}} = -\kappa\int d^4x\left(\frac{1}{2}\partial_\mu\varphi^{(0)}\partial^\mu\varphi^{(0)} + \sum_{n=1}^{\infty}\left[\frac{1}{4}F_{\mu\nu}^{(n)}F^{(n)\mu\nu} + \frac{1}{2}m_n^2V_\mu^{(n)}V^{(n)\mu}\right]\right), \tag{42}$$

where $F_{\mu\nu}^{(n)} = \partial_\mu V_\nu^{(n)} - \partial_\nu V_\mu^{(n)}$. Accordingly, $\varphi^{(0)}$ can be interpreted as pion meson, which is the Nambu–Goldstone boson associated with the chiral symmetry breaking. By analyzing the parity, it turns out that $\varphi^{(0)}$ is a pseudoscalar field, as expected.

The above discussion implicitly assumes that the gauge field A_M and its field strength F_{MN} should vanish at $|z| \to \infty$ in order to obtain a finite 4d mesonic action. However, there is an alternative gauge choice $A_z = 0$, which is recognized as a gauge transformation:

$$A_M \to A_M - \partial_M\Lambda, \tag{43}$$

to (37). Here, Λ is solved:

$$\Lambda(x,z) = \varphi^{(0)}(x)\psi_0(z) + \sum_{n=1}^{\infty} m_n^{-1}\varphi^{(n)}(x)\psi_n(z), \tag{44}$$

where

$$\psi_0(z) = \int dz\phi_0(z) = \frac{1}{\sqrt{2\pi\kappa}}\frac{1}{M_{KK}}\arctan\left(\frac{z}{U_{KK}}\right). \tag{45}$$

Thus, the components of A_M under gauge condition $A_z = 0$ become

$$\begin{aligned} A_\mu(x,z) &= -\partial_\mu\varphi^{(0)}(x)\psi_0(z) + \textstyle\sum_{n=1}^{\infty}\left[B_\mu^{(n)}(x) - m_n^{-1}\partial_\mu\varphi^{(n)}\right]\psi_n(z) \\ &= -\partial_\mu\varphi^{(0)}(x)\psi_0(z) + \textstyle\sum_{n=1}^{\infty}V_\mu^{(n)}(x)\psi_n(z), \\ A_z(x,z) &= 0. \end{aligned} \tag{46}$$

In the region $|z| \to \infty$, the gauge potential $A_\mu(x,z) \to \pm\sqrt{\frac{\pi}{8\kappa}}\frac{1}{M_{KK}}$, which implies that the gauge field strength remains vanished and the effective 4d action remains finite.

The above setup for mesons can be generalized into multiflavor case by taking into account the non-Abelian version of (33),

$$S_{\mathrm{YM}}^{(N_f)} = -\kappa N_f\int d^4x dZ\left[\frac{1}{2}K^{-1/3}\eta^{\mu\rho}\eta^{\nu\sigma}\mathrm{Tr}\left(F_{\mu\nu}F_{\rho\sigma}\right) + KM_{KK}^2\eta^{\mu\nu}\mathrm{Tr}\left(F_{\mu Z}F_{\nu Z}\right)\right], \tag{47}$$

where $F_{MN} = \partial_M A_N - \partial_N A_M + [A_M, A_N]$, $M, N = 0,1,2,3,z$ is the gauge field strength of $U\left(N_f\right)$. As has been discussed, in order to obtain a finite 4d action, the gauge field strength must vanish in the limit $|z| \to \infty$. Under the gauge condition $A_z = 0$, A_μ must asymptotically take a pure gauge configuration for $|z| \to \infty$:

$$A_\mu(x,z)|_{z\to\pm\infty} \to \xi_\pm(x)\partial_\mu\xi_\pm^{-1}(x). \tag{48}$$

Compare this with (46); the gauge potential can be expanded with boundary condition (48),

$$\begin{aligned} A_\mu(x,z) = & \ \xi_+(x)\partial_\mu\xi_+^{-1}(x)\psi_+(z) + \xi_-(x)\partial_\mu\xi_-^{-1}(x)\psi_-(z) + \textstyle\sum_{n=1}^\infty V_\mu^{(n)}(x)\psi_n(z) \\ \equiv & \ \alpha_\mu(x)\hat{\psi}_0(z) + \beta_\mu(x) + \textstyle\sum_{n=1}^\infty V_\mu^{(n)}(x)\psi_n(z), \end{aligned} \tag{49}$$

with

$$\begin{aligned} \psi_\pm = & \ \tfrac{1}{2} \pm \hat{\psi}_0, \hat{\psi}_0 = \tfrac{1}{\pi}\arctan\left(\tfrac{z}{U_{KK}}\right). \\ \alpha_\mu(x) = & \ \xi_+(x)\partial_\mu\xi_+^{-1}(x) - \xi_-(x)\partial_\mu\xi_-^{-1}(x) \\ \beta_\mu(x) = & \ \tfrac{1}{2}\left[\xi_+(x)\partial_\mu\xi_+^{-1}(x) + \xi_-(x)\partial_\mu\xi_-^{-1}(x)\right]. \end{aligned} \tag{50}$$

To obtain the chiral Lagrangian for mesons from the Yang–Mills action (47), we identify the lowest vector meson field $V_\mu^{(n)}$ as the ρ meson $V_\mu^{(1)} = \rho_\mu$ and choose the following gauge conditions:

$$\xi_+^{-1}(x) = U(x), \xi_-(x) = 1, \tag{51}$$

or

$$\xi_+^{-1}(x) = \xi_-(x) = \exp[i\pi(x)/f_\pi]. \tag{52}$$

Inserting (49) into action (47) with the gauge condition (51), the 4d Yang–Mills action (47) includes a part of Skyrme model [61],

$$S_{\mathrm{YM}}^{(N_f)} = \int d^4x \left[\frac{f_\pi^2}{4}\mathrm{Tr}\left(U^{-1}\partial_\mu U\right)^2 + \frac{1}{32e^2}\mathrm{Tr}\left(U^{-1}\partial_\mu U, U^{-1}\partial_\mu U\right)^2 + ...\right], \tag{53}$$

where the coupling constants f_π, e are given as

$$\begin{aligned} f_\pi^2 & = 6R^{3/2}U_{KK}^{1/2}T_{\mathrm{D8}}\Omega_4(2\pi\alpha')^2\int dz\frac{U(z)^3}{U_{KK}}(\partial_z\psi_+)^2 = \frac{\lambda M_{KK}N_c}{54\pi^2}, \\ e^2 & = \left[\tfrac{32}{3}R^{3/2}U_{KK}^{1/2}T_{\mathrm{D8}}\Omega_4(2\pi\alpha')^2\int dz\frac{R^3}{U(z)}\psi_+^2(\psi_+-1)^2\right]^{-1} = \frac{27\pi^7}{2b\lambda N_c}, \\ b & = \int\frac{dZ}{(1+Z^2)^{1/3}}\left(\arctan Z + \tfrac{\pi}{2}\right)^2\left(\arctan Z - \tfrac{\pi}{2}\right)^2 \simeq 15.25. \end{aligned} \tag{54}$$

Moreover, the interaction terms of π, ρ mesons would be determined by the Yang–Mills action (47) with the gauge condition (52), as

$$\begin{aligned} S_{\mathrm{YM}}^{(N_f)} = & \int d^4x\mathrm{Tr}\left[-\partial_\mu\pi\partial^\mu\pi + \tfrac{1}{2}W_{\mu\nu}^2 + m_v^2\rho_\mu^2 + a_{\rho^3}\left[\rho_\mu,\rho_\nu\right]W^{\mu\nu} + a_{\rho\pi^2}\left[\partial_\mu\pi,\partial_\nu\pi\right]W^{\mu\nu}\right] \\ & +\mathcal{O}\left(\pi^4,\rho_\mu^4\right), \end{aligned} \tag{55}$$

where $W_{\mu\nu}$ is the gauge field strength of ρ_μ, and the associated coupling constants are given as

$$\begin{aligned} m_\rho^2 & = \Lambda_1 M_{KK}^2, a_{\rho^3} = \frac{(6\pi)^{3/2}}{\sqrt{\lambda N_c}}b_{\rho^3}, a_{\rho\pi^2} = \frac{\pi(3\pi)^{3/2}}{M_{KK}^2\sqrt{2\lambda N_c}}b_{\rho\pi^2}, \\ b_{\rho^3} & \simeq 0.45, b_{\rho\pi^2} \simeq 1.6, \Lambda_1 \simeq 0.67. \end{aligned} \tag{56}$$

Therefore, we can reach the meson tower or chiral Lagrangian starting with the D8-brane action, which provides a description of the meson in holography.

To close this section, let us finally take a look at the WZ term presented in action (22), which can be integrated as

$$\begin{aligned} S_{\mathrm{WZ}}^{\mathrm{D8}} &= \tfrac{g_s}{3!}(2\pi\alpha')^3 T_{\mathrm{D8}} \int_{\mathrm{D8}} C_3 \wedge \mathrm{Tr}(F \wedge F \wedge F) \\ &= \tfrac{g_s}{3!}(2\pi\alpha')^3 T_{\mathrm{D8}} \int_{\mathrm{D8}} F_4 \wedge \omega_5 \\ &= \tfrac{N_c}{24\pi^2} \mathrm{Tr} \int_{M_4 \times \mathbb{R}} \omega_5(A). \end{aligned} \tag{57}$$

Here, $F_4 = dC_3$ is the Ramond–Ramond field given in (14), and $\omega_5(A)$ is the Chern–Simons (CS) 5-form, given as

$$\omega_5(A) = AF^2 - \frac{1}{2}A^3F + \frac{1}{10}A^5, \tag{58}$$

where $F = dA + \frac{1}{2}[A, A]$ is the gauge field strength. Under the gauge transformation on the D8-brane,

$$\delta_\Lambda A = d\Lambda + [A, \Lambda], \delta_\Lambda F = [F, \Lambda], \tag{59}$$

we can compute

$$\begin{aligned} \mathrm{Tr}(\delta_\Lambda \omega_5) &= \mathrm{Tr}\left[d\Lambda d\left(AdA + \tfrac{1}{2}A^3\right)\right] \\ &= d\left(\mathrm{Tr}\left[\Lambda d\left(AdA + \tfrac{1}{2}A^3\right)\right]\right) \\ &\equiv d\chi_4(\Lambda, A). \end{aligned} \tag{60}$$

Hence, by defining the boundary value of the gauge potential as

$$A_\mu^L(x) = \lim_{z\to+\infty} A_\mu(x,z), A_\mu^R(x) = \lim_{z\to-\infty} A_\mu^R(x,z), \tag{61}$$

the WZ term is reduced to the chiral anomaly of $U\left(N_f\right)_L \times U\left(N_f\right)_R$ in QCD,

$$\begin{aligned} \delta_\Lambda S_{\mathrm{WZ}}^{\mathrm{D8}} &= \tfrac{N_c}{24\pi^2} \mathrm{Tr} \int_{M_4 \times \mathbb{R}} \delta_\Lambda \omega_5(A) = \tfrac{N_c}{24\pi^2} \int_{M_4} \chi_4(\Lambda, A)\Big|_{z\to-\infty}^{z\to+\infty} \\ &= \tfrac{N_c}{24\pi^2} \int_{M_4} [\chi_4(\Lambda_L, A_L) - \chi_4(\Lambda_R, A_R)]. \end{aligned} \tag{62}$$

Moreover, the formula for the chiral anomaly can also be expressed in the gauge condition $A_z = 0$, which is used to perform the gauge transformation

$$A^g = gAg^{-1} + gdg^{-1}. \tag{63}$$

Then, the CS 5-form is reduced to

$$\omega_5(A^g) = \omega_5(A) + \frac{1}{10}\left(gdg^{-1}\right)^5 + d\alpha_4, \tag{64}$$

where

$$\begin{aligned} &\alpha_4 = -\frac{1}{2}W_1\left(AdA + dAA + A^3\right) + \frac{1}{4}W_1AW_1A - W_1^3A, \\ &W_1 = dg^{-1}g. \end{aligned} \tag{65}$$

Recalling Formulas (49) in the gauge $A_z = 0$ and choosing gauge condition (51), the WZ term (57) can be rewritten, after somewhat lengthy but straightforward calculations, as

$$S_{\mathrm{WZ}}^{\mathrm{D8}} = -\frac{N_c}{48\pi^2}\mathrm{Tr}\int_{M_4} L_{\mathrm{WZW}} - \frac{N_c}{240\pi^2}\mathrm{Tr}\int_{M_4\times\mathbb{R}}\left(gdg^{-1}\right)^5, \tag{66}$$

where L_{WZW} is the Wess–Zumino–Witten (WZW) term in [62,63], given as

$$\begin{aligned} L_{\text{WZW}} = \quad & \left[\left(A_R dA_R + dA_R A_R + A_R^3\right)\left(U^{-1}A_L U + U^{-1}dU\right) - \text{p.c.}\right] \\ & + \left(dA_R dU^{-1}A_L U - \text{p.c.}\right) + \left[A_R\left(dU^{-1}U\right)^3 - \text{p.c.}\right] \\ & + \frac{1}{2}\left[\left(A_R dU^{-1}U\right)^2 - \text{p.c.}\right] + \left[UA_R U^{-1}A_L dU dU^{-1} - \text{p.c.}\right] \\ & - \left[A_R dU^{-1}UA_R U^{-1}A_L U - \text{p.c.}\right] + \frac{1}{2}\left(A_R U^{-1}A_L U\right)^2. \end{aligned} \tag{67}$$

Note that "p.c." refers to the terms by exchanging $A_L \leftrightarrow A_R, U \leftrightarrow U^{-1}$. One can further work out the couplings to the vector mesons by using (49) with $A_z = 0$.

2.5. The Wrapped D4-Brane and Baryon Vertex

In the $SU(N_c)$ gauge theory, a baryon vertex connects to N_c external fundamental quarks with the color wave function combined together by an N_c-th antisymmetric tensor of $SU(N_c)$ group. Accordingly, the baryon vertex in gauge–gravity duality is recognized as a D-brane wrapped on the internal sphere [26,64]. To clarify this briefly, let us first recall the baryon vertex in the holographic duality between $\mathcal{N} = 4$ super Yang–Mills theory and IIB string theory on $\text{AdS}_5 \times S^5$. As the fundamental quark in the super Yang–Mills theory is created by the N_c elementary superstrings in $\text{AdS}_5 \times S^5$, it is represented by the endpoints of elementary superstrings at the boundary of AdS_5. Hence, we need N_c elementary superstrings with the same orientation to somehow terminate in the $\text{AdS}_5 \times S^5$.

On the other hand, since the baryon current must be conserved, one needs to find a source to cancel the N_c charges (baryon charge) contributed by the N_c elementary superstrings. To figure out these problems and work out a baryon vertex, a probe D5-brane wrapped on S^5 provides us with a good answer. The N_c elementary superstrings ending on the D5-brane contribute N_c to the D5-brane; however, the WZ action for such a wrapped D5-brane,

$$S_{\text{WZ}}^{(\text{D5})} \sim \int_{S^5\times\mathbb{R}} C_4 F \sim \int_{S^5\times\mathbb{R}} F_5 A \sim N_c \int_{\mathbb{R}} A, \tag{68}$$

where $F_5 = dC_4$ is the Ramond–Ramond field strength, nicely provides N_c charges to cancel the charges given by N_c elementary superstrings (the sign of the N_c charge depends on the orientation of the elementary superstrings and D5-branes.). Therefore, the A current would be conserved, which implies that the D5-brane is a baryon vertex.

The construction of the baryon vertex can also been employed in the D4/D8 model, which is identified as a D4-brane (to distinguish the D4-branes as the baryon vertex from the N_c D4-branes, we denote the baryon vertex as D4$'$-brane in the rest of this paper) wrapped on S^4 with N_c elementary superstrings ending on it. A remarkable point here is that the D4$'$-branes can be described equivalently by the instanton configuration of the gauge field on the D8-branes [65,66]. To see this clearly, let us consider a D_p-brane with its worldvolume gauge field strength F. According to (20), The WZ action for such a D_p-brane includes a term as a source,

$$S_{\text{WZ}} \sim g_s T_{D_p}\left(2\pi\alpha'\right)^2 \int C_{p-3}\text{Tr}F^2. \tag{69}$$

For the single instanton configuration, the gauge field strength can be integrated as follows:

$$\text{Tr}\int F^2 = 8\pi^2. \tag{70}$$

Hence, (69) can be written as

$$g_s T_{D_p}\left(2\pi\alpha'\right)^2 \int C_{p-3}\text{Tr}F^2 = g_s T_{D_{p-4}} \int C_{p-3},$$

giving rise to a same source included by a D_{p-4}-brane. Accordingly, we obtain a simple and interesting conclusion here, that is, the instanton in the D_p-brane is the same object as a D_{p-4}-brane inside it.

Let us return to the D4/D8 model; it implies that the D4′-branes as the baryon vertex are equivalent to the instanton in the D8/$\overline{\text{D8}}$-branes. For multiple instantons, (70) is replaced by

$$\mathrm{Tr}\int F^2 = 8\pi^2 n, \tag{71}$$

where n refers to the instanton number. Inserting the instanton configuration of the gauge field denoted as A_{cl} with a $U\left(N_f\right)_V$ fluctuation $\tilde{A}$ into the WZ action (57) of D8-brane, it reduces to

$$\frac{N_c}{8\pi^2}\int \tilde{A}\mathrm{Tr}F^2 = nN_c\int \tilde{A}, \tag{72}$$

which implies that the instantons take $U(1)_V$ charge nN_c. Since the baryon number is defined as $1/N_c$ times the charge of the diagonal $U(1)_V$ subgroup of the $U\left(N_f\right)_V$ symmetry, it is obvious that the instanton number is equivalent to the baryon number in this holographic system.

Moreover, when (71) is integrated out to be a Chern–Simons 3-form ω_3, as

$$\int_{M_4}\mathrm{Tr}F^2 = \int_{\partial M_4}\mathrm{Tr}\omega_3 = \int \mathrm{Tr}\left(AF - \frac{1}{3}A^3\right), \tag{73}$$

the baryon number can be obtained:

$$n = \frac{1}{8\pi^2}\mathrm{Tr}\int_{\mathbb{R}^4} F^2 = \mathrm{Tr}\int_{\mathbb{R}^3}\omega_3|_{z\to-\infty}^{z\to+\infty} = -\frac{1}{24\pi^2}\mathrm{Tr}\int_{\mathbb{R}^3}\left(U^{-1}dU\right)^3, \tag{74}$$

where we impose a similar boundary condition as is given in (51):

$$\lim_{z\to+\infty}A_\mu(x^\mu,z) = U^{-1}\left(x^i\right)\partial_i U\left(x^i\right), \lim_{z\to-\infty}A_\mu(x^\mu,z) = 0. \tag{75}$$

Equation (74) gives the winding number of U, which means the homotopy is $\pi_3\left[U\left(N_f\right)\right] \simeq \mathbb{Z}$. This agrees with the baryon number charge in the Skyrme model [62,67].

The baryon mass m_B can be roughly obtained by evaluating the energy carried by the D4′-branes, which can be read from its DBI action as

$$\begin{aligned} S_{\mathrm{D4}'} &= -T_{\mathrm{D4}}\int dx^0 d\Omega_4 e^{-\phi}\sqrt{-g_{00}g_{S^4}} \\ &= -\tfrac{1}{27}M_{KK}\lambda N_c^2\int_{\mathbb{R}}dx^0, \\ &= -m_B\int_{\mathbb{R}}dx^0 \end{aligned} \tag{76}$$

where the bubble D4-brane background has been chosen for the confined property of baryon, and g_{S^4} refers to the metric on S^4 presented in (16). This formula illustrates a stable position of the baryonic D4′-brane by minimizing its energy, which is $U = U_{KK}$, since the bubble geometry shrinks at $U = U_{KK}$. In the black D4-brane, one can follow the same formula (76) to evaluate the baryon mass. However, if the baryonic D4′-brane is the only probe brane, it can not stay at $U = U_H$ stably in the black D4-brane background, since gravity will pull it into the horizon. In this sense, the baryon vertex exists in the bubble D4-brane background only, and it is consistent with its property of confinement. When the probe D8/$\overline{\text{D8}}$-branes are embedded into the bulk geometry, due to the balance condition, the baryonic D4′-brane can be restricted inside the D8-branes if D8/$\overline{\text{D8}}$-branes are connected, as is displayed in Figure 4 (the authors of [68] claim thataccording to the numerical calculation, there is not a wrapped configuration for the baryonic D4′-brane in the black D4-brane background; thus, this background may correspond to the deconfinement phase of QCD. We note that this issue is not figured out, even if the baryon vertex is introduced into the black D4-brane background).

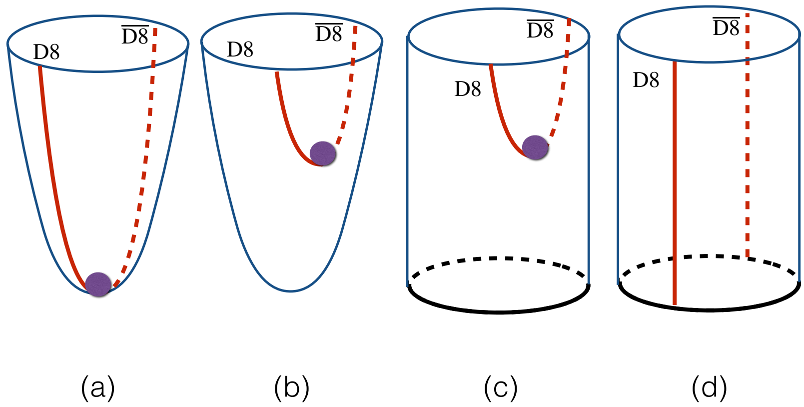

Figure 4. Various D-brane configurations in the D4/D8 model. Purple refers to the baryon vertex (D4′-brane) located at the stable position. When the D8/$\overline{\mathrm{D8}}$-branes are connected as in (**a**–**c**), the baryon vertex can be located stably at the connected position inside the D8/$\overline{\mathrm{D8}}$-branes. There is no stable position for baryon vertex if D8/$\overline{\mathrm{D8}}$-branes are parallel, as in (**d**).

Therefore, it can be described equivalently by the instanton configuration on the D8-branes.

To obtain the baryon mass or baryon spectrum in this model, it is worth searching for an exact instanton solution for the gauge field on the D8-branes. As baryon lives in the low-energy region of QCD, we may find an approximated solution for the instanton configuration in the strong coupling limit, i.e., $\lambda \to \infty$. To achieve this goal, let us take a look at the gauge field on the D8-branes, whose dynamic is described by the Yang–Mills action (33) and the Chern–Simons action presented in (57) (as the size of instanton takes order of $\lambda^{-1/2}$, it may lead to a puzzle if the Yang–Mills action is taken into account, only because the high-order derivatives in the DBI action contribute more importantly. However, according to the holographic duality, taking the near-horizon limit requires $\alpha' \to 0$, which implies that the Yang–Mills action dominates the dynamics in the DBI action. This puzzle is not figured out completely in [27,28], and we may additionally set $\alpha'\lambda \to 0$ when Yang–Mills action is taken into account only in this setup.). Since the size of instanton is of order $\lambda^{-1/2}$, it would be convenient to rescale the coordinate $\{x^0, x^i, z\}$ and the gauge potential A as

$$\begin{aligned} x^M &\to \lambda^{-1/2} x^M, \quad x^0 \to x^0 \\ A_M &\to \lambda^{1/2} A_M, \quad A_0 \to A_0 \\ F_{MN} &\to \lambda F_{MN}, \quad F_{0M} \to \lambda^{1/2} F_{0M}, \end{aligned} \tag{77}$$

where $M, N = 1,2,3,z$. In the large λ limit, the Yang–Mills action (33) can be expanded as follows:

$$\begin{aligned} S_{\mathrm{YM}} = \; & -\tfrac{\kappa}{\lambda}\int d^4xdz\mathrm{Tr}\left[\tfrac{\lambda}{2}F_{MN}^2 + \left(-\tfrac{z^2}{6}F_{ij}^2 + z^2F_{iz}^2 - F_{0M}^2\right) + \mathcal{O}\left(\lambda^{-1}\right)\right] \\ & -\tfrac{\kappa}{2\lambda}\int d^4xdz\left[\tfrac{\lambda}{2}\hat{F}_{MN}^2 + \left(-\tfrac{z^2}{6}\hat{F}_{ij}^2 + z^2\hat{F}_{iz}^2 - \hat{F}_{0M}^2\right) + \mathcal{O}\left(\lambda^{-1}\right)\right], \end{aligned} \tag{78}$$

while the Chern–Simons action (57) remains under the rescaling (77). We employed the D-brane configuration presented in Figure 4a. The $U\left(N_f\right)$ group is decomposed as $U\left(N_f\right) \simeq U(1) \times SU\left(N_f\right)$, and correspondingly, its generator is decomposed as follows:

$$A + \frac{1}{\sqrt{2N_f}}\hat{A} = A^a t^a + \frac{1}{\sqrt{2N_f}}\hat{A}, \tag{79}$$

where $\hat{A}, A$ refers to the generators of $U(1), SU\left(N_f\right)$, respectively, and t^a $(a = 1,2...N_f^2 - 1)$ are the normalized bases, satisfying

$$\mathrm{Tr}\left(t^a t^b\right) = \frac{1}{2}\delta^{ab}. \tag{80}$$

So, the Chern–Simons action (57) can be derived as follows:

$$\begin{aligned} S_{\mathrm{CS}} = & \frac{N_c}{24\pi^2}\int \omega_5^{SU(N_f)}(A) + \frac{N_c}{24\pi^2}\sqrt{\frac{2}{N_f}}\epsilon_{MNPQ}\int d^4x dz\Big[\frac{3}{8}\hat{A}_0 \mathrm{Tr}\big(F_{MN}F_{PQ}\big) \\ & -\frac{3}{2}\hat{A}_M \mathrm{Tr}\big(\partial_0 A_N F_{PQ}\big) + \frac{3}{4}\hat{F}_{MN}\mathrm{Tr}\big(A_0 F_{PQ}\big) + \frac{1}{16}\hat{A}_0\hat{F}_{MN}\hat{F}_{PQ} - \frac{1}{4}\hat{A}_M\hat{F}_{0N}\hat{F}_{PQ} \\ & +(\text{total derivatives})\Big]. \end{aligned} \tag{81}$$

Furthermore, the equation of motion for $\hat{A}, A$ can be derived by varying actions (78) and (81), which allows for an instanton solution as follows:

$$A_M^{\mathrm{cl}} = -if(\xi)g(x)\partial_M g^{-1}, \tag{82}$$

where

$$\begin{aligned} f(\xi) &= \frac{\xi^2}{\xi^2+\rho^2}, \xi = \sqrt{\left(x^M - X^M\right)^2}, \\ g(x) &= \begin{pmatrix} g^{SU(2)}(x) & 0 \\ 0 & \mathbf{1}_{N_f-2} \end{pmatrix}, g^{SU(2)}(x) = \frac{1}{\xi}\left[(z-Z)\mathbf{1}_2 - i\left(x^i - X^i\right)\tau^i\right]. \end{aligned} \tag{83}$$

Here, $\mathbf{1}_N$ is an $N \times N$ identity matrix and τ^i's are the Pauli matrices. The position and the size of the instanton are denoted by the constants $X^M = \{X^i, Z\}$ and ρ, respectively which have been rescaled as (77). The configuration (82) and (83) is the Belavin–Polyakov–Schwartz–Tyupkin (BPST) solution embedding into $SU\left(N_f\right)$, which represents the $SU(2)$ Euclidean instanton, and one may verify that this solution satisfies (70). Then, the $U(1)$ part of the gauge field is solved as follows:

$$\hat{A}_0^{\mathrm{cl}} = \sqrt{\frac{2}{N_f}}\frac{1}{8\pi^2 a}\frac{1}{\xi^2}\left[1 - \frac{\rho^4}{\left(\xi^2+\rho^2\right)^2}\right], \hat{A}_M^{\mathrm{cl}} = 0. \tag{84}$$

which leads to a nonzero A_0,

$$A_0^{\mathrm{cl}} = \frac{1}{16\pi^2 a}\frac{1}{\xi^2}\left[1 - \frac{\rho^4}{\left(\xi^2+\rho^2\right)^2}\right]\left(\mathcal{P}_2 - \frac{2}{N_f}\mathbf{1}_{N_f}\right), \tag{85}$$

where $\mathcal{P}_2$ is an $N_f \times N_f$ matrix $\mathcal{P}_2 = \mathrm{diag}(1,1,0,...0)$.

Keeping these in hand, it is possible to evaluate the classical baryon mass through the soliton mass M with respect to the D8-brane action as $S\left[A^{\mathrm{cl}}\right] = -\int M dt$, which is obtained as follows:

$$M = 8\pi^2\kappa + \frac{8\pi^2\kappa}{\lambda}\left(\frac{\rho^2}{6} + \frac{Z^2}{3} + \frac{1}{320\pi^4 a^2\rho^2}\right), \tag{86}$$

by inserting (82)–(85) into action (78) plus (81). On the other hand, since the low-energy effective theory on the D8-branes can reduce to Skyrme model, we can further employ the idea in the Skyrme model of baryon, which is identified as the excitation of the collective modes, in order to search for the baryon spectrum. The classically effective Lagrangian for baryon describes the dynamics of the collective coordinates $\mathcal{X}^\alpha$ in the moduli space by the one instanton solution, which refers to the world line element with a baryonic potential $U(\mathcal{X}^\alpha)$ in the moduli space:

$$L(\mathcal{X}^\alpha) = \frac{m_X}{2}\mathcal{G}_{\alpha\beta}\dot{\mathcal{X}}^\alpha\dot{\mathcal{X}}^\beta - U(\mathcal{X}^\alpha) + \mathcal{O}\left(\lambda^{-1}\right), \tag{87}$$

where "$\cdot$" refers to the derivative respected to time; the collective coordinates $\mathcal{X}^\alpha$ denote $\{X^M, \rho, y^a\}$; and $W = y^a t^a$ is the $SU\left(N_f\right)$ orientation of the instanton. The potential

$U(\mathcal{X}^\alpha)$ is the classical soliton mass given by $S\left[\mathcal{A}^{\text{cl}}\right] = -\int dt U(\mathcal{X}^\alpha)$. The basic idea to quantize the classical Lagrangian (87) is to slowly move the classical soliton so that the collective coordinates $\mathcal{X}^\alpha$ are promoted to be time-dependent [69]. Approximately, the $SU\left(N_f\right)$ gauge field potential becomes time-dependent by a gauge transformation,

$$\begin{aligned} A_M(t,x) &= W(t)A_M^{\text{cl}}(x,\mathcal{X}^\alpha)W(t)^{-1} - iW(t)\partial_M W(t)^{-1}, \\ A_0(t,x) &= W(t)A_0^{\text{cl}}(x,\mathcal{X}^\alpha)W(t)^{-1} + \Delta A_0, \\ \hat{A}_M(t,x) &= 0,\ \hat{A}_0(t,x) = \hat{A}_0^{\text{cl}}(t,x), \end{aligned} \tag{88}$$

and the associated field strength becomes

$$\begin{aligned} F_{MN} = &\ W(t)F_{MN}^{\text{cl}}W(t)^{-1}, \\ F_{0M} = &\ W(t)\left(\dot{\mathcal{X}}^\alpha \tfrac{\partial}{\partial \mathcal{X}^\alpha} A_M^{\text{cl}} - D_M^{\text{cl}}\Sigma - D_M^{\text{cl}}A_0^{\text{cl}}\right)W(t)^{-1}, \\ \hat{F}_{0M} = &\ \hat{F}_{0M}^{\text{cl}},\ \hat{F}_{MN} = \hat{F}_{MN}^{\text{cl}}, \end{aligned} \tag{89}$$

where

$$\begin{aligned} D_M^{\text{cl}}A_0 &= \partial_M A_0 + i\left[A_M^{\text{cl}}, A_0\right], \\ \Sigma &= W(t)^{-1}\Delta A_0 W(t) - i\dot{W}(t)^{-1}W(t). \end{aligned} \tag{90}$$

ΔA_0 must be determined by its equation of motion:

$$D_M^{\text{cl}}\left(\dot{X}^N \frac{\partial}{\partial X^N} A_M^{\text{cl}} + \dot{\rho}\frac{\partial}{\partial \rho} A_M^{\text{cl}} - D_M^{\text{cl}}\Sigma\right) = 0. \tag{91}$$

While for generic N_f, the exact solution for Σ may be out of reach, the solution with $N_f = 2,3$ is collected, respectively, in [27,28]. Accordingly, the Lagrangian of the collective modes is given by

$$\begin{aligned} S[\mathcal{A}] - S\left[\mathcal{A}^{\text{cl}}\right] &= \int dt[L_{\text{YM}}(\mathcal{X}^\alpha) + L_{\text{CS}}(\mathcal{X}^\alpha)] = \int dt L(\mathcal{X}^\alpha) \\ S_{\text{YM}}[\mathcal{A}] - S_{\text{YM}}\left[\mathcal{A}^{\text{cl}}\right] &= \int dt L_{\text{YM}}(\mathcal{X}^\alpha), \\ S_{\text{CS}}[\mathcal{A}] - S_{\text{CS}}\left[\mathcal{A}^{\text{cl}}\right] &= \int dt L_{\text{CS}}(\mathcal{X}^\alpha), \end{aligned} \tag{92}$$

which leads to

$$\begin{aligned} L(\mathcal{X}^\alpha) &= -M + aN_c \text{Tr}\int d^3x dz \left(\dot{X}^N F_{MN}^{\text{cl}} + \dot{\rho}\tfrac{\partial}{\partial \rho}A_M - \dot{X}^N D_M^{\text{cl}}A_N^{\text{cl}} - D_M^{\text{cl}}\Sigma\right)^2 + \mathcal{O}(\lambda^{-1}) \\ &= -M_0 + \tfrac{m_X}{2}\delta_{ij}\dot{X}^i\dot{X}^j + L_Z + L_\rho + L_{\rho W} + \mathcal{O}(\lambda^{-1}), \end{aligned} \tag{93}$$

where

$$\begin{aligned} L_Z = &\ \tfrac{m_Z}{2}\left(\dot{Z}^2 - \omega_Z^2 Z^2\right), L_\rho = \tfrac{m_\rho}{2}\left(\dot{\rho} - \omega_\rho^2\rho^2\right) - \tfrac{K}{m_\rho \rho^2}, \\ L_{\rho W} = &\ \tfrac{m_\rho \rho^2}{2}\sum_a C_a\left[\text{Tr}\left(-iW^{-1}\dot{W}t^a\right)\right]^2, a = 1,2 \ldots N_f^2 - 1 \end{aligned} \tag{94}$$

and

$$M_0 = 8\pi^2\kappa, m_X = m_Z = \frac{m_\rho}{2} = 8\pi^2\kappa\lambda^{-1}, K = \frac{2}{5}N_c^2, \omega_Z^2 = 4\omega_\rho^2 = \frac{2}{3}. \tag{95}$$

Here, we note that the formulas in the unit of $M_{KK} = 1$, C_a's are constants dependent on the $SU\left(N_f\right)$ instanton, solution and the metric of the moduli space can be further obtained by comparing (93) with (87). For example, we have $C_{1,2,3} = 1$ for $N_f = 2$, and $C_{1,2,3} = 1, C_{4,5,6,7} = 1/2, C_8 = 0$ for $N_f = 3$. Afterwards, the baryon states can be obtained by quantizing the Lagrangian (93), that is, to replace the derivative term by $\dot{X}^\alpha \to -\frac{i}{m_X}\partial_\alpha$ straightforwardly. Hence, the quantized Hamiltonian associated with (93) is collected as follows (we note that for generic N_f, the baryonic Hamiltonian must be supported by additional constraint, according to [70] although it may not change the baryon spectrum):

$$
\begin{aligned}
H = &\ M_0 + H_Z + H_\rho + H_{\rho W}, \\
H_Z = &\ -\tfrac{1}{2m_Z}\partial_Z^2 + \tfrac{1}{2}m_Z\omega_Z^2 Z^2, \\
H_\rho = &\ -\tfrac{1}{2m_\rho}\tfrac{1}{\rho^\eta}\partial_\rho\left(\rho^\eta\partial_\rho\right) + \tfrac{1}{2}m_\rho\omega_\rho^2\rho^2 + \tfrac{K}{m_\rho\rho^2}, \\
H_{\rho W} = &\ \tfrac{m_\rho\rho^2}{2}\sum_a C_a\left[\mathrm{Tr}\left(-iW^{-1}\dot{W}t^a\right)\right]^2 = \tfrac{2}{m_\rho\rho^2}\sum_a C_a\left(J^a\right)^2,
\end{aligned}
\tag{96}
$$

where $\eta = N_f^2 - 1$ and J^a's are the operators of the angular momentum of $SU\left(N_f\right)$. The baryon spectrum can be finally obtained by evaluating the eigenvalues of the Hamiltonian (96), which fortunately takes an analytical formula [27,28].

2.6. Gravitational Wave as Glueball

According to AdS/CFT and gauge–gravity duality [29–32], the glueball operator $\hat{O}$ can be identified as the source of gravitational fluctuation in bulk, since it is included in energy–momentum tensor of Yang–Mills theory in the dual theory as $\hat{O} \sim F_{\mu\nu}F^{\mu\nu} \sim T_{\mu\nu}$ coupling to metric. Thus, due to the confined property of glueball, we can choose the bubble D4-brane background (16) compactified on a circle with gravitational fluctuation in order to investigate glueball in holography.

The dual field to the glueball operator is the gravitational fluctuation coupling the energy–momentum, which therefore refers to the gravitational polarization. By employing the relation of 11d M-theory and 10d type IIA string theory in Section 2.1, it would be convenient to find the gravitational polarization in 11d theory. For example, the lowest exotic scalar glueball with quantum number $J^{CP} = 0^{++}$ corresponds to the exotic polarizations of the bulk gravitational polarization, and its 11d components are given as ($\mu, \nu = 0,1,2,3$):

$$
\begin{aligned}
\delta g_{44} &= -\tfrac{r^2}{L^2}f(r)H_E(r)G_E(x), \\
\delta g_{\mu\nu} &= \tfrac{r^2}{L^2}H_E(r)\left[\tfrac{1}{4}\eta_{\mu\nu} - \left(\tfrac{1}{4} + \tfrac{3r_{KK}^6}{5r^6 - 2r_{KK}^6}\right)\tfrac{\partial_\mu\partial_\nu}{M_E^2}\right]G_E(x), \\
\delta g_{55} &= \tfrac{r^2}{4L^2}H_E(r)G_E(x), \\
\delta g_{rr} &= -\tfrac{L^2}{r^2}\tfrac{1}{f(r)}\tfrac{3r_{KK}^6}{5r^6 - 2r_{KK}^6}H_E(r)G_E(x), \\
\delta g_{r\mu} &= \tfrac{90r^7 r_{KK}^6}{M_E^2 L^2\left(5r^6 - 2r_{KK}^6\right)^2}H_E(r)\partial_\mu G_E(x),
\end{aligned}
\tag{97}
$$

where $H_E(r)$ must be determined by its eigen equation, given as

$$
\frac{1}{r^3}\frac{d}{dr}\left[r\left(r^6 - r_{KK}^6\right)\frac{d}{dr}H_E(r)\right] + \left[\frac{432r^2 r_{KK}^{12}}{\left(5r^6 - 2r_{KK}^6\right)^2} + L^4M_E^2\right]H_E(r) = 0, \tag{98}
$$

and $G_E(x)$ refers to the 4d glueball field. By imposing the metric with gravitational fluctuation (97) as $g_{MN} = g_{MN}^{(0)} + \delta g_{MN}$ and solution of C_3 into 11d SUGRA action (1), we can obtain

$$
S_{\mathrm{SUGRA}}^{\mathrm{11d}} = -\frac{1}{2}\mathcal{C}_E\beta_4\beta_5\int d^4x\left[\left(\partial_\mu G_E\right)^2 + M_E^2G_E^2\right], \tag{99}
$$

representing the standard kinetic action for scalar glueball field G_E, where β_5, $g_{MN}^{(0)}$ refer, respectively, to the size of x^5 and the bubble version of (10). $\mathcal{C}_E$ is a numerical constant, given as

$$
\begin{aligned}
\mathcal{C}_E &= 0.057396\left[H_E(r_{KK})\right]^2\tfrac{r_{KK}^4}{L^3}, \\
\left[H_E(r_{KK})\right]^{-1} &= 0.0069183\lambda^{1/2}N_cM_{KK}.
\end{aligned}
\tag{100}
$$

Hence, the eigenvalue of (98) determines the mass spectrum of exotic scalar glueball. The mass spectrum for various glueballs can be obtained by taking into account different gravitational polarizations, e.g., dilatonic scalar glueball with $J^{CP} = 0^{++}$,

$$\begin{aligned} \delta G_{11,11} &= -3\frac{r^2}{L^2} H_D(r) G_D(x), \\ \delta G_{\mu\nu} &= \frac{r^2}{L^2} H_D(r) \left[\eta^{\mu\nu} - \frac{\partial^\mu \partial^\nu}{M_D^2} \right] G_D(x), \end{aligned} \tag{101}$$

and tensor glueball with $J^{CP} = 2^{++}$,

$$\delta G_{\mu\nu} = -\frac{r^2}{L^2} H_T(r) T_{\mu\nu}(x). \tag{102}$$

The eigen equations for $H_D(r)$ and $H_T(r)$ are given as

$$\frac{1}{r^3}\frac{d}{dr}\left[r\left(r^6 - r_{KK}^6\right)\frac{d}{dr} H_{D,T}(r) \right] + L^4 M_{D,T}^2 H_{D,T}(r) = 0, \tag{103}$$

which determines the mass spectrum of dilatonic scalar and tensor glueball. The mass spectrum of various glueballs are collected in Table 3 for the reader's convenience. The labels S, T, V, N, M, L refer to the solutions for six independent wave equations for various scalar, vector and tensor modes of glueballs.

Table 3. Glueball mass spectrum m_n^2 of AdS_7 in the units of $r_{KK}^2/L^4 = M_{KK}^2/9$ in [32].

Mode J^{PC}	$\mathbf{S_4}$ 0^{++}	$\mathbf{T_4}$ $0^{++}/2^{++}$	$\mathbf{V_4}$ 0^{-+} 1^{+-}	$\mathbf{N_4}$ 1^{--}	$\mathbf{M_4}$ 0^{++}	$\mathbf{L_4}$
$n=0$	7.30835	22.0966	31.9853	53.3758	83.0449	115.002
$n=1$	46.9855	55.5833	72.4793	109.446	143.581	189.632
$n=2$	94.4816	102.452	126.144	177.231	217.397	227.283
$n=3$	154.963	162.699	193.133	257.959	304.531	378.099
$n=4$	228.709	236.328	273.482	351.895	405.011	492.171

This model predicts the properties of glueballs in a very simple and powerful way.

3. Developments and Holographic Approaches to QCD

In this section, we will review some holographic approaches to QCD by using the D4/D8 model and some developments of this model in recent years, which includes the topics of phase transition, heavy flavor, hadron interaction and the theta angle in QCD.

3.1. QCD Deconfinement Transition

While the confinement phase of QCD corresponds to the bubble D4-brane geometry given in (16), it is less clear whether the black D4-brane background (14) corresponds exactly to the deconfinement phase in holography [58,59]. This issue is recognized by investigating the associated Wilson loop in the bubble (16) and black brane backgrounds, (14) respectively. Nonetheless, it would be interesting to compare the deconfinement transition in QCD with the Hawking–Page transition in the D4-brane system through the gauge–gravity duality to find an exact holographic description of the deconfinement transition. To achieve this goal, let us first recall the holographic relation between the partition functions Z of the bulk gravity and its dual field theory,

$$Z = e^{-F} = e^{-S_{\mathrm{SUGRA}}^{ren}}, \tag{104}$$

which implies that the classical (onshell) renormalized SUGRA action S^{ren}_{SUGRA} is equivalent to the free energy F of the dual theory (in the Euclidean version). The classical SUGRA action S^{ren}_{SUGRA} can be collected by

$$S^{ren}_{\mathrm{SUGRA}} = S^{E}_{\mathrm{IIA}} + S_{\mathrm{GH}} + S^{\mathrm{bulk}}_{\mathrm{CT}}, \tag{105}$$

where S^{E}_{IIA} refers to the Euclidean version of the IIA SUGRA action given in (15), and S_{GH} refers to the standard Gibbons–Hawking term given as [71]

$$S_{\mathrm{GH}} = \frac{1}{\kappa_{10}^2} \int_{\partial\mathcal{M}} e^{-2\Phi} \sqrt{h} K, \tag{106}$$

where h_{MN} refers to the metric on the holographic boundary $\partial\mathcal{M}$ with $\partial\mathcal{M} = \{r = \varepsilon\}$, and

$$K = h^{MN} \nabla_M n_N = -\frac{1}{\sqrt{|g|}} \partial_r \left(\frac{\sqrt{|g|}}{\sqrt{g_{rr}}} \right) \Big|_{r=\varepsilon}, \tag{107}$$

is the trace of the extrinsic curvature. $S^{\mathrm{bulk}}_{\mathrm{CT}}$ refers to the counterterm of the bulk fields presented in action (15), given as [72]

$$S^{\mathrm{bulk}}_{\mathrm{CT}} = -\frac{5}{2\kappa_{10}^2} \frac{g_s^{1/3}}{R} \int d^9 x e^{-7\Phi/3} \sqrt{h}. \tag{108}$$

Using (105)–(108), by picking up the bubble (16) and black brane background (14) solutions, respectively, we can obtain the free energy of the dual theory by a simple formula:

$$\begin{aligned} F_{\mathrm{conf.}} &= S^{ren,\mathrm{bub}}_{\mathrm{SUGRA}} = -\frac{2N_c^2 M_{KK}^4 \lambda V_4}{3^7 \pi^2}, \\ F_{\mathrm{deconf.}} &= S^{ren,\mathrm{black}}_{\mathrm{SUGRA}} = -\frac{2^7 N_c^2 T^6 \pi^4 \lambda V_4}{3^7 M_{KK}^2}, \end{aligned} \tag{109}$$

where V_4 refers to the volume of $\mathbb{R}^4$; T is the Hawking temperature in the black D4-brane solution (16). Comparing the free energies given in (109), we obtain the critical temperature with $F_{\mathrm{conf.}} = F_{\mathrm{deconf.}}(T = T_c)$ for the Hawking–Page transition as follows:

$$T_c = \frac{M_{KK}}{2\pi}, \tag{110}$$

which is expected to be the deconfinement transition in QCD in the large N_c limit. While this may be a trivial result for QCD, it is theoretically expected in the gravity side since, the bubble solution (14) is obtained by a double Wick rotation to the black brane solution (16), i.e., (110) means exactly $\beta_4 = \beta_T$. However, this does not mean that the Hawking–Page transition has nothing to do with the QCD deconfinement transition, because the fundamental flavored matter has not been taken into account.

In order to obtain a critical temperature close to the realistic QCD with the D4/D8 model, the flavored matter on the D8-branes must somehow contribute to the free energy. This means that in the gravity side, flavor branes have to back-react to the bulk geometry; thus, they would not be probes. For such a holographic setup, we require N_f/N_c to be fixed in the large N_c limit in order to go beyond the probe approximation for the flavor branes. Moreover, we further need $N_f/N_c \ll 1$, otherwise the dynamics of the dual theory is determined by flavors instead of colors, and in the gravity side, $N_f/N_c \ll 1$ is also necessary, since N_c D4-branes must dominate the bulk geometry, otherwise the holographic duality given in the previous sections would not be valid (see similar setups in [73–75] for the D3/D7 system).

Then, the next step is to confirm the embedding configuration of the D8/$\overline{\mathrm{D8}}$-branes. Since the configuration of the D8/$\overline{\mathrm{D8}}$-branes relates to the chiral symmetry discussed in Sections 2.2 and 2.3, we can identify, respectively, the bubble D4-brane background, where D8/$\overline{\text{D8}}$-branes are located at the antipodal points of x^4 (the left one in Figure 2) to the confined phase with broken chiral symmetry; and the black D4-brane background, where D8/$\overline{\text{D8}}$-branes are parallel (the left one in Figure 3) to the deconfined phase with the restored chiral symmetry. does not exactly distinguish the chiral transition from the deconfinement transition and is not unique, it is the most simple setup to include the elementary features in the QCD deconfinement transition. However, keeping the above requirements in hand, it is not enough to give a holographic setup quantitatively, because when the flavored backreaction is considered, it would be extremely challenging to search for a SUGRA solution technologically with respect to the D-brane configuration in the D4/D8 model as in Table 1. To simplify the calculation and keep the fundamental features of QCD, the authors of [34,35] suggest to consider the case that the D8/$\overline{\text{D8}}$-branes are smeared on the x^4 direction homogeneously so that the harmonic function for the D8-branes is identified uniquely; thus, it is possible to search for a geometric solution in this setup.

Altogether, let us write down the IIA SUGRA action plus the dynamics of N_f D8-branes smeared on x^4 as the total action S,

$$\begin{aligned} S = \; & \tfrac{1}{2\kappa_{10}^2}\int d^{10}x\sqrt{-G}e^{-2\phi}\left[\mathcal{R}^{(10)}+4\partial_\mu\phi\partial\phi\right]-\tfrac{1}{4\kappa_{10}^2}\int d^{10}x\sqrt{-G}|F_4|^2 \\ & -\tfrac{g_sN_fT_{\mathrm{D8}}M_{KK}}{\pi}\int d^{10}x\tfrac{\sqrt{-\det[g+(2\pi\alpha')F]}}{\sqrt{g_{44}}}e^{-\phi}. \end{aligned} \tag{111}$$

To search for an approximate solution under the condition $N_f/N_c \ll 1$, the solution with $N_f = 0$ is therefore the zero-th order solution to the equations of motion from (111), which is nothing but the bubble and black D4-brane solution given in (14) and (16). Then, let us attempt to find a solution of $\mathcal{O}\left(N_f/N_c\right)$ to the bubble D4-brane (16) first. For a homogeneous solution, the ansatz of the metric to solve the action (111) can be chosen as [33–35]

$$\begin{aligned} ds^2 &= e^{2\hat{\lambda}}\left(-dt^2+dx_idx^i\right)+e^{2\tilde{\lambda}}\left(dx^4\right)^2+l_s^2e^{-2\varphi}d\rho^2+l_s^2e^{2\nu}d\Omega_4^2, \\ \varphi &= 2\Phi-4\lambda-\tilde{\lambda}-4\nu, \end{aligned} \tag{112}$$

where Φ refers to the dilaton field; $\hat{\lambda},\tilde{\lambda},\varphi,\nu$ are unknown functions depending on the holographic coordinate ρ only. ρ is the logarithmic coordinate, defined as

$$e^{-3a\rho} = 1-\frac{U_{KK}^3}{U^3}, a = \frac{\sqrt{2}Q_cU_{KK}^3}{3R^3g_s} = \frac{U_{KK}^3}{l_s^3g_s^2}. \tag{113}$$

Impose the ansatz (112) into (111); it reduces to a 1d effective action,

$$\begin{aligned} S &= \mathcal{V}\int d\rho\left[-4\dot{\hat{\lambda}}^2-\dot{\tilde{\lambda}}^2-4\dot{\nu}^2+\dot{\varphi}^2+V\right], \\ V &= 12e^{-2\nu-2\varphi}-Q_c^2e^{4\hat{\lambda}+\tilde{\lambda}-4\nu-4\varphi}-Q_fe^{2\hat{\lambda}-\frac{\tilde{\lambda}}{2}+2\nu-\frac{3}{2}\varphi}, \end{aligned} \tag{114}$$

which has to be supported by the zero-energy constraint (dot refers to the derivative with respect to ρ)

$$-4\dot{\hat{\lambda}}^2-\dot{\tilde{\lambda}}^2-4\dot{\nu}^2+\dot{\varphi}^2-V = 0, \tag{115}$$

with

$$Q_c = \frac{3\pi N_c}{\sqrt{2}} = \frac{3}{\sqrt{2g_s}}\frac{R^3}{l_s^3}, Q_f = \frac{2\kappa_{10}^2N_fg_sT_{\mathrm{D8}}M_{KK}l_s^2}{\pi}, \mathcal{V} = \frac{1}{2\kappa_{10}^2}V_3\Omega_4\beta_T\frac{2\pi}{M_{KK}}l_s^3. \tag{116}$$

Here, β_T is the size of x^0, representing the temperature in the dual theory $\beta_T = 1/T$, and the only nonzero component of the gauge field potential on the D8-branes is a constant

A_0, representing the chemical potential in the dual theory. Next, we expand all the relevant functions $\hat{\lambda}, \tilde{\lambda}, \varphi, \nu$ up to N_f/N_c, as follows:

$$\Psi = \Psi_0 + \epsilon_f \Psi_1 + \mathcal{O}\left(\epsilon_f^2\right), \tag{117}$$

where

$$\epsilon_f = \frac{R^{3/2} u_0^{1/2} g_s}{l_s} Q_f = \frac{1}{12\pi^3} \lambda^2 \frac{N_f}{N_c} \ll 1. \tag{118}$$

So, the zero-th order solution of $\hat{\lambda}, \tilde{\lambda}, \varphi, \nu$ reads by comparing the metric ansatz (112) with the bubble D4-brane solution (16) as follows:

$$\begin{aligned} \hat{\lambda}_0 &= f_0 + \tfrac{3}{4} \log \tfrac{U_{KK}}{R}, \\ \tilde{\lambda}_0 &= f_0 - \tfrac{3}{2} a\rho + \tfrac{3}{4} \log \tfrac{U_{KK}}{R}, \\ \Phi_0 &= f_0 + \tfrac{3}{4} \log \tfrac{U_{KK}}{R} + \log g_s, \\ \nu_0 &= \tfrac{1}{3} f_0 + \tfrac{1}{4} \log \tfrac{U_{KK}}{R} + \log \tfrac{R}{l_s}, \\ f_0 &= -\tfrac{1}{4} \log\left(1 - e^{-3a\rho}\right), \end{aligned} \tag{119}$$

Putting (117)–(119) back into the equation of motion varied from action (114), we can obtain a series of equations for $\hat{\lambda}_1, \tilde{\lambda}_1, \varphi_1, \nu_1$:

$$\begin{aligned} \frac{\ddot{\hat{\lambda}}_1}{a^2} - \frac{9}{2} \frac{e^{-3a\rho}}{\left(1-e^{-3a\rho}\right)^2} \left(4\hat{\lambda}_1 + \tilde{\lambda}_1 - \Phi_1\right) &= \frac{1}{4} \frac{e^{-\frac{3}{2}a\rho}}{\left(1-e^{-3a\rho}\right)^{13/6}}, \\ \frac{\ddot{\tilde{\lambda}}_1}{a^2} - \frac{9}{2} \frac{e^{-3a\rho}}{\left(1-e^{-3a\rho}\right)^2} \left(4\hat{\lambda}_1 + \tilde{\lambda}_1 - \Phi_1\right) &= -\frac{1}{4} \frac{e^{-\frac{3}{2}a\rho}}{\left(1-e^{-3a\rho}\right)^{13/6}}, \\ \frac{\ddot{\Phi}_1}{a^2} - \frac{9}{2} \frac{e^{-3a\rho}}{\left(1-e^{-3a\rho}\right)^2} \left(4\hat{\lambda}_1 + \tilde{\lambda}_1 - \Phi_1\right) &= \frac{5}{4} \frac{e^{-\frac{3}{2}a\rho}}{\left(1-e^{-3a\rho}\right)^{13/6}}, \\ \frac{\ddot{\nu}_1}{a^2} - \frac{3}{2} \frac{e^{-3a\rho}}{\left(1-e^{-3a\rho}\right)^2} \left(4\hat{\lambda}_1 + \tilde{\lambda}_1 - 5\Phi_1 + 12\nu_1\right) &= \frac{1}{4} \frac{e^{-\frac{3}{2}a\rho}}{\left(1-e^{-3a\rho}\right)^{13/6}}, \end{aligned} \tag{120}$$

which can be solved analytically by

$$\begin{aligned} \hat{\lambda}_1 &= \tfrac{3}{8} f + y - \tfrac{1}{4}(A_2 - A_1) - \tfrac{1}{4}(B_2 - B_1) a\rho, \\ \tilde{\lambda}_1 &= -\tfrac{1}{8} f + y - \tfrac{1}{4}(A_2 + B_2 a\rho) - \tfrac{3}{4}(A_1 + B_1 a\rho), \\ \Phi_1 &= \tfrac{11}{8} f + y + \tfrac{1}{4}(A_1 + B_1 a\rho) - \tfrac{5}{4}(A_2 + B_2 a\rho), \\ \nu_1 &= \tfrac{11}{24} f + q, \end{aligned} \tag{121}$$

with hypergeometrical functions

$$\begin{aligned} f =& \ \tfrac{4}{9} e^{-3a\rho/2} \, {}_3F_2\left(\tfrac{1}{2}, \tfrac{1}{2}, \tfrac{13}{6}; \tfrac{3}{2}, \tfrac{3}{2}; e^{-3a\rho}\right), \\ y =& \ C_2 - \coth\left(\tfrac{3a\rho}{2}\right) \left[C_1 + C_2\left(\tfrac{3}{2} a\rho + 1\right)\right] + z, \\ q =& \ \tfrac{1}{12}\left[A_1 - 5A_2 + a\rho(B_1 - 5B_2)\right] + \tfrac{5}{3} z - \coth\left(\tfrac{3a\rho}{2}\right)\left[M_1 + M_2(3a\rho + 2)\right] + 2M_2, \\ z =& \ -\frac{e^{-9a\rho/2}\left(e^{-3a\rho}+1\right)\left[9e^{3a\rho} \, {}_3F_2\left(\tfrac{1}{2}, \tfrac{1}{2}, \tfrac{19}{6}; \tfrac{3}{2}, \tfrac{3}{2}; e^{-3a\rho}\right) + {}_3F_2\left(\tfrac{3}{2}, \tfrac{3}{2}, \tfrac{19}{6}; \tfrac{5}{2}, \tfrac{5}{2}; e^{-3a\rho}\right)\right]}{162\left(1-e^{-3a\rho}\right)} \\ & -\frac{8e^{-3a\rho/2}\left(10e^{-3a\rho}+3\right)}{819\left(1-e^{-3a\rho}\right)} \, {}_2F_1\left(\tfrac{1}{6}, \tfrac{1}{2}; \tfrac{3}{2}; e^{-3a\rho}\right) + -\frac{e^{-15a\rho/2}\left(38e^{3a\rho} + 8e^{6a\rho} - 40\right)}{273\left(1-e^{-3a\rho}\right)^{13/6}}, \end{aligned} \tag{122}$$

where $A_{1,2}, B_{1,2}, C_{1,2}, M_{1,2}$ are integration constants. The integration constants can be determined by analyzing the asymptotics and using the zero-energy constraint (115), which leads to

$$\begin{aligned} A_2 &= -2A_1, A_1 = \frac{81\sqrt{3}\pi^2\left(-9+\sqrt{3}\pi - 12\log 2 + 9\log 3\right)}{43120(2)^{2/3}\Gamma(-14/3)\Gamma(-2/3)^2}, \\ k &= C_1 + C_2 = \frac{\pi^{3/2}\left(3+\sqrt{3}\pi - 12\log 2 + 9\log 3\right)}{78\Gamma(-2/3)\Gamma(1/6)}, \\ \tfrac{5k}{3} &= M_1 + M_2, \end{aligned} \tag{123}$$

while the other constants must be confirmed by imposing additional physical conditions. Nevertheless, one may find that the phase transition depends only on the integration constants given in (123).

Following the same step, it is also possible to obtain a solution of order N_f/N_c to the black D4-brane solution by using the metric ansatz:

$$\begin{aligned} ds^2 &= -e^{2\tilde{\lambda}}dt^2 + e^{2\hat{\lambda}}dx_i dx^i + e^{2\lambda_s}\left(dx^4\right)^2 + l_s^2 e^{-2\varphi}d\rho^2 + l_s^2 e^{2\nu}d\Omega_4^2, \\ \varphi &= 2\Phi - 3\hat{\lambda} - \tilde{\lambda} - \lambda_s - 4\nu, \end{aligned} \tag{124}$$

with a nonzero dynamical chemical potential:

$$2\pi\alpha' A = A_t dt. \tag{125}$$

We note that U_{KK} is replaced by U_H in the black brane case. Putting (124) and (125) into action (111), it leads to a 1d action:

$$\begin{aligned} S &= \mathcal{V}\int d\rho\left[-3\dot{\hat{\lambda}}^2 - \dot{\tilde{\lambda}}^2 - \dot{\lambda}_s^2 - 4\dot{\nu}^2 + \dot{\varphi}^2 + V\right], \\ V &= 12e^{-2\nu-2\varphi} - Q_c^2 e^{3\hat{\lambda}+\tilde{\lambda}+\lambda_s-4\nu-4\varphi} - Q_f e^{\frac{3}{2}\hat{\lambda}-\frac{1}{2}\lambda_s+\frac{\tilde{\lambda}}{2}+2\nu-\frac{3}{2}\varphi}\sqrt{1-\frac{1}{l_s^2}e^{-2\tilde{\lambda}+2\varphi}\dot{A}_t^2}. \end{aligned} \tag{126}$$

Taking into account the near-horizon geometry, the DBI action presented in (126) can be expanded with respect to small gauge field potential. Then, keeping the quadratic action for A_t, we can obtain an analytical leading-order solution by the equations of motion derived from (126):

$$\begin{aligned} A_t &= \frac{2}{3}qU_H\left(1-\sqrt{1-e^{-3a\rho}}\right), q = \frac{g_s l_s^4}{R^{3/2}U_H^{5/2}}n \\ \hat{\lambda}_1 &= \frac{f}{28} - \frac{3}{16}q^2 g + y - \frac{1}{4}(a_2 - a_1 - a_3) - \frac{1}{4}(b_2 - b_1 - b_3)a\rho, \\ \lambda_{s1} &= \hat{\lambda}_1 - \frac{f}{21} + \frac{q}{4}g - a_1 - b_1 a\rho, \\ \tilde{\lambda}_1 &= \hat{\lambda}_1 + \frac{q^2}{2}g - a_3 - b_3 a\rho, \\ \Phi_1 &= \hat{\lambda}_1 + \frac{2}{21}f - a_2 - b_2 a\rho, \\ \nu_1 &= \frac{11}{252}f - \frac{q^2}{16}g + w, \end{aligned} \tag{127}$$

with

$$\begin{aligned} f =& \frac{6}{\left(1-e^{-3a\rho}\right)^{1/6}} + \sqrt{3}\tan^{-1}\left[\frac{2\left(1-e^{-3a\rho}\right)^{1/6}-1}{\sqrt{3}}\right] + \sqrt{3}\tan^{-1}\left[\frac{2\left(1-e^{-3a\rho}\right)^{1/6}+1}{\sqrt{3}}\right] \\ & -2\tanh^{-1}\left[\left(1-e^{-3a\rho}\right)^{1/6}\right] - \coth^{-1}\left[\left(1-e^{-3a\rho}\right)^{1/6} + \frac{1}{\left(1-e^{-3a\rho}\right)^{1/6}}\right], \\ g =& \frac{4}{9}\log\left(e^{-3a\rho/2}\sqrt{e^{3a\rho}-1}+1\right) - \frac{4}{9}e^{-3a\rho/2}\sqrt{e^{3a\rho}-1}, \\ y =& c_2 - \left[c_1 + \left(1+\frac{3}{2}a\rho\right)c_2\right]\coth\left(\frac{3a\rho}{2}\right) + q^2 j + z, \\ w =& 2m_2 - \left[m_1 + (2+3r)m_2\right]\coth\left(\frac{3a\rho}{2}\right) + \frac{1}{12}(a_1 - 5a_2 + a_3 + b_1 a\rho - 5b_2 a\rho + b_3 a\rho) \\ & +\frac{5}{3}z - q^2 j, \\ j =& \frac{1}{72}\left[4\sqrt{1-e^{-3a\rho}} + \left(-9a\rho + 6\sqrt{1-e^{-3a\rho}} - 6\log\left(\sqrt{1-e^{-3a\rho}}+1\right)\right)\coth\left(\frac{3a\rho}{2}\right)\right], \\ z =& \frac{3e^{3a\rho}\left(1-e^{-3a\rho}\right)^{5/6} - \frac{\sqrt{3}}{2}\left(e^{3a\rho}+1\right)\left[\tan^{-1}\left(\frac{2\sqrt[6]{1-e^{-3a\rho}}-1}{\sqrt{3}}\right) + \tan^{-1}\left(\frac{2\sqrt[6]{1-e^{-3a\rho}}+1}{\sqrt{3}}\right)\right]}{546\left(e^{3a\rho}-1\right)} \\ & +\frac{1}{2}\left(e^{3a\rho}+1\right)\frac{2\tan^{-1}\left(\frac{2\sqrt[6]{1-e^{-3a\rho}}-1}{\sqrt{3}}\right) + \coth^{-1}\left[\left(1-e^{-3a\rho}\right)^{1/6} + \frac{1}{\left(1-e^{-3a\rho}\right)^{1/6}}\right]}{546\left(e^{3a\rho}-1\right)}, \end{aligned} \tag{128}$$

where $a_{1,2,3}, b_{1,2,3}, c_{1,2}, m_{1,2}$ are integration constants and n refers to the $U(1)$ charge density. The zero-energy constraint is given by

$$-3\dot{\hat{\lambda}}^2 - \dot{\lambda}_s^2 - \dot{\tilde{\lambda}}^2 - 4\dot{\nu}^2 + \dot{\varphi}^2 + \frac{Q_f}{2l_s} e^{\frac{3}{2}\hat{\lambda} - \frac{1}{2}\lambda_s + \frac{3\tilde{\lambda}}{2} + 2\nu + \frac{1}{2}\varphi} \dot{A}_t^2 - \mathcal{P} = 0, \tag{129}$$

with

$$\mathcal{P} = 12e^{-2\nu - 2\varphi} - Q_c^2 e^{3\hat{\lambda} + \tilde{\lambda} + \lambda_s - 4\nu - 4\varphi} - Q_f e^{\frac{3}{2}\hat{\lambda} - \frac{1}{2}\lambda_s + \frac{\tilde{\lambda}}{2} + 2\nu - \frac{3}{2}\varphi}. \tag{130}$$

Now. it is possible to obtain the free energy of the dual theory involving the flavored matters by imposing the above leading-order solutions into the action given in (111) after holographic renormalization. Before this, we need to add an additional holographic counterterm to (105) in order to cancel the divergence in the DBI action presented in (111), which turned out to be [34,76–78]

$$S_{\mathrm{CT}}^{\mathrm{D8}} = \frac{Q_f}{\kappa_{10}^2 l_s^2} \int_{\partial\mathcal{M}} d^9x \frac{\sqrt{h}}{\sqrt{h_{44}}} \left[\frac{R}{g_s^{1/3}} \chi_1 e^{-2\Phi/3} - \frac{2R^2}{g_s^{2/3}} \chi_2 e^{-\Phi/3} \left(K - \frac{8}{3} \boldsymbol{n} \cdot \nabla\Phi - \boldsymbol{n} \cdot \frac{\nabla\left(\sqrt{g_{44}}\right)}{\sqrt{g_{44}}} \right) \right]. \tag{131}$$

Here, $\boldsymbol{n}$ refers to the normal vector of $\partial\mathcal{M}$, and $\chi_{1,2}$ are renormalized constants. For example, with the back reaction from D8-branes to the bubble background, it leads to

$$\chi_1 = -\frac{631}{5005}, \chi_2 = -\frac{2}{2145}. \tag{132}$$

For the black brane background, it leads to

$$\chi_1 = -\frac{607}{5005}, \chi_2 = -\frac{4}{15015}. \tag{133}$$

Hence, we finally obtained the renormalized SUGRA action,

$$F = S_{\mathrm{SUGRA}}^{ren} = S_{\mathrm{IIA}}^{E} + S_{\mathrm{GH}} + S_{\mathrm{CT}}^{\mathrm{bulk}} + S_{\mathrm{CT}}^{\mathrm{D8}}, \tag{134}$$

with suitable choice of $\chi_{1,2}$. Respectively, the confined and deconfined free energy with flavors can be computed straightforwardly by plugging the solutions of order N_f/N_c into (134)

$$\begin{aligned} F_{\mathrm{conf.}} &= -\frac{2N_c^2 M_{KK}^4 \lambda V_4}{3^7\pi^2} \left[1 - \frac{48}{7}\epsilon_f \frac{\pi^{3/2}}{\Gamma(-2/3)\Gamma(1/6)} \right], \\ F_{\mathrm{deconf.}} &= -\frac{2^7 N_c^2 T^6 \pi^4 \lambda V_4}{3^7 M_{KK}^2} \left[1 + \frac{4}{7}\epsilon_{fT}\left(1 + \frac{7}{6}q^2\right) \right], \end{aligned} \tag{135}$$

where

$$\epsilon_{fT} = \frac{R^{3/2} U_H^{1/2} g_s Q_f}{l_s^2} = \frac{\lambda^2}{12\pi^3} \frac{2\pi T}{M_{KK}} \frac{N_f}{N_c} \ll 1, \tag{136}$$

and we use the choice of the relevant constants given in (123). Therefore, comparing the free energy given in (135), we can obtain the critical temperature with flavors as follows:

$$\frac{2\pi T_c}{M_{KK}} = 1 - \frac{1}{126\pi^3} \lambda^2 \frac{N_f}{N_c} \left[1 + \frac{12\pi^{3/2}}{\Gamma(-2/3)\Gamma(1/6)} \right] - \frac{27}{16\pi} \frac{N_f}{N_c} \frac{\mu^2}{M_{KK}^2}, \tag{137}$$

where μ is the chemical potential in the dual theory given by $A_t\big|_{U\to\infty} = \mu$. The behavior of the Hawking–Page transition given in (137) agrees qualitatively with the QCD deconfinement transition [79–82].

Moreover, when the backreaction to the bulk geometry of the flavor branes is picked up, it is also possible to evaluate QCD deconfinement transition under an external magnetic field, because extremely strong magnetic field may also give rise to deconfinement transition in QCD [83–86]. The setup mostly follows the same discussion given above, while we need to turn on a constant magnetic field in the DBI action is presented in (111), as the only nonzero component of the gauge field strength. Then, we can derive the effective 1d action by using the metric ansatz (112) and (124) with respect to the bubble and black D4-brane background. Fortunately, it is possible to find an analytical solution, which leads to critical temperature T_c as

$$\frac{2\pi T_c}{M_{KK}} = 1 + \frac{N_f}{N_c}\left(X\lambda^2 + \frac{B^2}{M_{KK}^4}Y\right), \tag{138}$$

by comparing free energy in the same way. Here, B refers to the external magnetic field, and X, Y are numerical numbers. For the probe approximation limit of the D8-brane, X, Y are calculated as

$$\begin{aligned} X &= -\frac{1}{126\pi^3}\left[1 - \frac{8\pi^{3/2}}{3\Gamma(1/6)\Gamma(4/3)}\right] \simeq 5\times 10^{-4}, \\ Y &= -\frac{81}{16\pi}\left[1 - \frac{2\pi^{3/2}}{3\Gamma(1/6)\Gamma(4/3)}\right] \simeq -0.408. \end{aligned} \tag{139}$$

By considering the backreaction of the D8-branes, X, Y are calculated as

$$X \simeq 5\times 10^{-4}, Y \simeq -2.44. \tag{140}$$

The behavior of the critical temperature illustrated in (138) also coincides qualitatively with the QCD deconfinement transition under external magnetic field predicted by lattice QCD [83]. We plot out the behavior of the critical temperature given in (137) and (138) in Figure 5. In this sense, we could conclude, at least, that investigating the Hawking–Page transition in the D4/D8 model is very suggestive to study the QCD deconfinement transition in holography, which also partly covers the discussion in some bottom-up approaches [87,88].

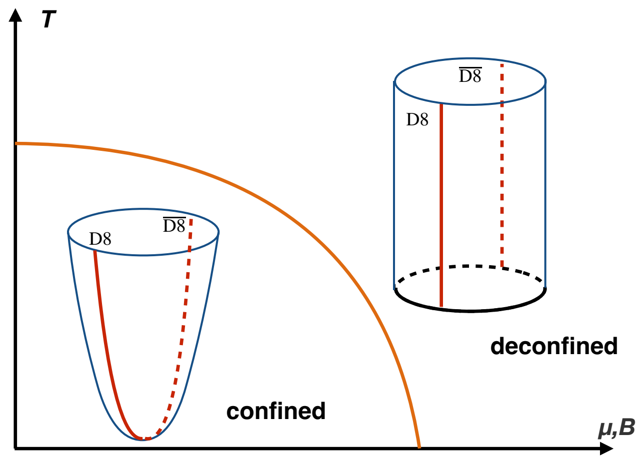

Figure 5. The critical temperature of Hawking–Page transition as the temperature of QCD deconfinement transition in the D4/D8 model with chemical potential μ or magnetic field B.

3.2. Phase Diagram with Chiral Transition

As we have reviewed the deconfinement transition in the D4/D8 model, which can not be distinguished from the chiral transition, let us focus on the chiral transition in the D4/D8 model, since QCD has various phases with chiral symmetry.

Recalling the relation of D8/$\overline{\text{D8}}$-brane configuration and chiral symmetry, the chiral transition is identified as the transition from connected to disconnected configuration of the D8/$\overline{\text{D8}}$-branes. Hence, we need to choose the black D4-brane background in order to include both the connected and disconnected D8/$\overline{\text{D8}}$-brane configurations. The main idea for evaluating the phase transition follows Section 3.1, which is to compute the free energy in holography. As we will work with respect to the black D4-brane background only, the contribution from the bulk geometry would be irrelevant, because the difference of the free energy determines the phase transition. Keeping this in mind, we can quickly write down the D8-brane action for mesonic (broken chiral symmetry) and quark matter phases (restored chiral symmetry) with a $U(1)$ chemical potential $\hat{A}_0$, which corresponds to the connected and disconnected D8-brane configuration, respectively, in Figure 3 as follows (we note that in this setup, the Chern–Simons action vanishes):

$$S_{\mathrm{DBI}}^{\mathrm{D8}} = \mathcal{N}\frac{V_3}{T}\int_{u_0}^{\infty} du u^{5/2}\sqrt{1+u^3 f_T\left(x_4'\right)^2 - \hat{a}_0'^2}, \tag{141}$$

where the variables in (141) are dimensionless, as follows:

$$x_4 = x^4 M_{KK}, u = \frac{U}{R}\frac{1}{\left(M_{KK}R\right)^2}, \hat{a}_0 = \hat{A}_0\frac{4\pi}{\lambda M_{KK}}, \mathcal{N} = 2T_{\mathrm{D8}}\Omega_4 R^5 \left(M_{KK}R\right)^7. \tag{142}$$

The equation of motion can be obtained by varying (141) with respect to x_4 and $\hat{a}_0$, which are

$$\begin{aligned} \frac{u^{5/2}\hat{a}_0'}{\sqrt{1+u^3 f_T x_4'^2 - \hat{a}_0'^2}} &= n_I, \\ \frac{u^{11/2} f_T x_4'}{\sqrt{1+u^3 f_T x_4'^2 - \hat{a}_0'^2}} &= f_T^{1/2}(u_0) u_0^4, \end{aligned} \tag{143}$$

where "$\prime$" refers to the derivative with respect to u. The constant n_I corresponds to the $U(1)$ charge density, which is therefore the baryon number in this setup. In the mesonic phase, the baryon number is zero, i.e., $n_I = 0$, and the equations of motion in (143) can be solved by the following boundary condition, according to the connected configuration in Figure 3:

$$\begin{aligned} \hat{a}_0'(u_0) &= 0,\ \hat{a}_0(\infty) = \mu, \\ x_4'(u_0) &= \infty,\ \tfrac{l}{2} = \textstyle\int_{u_0}^{\infty} du x_4', \end{aligned} \tag{144}$$

where constant μ refers to the chemical potential in the dual theory; constant l refers to the separation of the D8/$\overline{\mathrm{D8}}$-branes at boundary $u \to \infty$. Thus, the solution is

$$\hat{a}_0 = \mu, x_4' = \frac{f_T^{1/2}(u_0)u_0^4}{f_T^{1/2}(u)u^{3/2}\sqrt{u^8 f_T(u) - u_0^8 f_T(u_0)}}. \tag{145}$$

Putting the solution (145) back into action (141), we can obtain the free energy as follows:

$$F_{\mathrm{mesonic}} = \mathcal{N}\int_{u_0}^{\infty} du u^{5/2}\frac{u^4 f_T^{1/2}(u)}{\sqrt{u^8 f_T(u) - u_0^8 f_T(u_0)}}. \tag{146}$$

For the quark matter phase, the boundary condition reads from the disconnected configuration in Figure 3 as

$$\hat{a}_0(u_H) = 0, \hat{a}_0(\infty) = \mu, x_4' = 0, \tag{147}$$

which leads to a solution with the hypergeometrical functions

$$\hat{a}_0(u) = \mu - \frac{n_I^{2/5}\Gamma(3/10)\Gamma(6/5)}{\sqrt{\pi}} + u\,{}_2F_1\left(\frac{1}{5},\frac{1}{2},\frac{6}{5},-\frac{u^5}{n_I^2}\right). \tag{148}$$

Therefore, the free energy is computed as follows:

$$F_{\mathrm{quarkmatter}} = \mathcal{N}\int_{u_H}^{\infty} du \frac{u^5}{\sqrt{u^5 + n_I^5}}. \tag{149}$$

We note that the condition $\hat{a}_0(u_H) = 0$ implies that n_I is a function of μ:

$$0 = \mu - \frac{n_I^{2/5}\Gamma(3/10)\Gamma(6/5)}{\sqrt{\pi}} + u_H\, {}_2F_1\left(\frac{1}{5}, \frac{1}{2}, \frac{6}{5}, -\frac{u_H^5}{n_I^2}\right). \tag{150}$$

Then, the phase diagram can be obtained by comparing the free energies given in (146) and (150) with constraint (149). Notice that while the free energies given in (146) and (150) are divergent, their difference, which determines the phase diagram, remains finite. Thus, it is not necessary to perform holographic renormalization in this case.

For a more ambitious approach, let us include the baryonic phase in the black D4-brane background, that is, to take into account the configuration (c) in Figure 4, which has broken chiral symmetry with baryon vertex. Since baryon vertex is identified as D4′-brane, described equivalently by instantons on the D8-branes, we employ the BPST instanton solution given in (83) to represent baryon on the flavor brane. For multiple baryons, we can summarize the instanton field strength as what we have discussed in Section 2.5; in this sense, baryons are treated as instanton gas on the flavor brane. On the other hand, as the instanton size takes order of $\lambda^{-1/2}$ and the DBI action (20) does not define how to treat it with non-Abelian gauge field (the symmetrized trace in DBI action is usually used for all terms of $\mathcal{O}(F^4)$ and higher; however, it is known to be incomplete, starting from $\mathcal{O}(F^6)$ [89]), we may generalize the DBI action by taking all orders of gauge field strength into non-Abelian case through the identity of Abelian gauge field strength $\hat{F}$ as

$$\begin{aligned}\sqrt{\det(g + 2\pi\alpha'\hat{F})} = \; & U^4\left(\frac{R}{U}\right)^{3/4}\Big\{(2\pi\alpha')^2 f_T \hat{F}_{iU}^2 + \left(1 + u^3 f_T x_4'^2 - \hat{a}_0'^2\right)\left[1 + \left(\frac{R}{U}\right)^3 \frac{(2\pi\alpha')^2}{2}\hat{F}_{ij}^2\right] \\ & + \left(\frac{R}{U}\right)^3 \frac{(2\pi\alpha')^4 f_T\left(\hat{F}_{ij}\hat{F}_{kU}\epsilon_{ijk}\right)^2}{4}\Big\}^{1/2}.\end{aligned} \tag{151}$$

For non-Abelian generalization, we follow [90] to replace the quadratic terms of $\hat{F}$ by its non-Abelian version F, then take trace of each term separately, as follows:

$$\hat{F}_{iU}^2 \to \mathrm{Tr}F_{iU}^2, \hat{F}_{ij}^2 \to \mathrm{Tr}F_{ij}^2, \hat{F}_{ij}\hat{F}_{kU} \to \mathrm{Tr}F_{ij}F_{kU}. \tag{152}$$

Afterwards, we impose the BPST instanton solution (83) with multiple numbers n_I to F in order to represent baryons (Refs. [27,28] illustrate that in the case of $N_f = 2$, the non-Abelian part of A_0 presented in (85) vanishes. We do not attempt to consider baryons with $N_f > 2$ in this section.). Altogether, we reach a generalized version of action for baryonic phase,

$$F_{\text{baryonic}} = S^{\text{D8}} = \mathcal{N}\frac{V_3}{T}\int_{u_c}^{\infty}\left[\sqrt{\left(1 + g_1 + u^3 f_T x_4'^2 - \hat{a}_0'^2\right)(1 + g_2)} - n_I\hat{a}_0(u)q(u)\right], \tag{153}$$

where

$$\begin{aligned} g_1(u) &= \frac{f_T(u)u^{1/2}}{3u_c^2\sqrt{f_c(u)}} n_I q(u), f_c(u) = 1 - \frac{u_c^3}{u^3}, \\ g_2(u) &= \frac{u_c^2\sqrt{f_c(u)}}{3u^{7/2}} n_I q(u), q(Z) = \frac{3\rho^4}{4(Z^2+\rho^2)^{5/2}}. \end{aligned} \tag{154}$$

We note that the last term in (153) is the Chern–Simons action and $q(Z)$ is the average instanton field strength defined by the summary of the BPST instanton (83), as [91]

$$\frac{1}{V_3}\sum_{n=1}^{N_I}\int d^3X \frac{4(\rho/\gamma)^4}{\left[\left(\vec{X} - \vec{X}_{0n}\right)^2 + (Z/\gamma)^2 + (\rho/\gamma)^2\right]^4} = \frac{2}{3}\pi^2\gamma q(Z) n_I, \tag{155}$$

with the normalization condition

$$\int_{-\infty}^{+\infty} q(Z)dZ = 1. \tag{156}$$

$\vec{X}_{0n}$ refers to the center of the n-th instanton. Z is the Cartesian coordinate, in the case in Figure 4c, it is defined as

$$U^3 = U_c^3 + U_c Z^2, \tag{157}$$

where we use U_c to denote the connected position of D8/$\overline{\text{D8}}$-branes with instantons to distinguish it from U_0, in which instantons are absent. N_I is the instanton number, which relates to its number density n_I, as $n_I = N_I 96\pi^4/\left(\lambda^2 M_{KK}^3\right)$. With the boundary condition

$$\frac{l}{2} = \int_{u_c}^{\infty} du x_4', \hat{a}_0(\infty) = \mu, \tag{158}$$

the equations of motion obtained by varying (153) are

$$\begin{aligned} \frac{u^{5/2}\hat{a}_0'\sqrt{1+g_2}}{\sqrt{1+g_1+u^3 f_T x_4'^2-\hat{a}_0'^2}} &= n_I Q \\ \frac{u^{11/2} f_T x_4'\sqrt{1+g_2}}{\sqrt{1+g_1+u^3 f_T x_4'^2-\hat{a}_0'^2}} &= k, \end{aligned} \tag{159}$$

where k is an integration constant to be determined, and

$$Q(u) = \int_{u_c}^{u} q(v)dv = \frac{u^{3/2}\sqrt{f_c}}{2}\frac{3\rho^2 u_c + 2\left(u^3 - u_c^3\right)}{\left(u^3 - u_c^3 + \rho^2 u_c\right)^{3/2}}, \tag{160}$$

can be solved as

$$\begin{aligned} \hat{a}_0'^2 &= \frac{(n_I Q)^2}{u^5}\frac{1+g_1}{1+g_2-\frac{k^2}{u^8 f_T}+\frac{(n_I Q)^2}{u^5}}, \\ x_4'^2 &= \frac{k^2}{u^{11} f_T^2}\frac{1+g_1}{1+g_2-\frac{k^2}{u^8 f_T}+\frac{(n_I Q)^2}{u^5}}. \end{aligned} \tag{161}$$

Plugging solution (161) back into (153), we can obtain the free energy of the baryonic phase. In order to obtain the phase transition, we need to further minimize the free energy given in (153) with respect to n_I, ρ, u_c as the parameters, which leads to three constraints:

$$\begin{aligned} 0 &= \int_{u_c}^{\infty}\left[\frac{u^{5/2}}{2}\left(\frac{\partial g_1}{\partial n_I}\zeta^{-1} + \frac{\partial g_2}{\partial n_I}\zeta\right) + \hat{a}_0' Q\right] - \mu, \\ 0 &= \int_{u_c}^{\infty}\left[\frac{u^{5/2}}{2}\left(\frac{\partial g_1}{\partial \rho}\zeta^{-1} + \frac{\partial g_2}{\partial \rho}\zeta\right) + n_I \hat{a}_0' \frac{\partial Q}{\partial \rho}\right], \\ u_c^{5/2}\sqrt{\left[1+g_1(u_c)\right]\left[1+g_2(u_c) - \frac{k^2}{u_c^8 f_T(u_c)}\right]} &= \int_{u_c}^{\infty}\left[\frac{u^{5/2}}{2}\left(\frac{\partial g_1}{\partial u_c}\zeta^{-1} + \frac{\partial g_2}{\partial u_c}\zeta\right) + n_I \hat{a}_0' \frac{\partial Q}{\partial u_c}\right], \end{aligned} \tag{162}$$

where

$$\zeta = \frac{\sqrt{1+g_1}}{\sqrt{1+g_2 - \frac{k^2}{u^8 f_T} + \frac{(n_I Q)^2}{u^5}}}. \tag{163}$$

With all of the above in hand, we can numerically obtain a holographic diagram including mesonic, baryonic and quark matter phases of QCD by comparing the associated free energies given in (146), (149) and (153). The resultant phase diagram is given in Figure 6.

We can see that the holographic diagram includes all the elementary phases in realistic QCD, although the confined geometry is not included in the current discussion.

We note that it is very difficult to work out a reasonable model describing QCD matter over a very wide density regime with traditional models or theories of QCD. For example, the quark–meson model (e.g., [92,93]) and the Nambu–Jona–Lasinio (NJL) model [94–98] are very useful to obtain some insight into the chiral and deconfinement phase transitions and quark matter phases; however, nuclear matter is usually not included in these models. In addition, nucleon–meson models, e.g., [99–102] are based on the properties of nuclear matter, and may be able to describe moderately dense nuclear matter realistically, but they give a poor description of quark matter with restored chiral symmetry. In this sense, this holographic model provides a very powerful way to study QCD phase diagrams in a very wide density regime based on string theory.

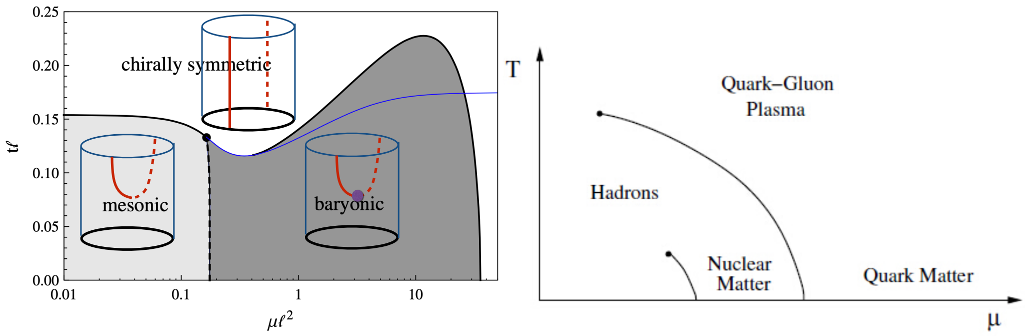

Figure 6. Holographic QCD phase diagram vs. realistic QCD phase diagram in the $T-\mu$ plane.

3.3. Higgs Mechanism and Heavy–Light Meson Field

One of the interesting developments of the D4/D8 model is including heavy flavor by using the Higgs mechanism in D-brane system. Recall that the fundamental quarks in the D4/D8 model are identified to be the 4–8 and 4–$\overline{8}$ strings; since N_c D4-branes and N_f D8-branes are coincident, we find that the 4–8 and 4–$\overline{8}$ strings have a vanishing vacuum expectation value (VEV). Therefore, the fundamental quarks created by 4–8 and 4–$\overline{8}$ strings are massless, which implies that this model can describe the mesons with light flavors only. Hence, it is naturally motivated to include the massive heavy flavor in this model. To achieve this goal, in this section, we review the Higgs mechanism in D-brane system and see how to use it to introduce heavy flavor.

First, we take a look at the Higgs mechanism in D-brane system by considering the configuration of an open string connecting two stacks of the separated D-branes, as illustrated in Figure 7a.

In this D-brane configuration, the worldvolume symmetry $U(N_1+N_2)$ breaks down to $U(N_1)\times U(N_2)$ when the D-branes move separately, where we use N_1, N_2 to refer to the D-branes number in each stack. Accordingly, the transverse modes of the D-brane acquire a nonzero VEV due to the separation of the D-branes. Hence, the multiplets created by the open string connecting the separated D-branes become massive, just like the Higgs mechanism in the standard model of particle physics [53,60]. Let us investigate this mechanism quantitatively by recalling the D-brane action in (20). In the holographic approach, we need the near-horizon limit, i.e., $\alpha' \to 0$; thus, the D-brane action can be expanded to be a Yang–Mills plus Wess–Zumino action, as it is in Section 2.4. Now, we pick up the transverse modes in the DBI action; it reduces to an additional quadratic action for the transverse modes Ψ^I with $\alpha' \to 0$:

$$\begin{aligned} S\left[\Psi^I\right] &= -T_{\mathrm{D}_p}\frac{(2\pi\alpha')^2}{4}\int_{\mathrm{D}_p} d^{p+1}x\sqrt{-\det g}e^{-\phi}\mathrm{Tr}\left\{2D_a\Psi^I D_a\Psi^I+\left[\Psi^I,\Psi^J\right]^2\right\}, \\ a &= 0,1\ldots p,\ I,J=p+1\ldots d, \end{aligned} \tag{164}$$

where the covariant derivative is

$$D_a\Psi^I = \partial_a\Psi^I + i\left[\mathbf{A}_a,\Psi^I\right], \tag{165}$$

and $\mathbf{A}_a$ is the gauge field potential on the D-brane. Consider a stack of coincident N_1+N_2 D-branes; $\mathbf{A}_a$ could be the $U(N_1+N_2)$ generator as an $(N_1+N_2)\times(N_1+N_2)$ matrix.

However, if the coincident $N_1 + N_2$ D-branes move apart to become two stacks of N_1 and N_2 D-branes, the gauge potential $\mathbf{A}_a$ becomes

$$\mathbf{A}_a = \begin{pmatrix} A_a & \Phi_a \\ \Phi_a^\dagger & 0 \end{pmatrix}, \tag{166}$$

where A_a is the $U(N_1)$ gauge potential as an $N_1 \times N_1$ matrix. Φ_a is the multiplet created by the open string connecting to the two stacks of the D-brane, which is an $N_1 \times N_2$ matrix-valued field, and the last element can be gauged away by residual symmetry. On the other hand, when the D-branes are separated, the transverse mode Ψ^I will have a nonzero VEV, since the open string connecting the separated D-branes cannot shrink to zero. Therefore, we can write Ψ^I with a VEV as

$$\Psi^I \to \Psi^I + V^I, \tag{167}$$

where

$$V^I \sim \begin{pmatrix} V & 0 \\ 0 & v \end{pmatrix}, \tag{168}$$

to represent $U(N_1 + N_2) \to U(N_1) \times U(N_2)$. Thus, plugging (165)–(168) into (164), one obtains a mass term in the action as follows:

$$\mathrm{Tr}\Big(V^2 \Phi_a^\dagger \Phi_a + v^2 \Phi_a \Phi_a^\dagger\Big), \tag{169}$$

and Φ_a can be interpreted as the heavy–light field acquiring a mass through the VEV of the transverse mode Ψ^I.

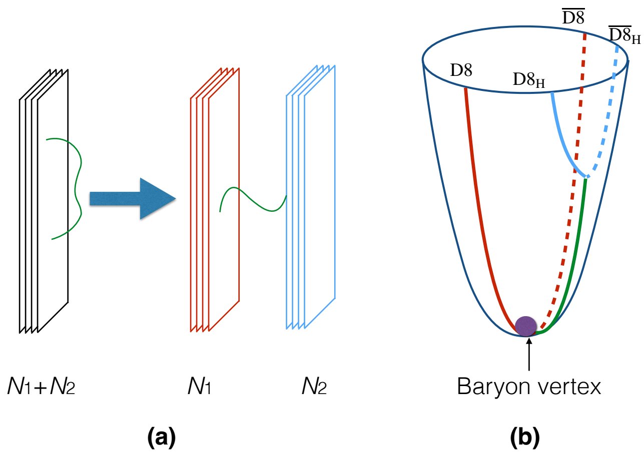

Figure 7. The Higgs mechanism in string theory (**a**) and the configuration of heavy flavor in D4/D8 model (**b**). (**a**) Higgs mechanism in string theory: The gauge symmetry on a stack of coincident $N_1 + N_2$ D-branes could be $U(N_1 + N_2)$, while it breaks down to $U(N_1) \times U(N_2)$ if the D-branes somehow move apart to become two stacks of coincident N_1 and N_2 D-branes. The open string connecting the two stacks of the D-branes has a nonzero VEV; hence, its ground states acquire nonzero mass, which corresponds to the separation of the D-branes. (**b**) Configuration of heavy flavor in D4/D8 model: Red line refers to the stack of N_f D8/$\overline{\text{D8}}$-branes in the original model, which now is identified as light flavor. Blue line refers to another pair of D8/$\overline{\text{D8}}$-branes separated from N_f D8/$\overline{\text{D8}}$-branes, which is identified as heavy flavor. The green line refers to the open string connecting the light and heavy brane, which is the heavy–light string, and it acquires nonzero VEV to create massive ground states.

With this Higgs mechanism in string theory, let us employ it in the D4/D8 model by considering Figure 7b. In this configuration, there is one pair of D8/$\overline{\text{D8}}$-branes separated from N_f D8/$\overline{\text{D8}}$-branes, which are identified as heavy flavor branes with an open string (the heavy–light string) connecting them. We note that the configuration in Figure 7b is a generalized version of Figure 7a in the curved spacetime. Then, we can write down the D8-brane action with heavy flavor by imposing the following replacement:

$$A_a \to \mathbf{A}_a = \begin{pmatrix} A_a & \Phi_a \\ \Phi_a^\dagger & 0 \end{pmatrix}, F_{ab} \to \mathbf{F}_{ab} = \begin{pmatrix} F_{ab} + i\alpha_{ab} & f_{ab} \\ f_{ab}^\dagger & i\beta_{ab} \end{pmatrix}, \tag{170}$$

to (33), where A_a, F_{ab} are $N_f \times N_f$ matrix-valued fields, as we have specified in Section 2. Φ_a is an $N_f \times 1$ matrix-valued multiplet created by the heavy–light string, which is interpreted as the heavy–light meson field, and the index in the square brackets is ranked as $T_{[ab]} = \frac{1}{2!}(T_{ab} - T_{ba})$, and we choose the gauge field as Hermitian field $\mathbf{A}_a^\dagger = \mathbf{A}_a$:

$$\begin{aligned} \alpha_{ab} =& \ 2\Phi_{[a}\Phi_{b]}^\dagger, \ \beta_{ab} = 2\Phi_{[a}^\dagger\Phi_{b]}, \\ f_{ab} =& \ 2\partial_{[a}\Phi_{b]} + 2iA_{[a}\Phi_{b]} \equiv 2D_{[a}\Phi_{b]}, \end{aligned} \tag{171}$$

we obtain the action (164) for Φ_a as follows:

$$\begin{aligned} S[\Phi_{\mu,z}] =& -2\kappa\mathrm{Tr}\int dzdx^4 f(z)\left(\partial_\mu\Phi_\nu^\dagger - \partial_\nu\Phi_\mu^\dagger\right)(\partial^\mu\Phi^\nu - \partial^\nu\Phi^\mu) \\ & -\kappa\mathrm{Tr}\int dzdx^4 g(z)\left(\partial_\mu\Phi_z^\dagger - \partial_z\Phi_\mu^\dagger\right)(\partial^\mu\Phi_z - \partial_z\Phi^\mu) \\ & -\tilde{v}\mathrm{Tr}\int dzdx^4 a(z)\left[2f(z)\Phi^{\dagger\mu}\Phi_\mu + g(z)\Phi_z^\dagger\Phi_z\right], \end{aligned} \tag{172}$$

where z is the Cartesian coordinates given in (34), and the VEV of T-dualized $\Psi^4 = 2\pi\alpha' x^4$ is chosen as [103]

$$\Psi^4 = \begin{pmatrix} -\frac{v}{N_f - 1}\mathbf{1}_{N_f - 1} & 0 \\ 0 & v \end{pmatrix}, \tag{173}$$

with

$$\tilde{v} = v\kappa/\left(2\pi\alpha'\right)^2, f(z) = \frac{R^3}{4U(z)}, g(z) = \frac{9}{8}\frac{U(z)^3}{U_{KK}}, a(z) = \left[\frac{U(z)}{R}\right]^{3/2}. \tag{174}$$

Note that Ψ^4 is the only transverse mode of D8-brane. The heavy–light meson tower can be obtained by expanding $\Phi_{\mu,z}$, as specified in Section 2.4. For example, the transverse modes of heavy–light meson field are suggested, given as [38,39]

$$\Phi_\mu = \sum_n \phi_{(n)}^H(z) B_\mu^{(n)}(x), \Phi_z = 0, \tag{175}$$

which leads to

$$S[\Phi_{\mu,z}] = \sum_n \int d^4x \left[\frac{1}{2}\partial_{[\mu} B_{\nu]}^{(n)\dagger}\partial^{[\mu} B^{(n)\nu]} + m_n^2 B_\mu^{(n)\dagger} B^{(n)\mu}\right], \tag{176}$$

with the normalization

$$4\kappa\int dz f(z)\phi_{(n)}^H\phi_{(m)}^H = \delta_{mn}, \tag{177}$$

and eigenvalue equation

$$-\frac{d}{dz}\left(g\frac{d\phi_{(n)}^H}{dz}\right) + 2f(z)\left[-m_n^2 + \tilde{v}^2 a(z)\right]\phi_n^H = 0. \tag{178}$$

For the transverse modes and longitudinal modes, the expansion is suggested as

$$\begin{aligned} \Phi_\mu =& -\sum_n \frac{1}{2a(z)f(z)m_n^2}\frac{d}{dz}[a(z)g(z)\epsilon_n(z)]\partial_\mu D_\nu(x), \\ \Phi_z =& \ \sum_n \epsilon_n(z) D_n(x), \end{aligned} \tag{179}$$

leading to

$$S\left[\Phi_{\mu,z}\right]=\sum_n\int d^4x\left(\partial_\mu D_n^\dagger\partial^\mu D_n+m_n^2D_n^\dagger D_n\right), \tag{180}$$

with the normalization

$$2\kappa=\int dza(z)g(z)\epsilon_n(z)\epsilon_m(z)=\frac{m_n^2}{\tilde{v}^2}\delta_{mn}. \tag{181}$$

We note that with the replacement (170), the Chern–Simons action (57) for the D8-branes reduces to additional terms as follows:

$$\begin{aligned}\mathcal{L}_{\mathrm{CS}}\left[\Phi_{\mu,z}\right]= & -\tfrac{N_c}{24\pi^2}\left(d\Phi^\dagger Ad\Phi+d\Phi^\dagger dA\Phi+\Phi^\dagger dAd\Phi\right)\\ & +\tfrac{iN_c}{16\pi^2}\left(d\Phi^\dagger A^2\Phi+\Phi^\dagger A^2d\Phi+\Phi^\dagger AdA\Phi+\Phi^\dagger dAA\Phi\right)\\ & +\tfrac{5N_c}{48\pi^2}\Phi^\dagger A^3\Phi+\mathcal{O}\left(\Phi^4,A\right).\end{aligned} \tag{182}$$

Using the expansions (175), (179) and (46), the DBI and CS term includes the interaction between light and heavy–light mesons.

It is also possible to obtain the baryon spectrum with heavy flavor by considering the baryon vertex as the instantons on the flavor brane [104–106]. Following the steps in Section 2.5, the equations of motion for the heavy–light meson field are derived as follows:

$$\begin{aligned}D_MD_M\Phi_N-D_ND_M\Phi_M+2iF_{MN}\Phi_M+\mathcal{O}\left(\lambda^{-1}\right) &=0,\\ D_M\left(D_0\Phi_M-D_M\Phi_0\right)-iF^{0M}\Phi_M &\\ -\tfrac{1}{64\pi^2a}\epsilon_{MNPQ}\mathcal{K}_{MNPQ}+\mathcal{O}\left(\lambda^{-1}\right) &=0,\end{aligned} \tag{183}$$

where $M,N=1,2,3,z$, and

$$\mathcal{K}_{MNPQ}=i\partial_MA_N\partial_P\Phi_Q-A_MA_N\partial_P\Phi_Q-\partial_MA_NA_P\Phi_Q-\frac{5i}{6}A_MA_NA_P\Phi_Q, \tag{184}$$

where $F=dA+\frac{i}{2}[A,A]$ is computed by the BPST instanton solution given in (82)–(85). Thus, $\Phi_{\mu,z}$ can be solved as $\Phi_{\mu,z}=e^{\pm im_Ht}\phi_{\mu,z}(x)$ with

$$\begin{aligned}\phi_0 &=-\tfrac{1}{1024a\pi^2}\left[\tfrac{25\rho}{2\left(x^2+\rho^2\right)^{5/2}}+\tfrac{7}{\rho\left(x^2+\rho^2\right)^{3/2}}\right]\chi,\\ \phi_M &=\tfrac{\rho}{\left(x^2+\rho^2\right)^{3/2}}\sigma_M\chi,\end{aligned} \tag{185}$$

where σ_M is the embedded Pauli matrices, as $\sigma_M/2=\left(t_i,-\mathbf{1}_{N_f}\right)$, and χ is the $SU\left(N_f\right)$ spinor independent on x,z. The soliton mass as the baryonic potential can be evaluated by inserting (185) and the BPST solution (82)–(85) to the full action for the D8-branes. Afterwards, one reaches to an effective Hamiltonian for baryon state by following Section 2.5, as given in [105,106]. We note that [40] also gives another generalization with heavy flavor into black D4-brane background.

3.4. Interactions of Hadrons and Glueballs

The interaction of hadrons relates to many significant topics in QCD and nuclear physics, and its holographic description by the D4/D8 model was reviewed briefly in Section 2 and [24,25]. In this section, we will take a look at the interactions in hadron physics involving glueballs, since the D4/D8 model provides explicit definitions of mesons, baryons and glueballs.

The main idea to include the interactions of mesons and glueballs is to consider the D8-brane action with a gravitational fluctuation. Recalling the discussion in Sections 2.4 and 2.6, since meson is identified as the gauge field on the D8-branes (created by 8–8 string) and glueball is identified as the gravitational polarization (closed string), the interaction of meson and glueball is nothing but the interaction of open and closed strings, which can therefore be included into the D8-brane action when the metric fluctuation is picked up.

For example, when we put the gravitational polarization (97) into the D8-brane action (32) with the meson tower given in (37), by integrating out the z dependence (the holographic coordinate), it reduces to an interaction action involving π, ρ meson and exotic glueball G_E, after some straightforward but messy calculations, as follows:

$$\begin{aligned}
S_{G_E}^{\pi-\rho} = & -\mathrm{Tr}\int d^4x \Bigg\{ c_1 \left[\frac{1}{2}\partial_\mu \pi \partial_\nu \pi \frac{\partial^\mu \partial^\nu}{M_E^2} G_E + \frac{1}{4}\left(\partial_\mu \pi\right)^2 \left(1 - \frac{\partial^2}{M_E^2}\right) G_E \right] \\
& + c_2 M_{KK}^2 \left[\frac{1}{2}\rho_\mu \rho_\nu \frac{\partial^\mu \partial^\nu}{M_E^2} G_E + \frac{1}{4}\left(\rho_\mu\right)^2 \left(1 - \frac{\partial^2}{M_E^2}\right) G_E \right] \\
& + c_3 \left[\frac{1}{2}\eta^{\sigma\lambda} \partial_{[\mu}\rho_{\sigma]} \partial_{[\nu}\rho_{\lambda]} \frac{\partial^\mu \partial^\nu}{M_E^2} G_E - \frac{1}{8}\partial_{[\mu}\rho_{\nu]} \partial^{[\mu}\rho^{\nu]} \left(1 + \frac{\partial^2}{M_E^2}\right) G_E \right] + c_4 \frac{3}{2M_E^2} \rho_\mu \partial^{[\mu}\rho^{\nu]} \partial_\nu G_E \\
& + c_5 \left[\partial_\mu \pi [\pi, \rho_\nu] \frac{\partial^\mu \partial^\nu}{M_E^2} G_E + \frac{1}{2}\partial_\mu \pi [\pi, \rho^\mu] \left(1 - \frac{\partial^2}{M_E^2}\right) G_E \right] \\
& + \left[\frac{1}{2}\tilde{c}_1 \left(\partial_\mu \pi\right)^2 + \frac{1}{2}\tilde{c}_2 M_{KK}^2 \left(\rho_\mu\right)^2 + \frac{1}{4}\tilde{c}_3 \partial_{[\mu}\rho_{\nu]} \partial^{[\mu}\rho^{\nu]} + \tilde{c}_5 \partial_\mu \pi [\pi, \rho^\mu] \right] G_E \Bigg\},
\end{aligned} \tag{186}$$

where the c_i and $\tilde{c}_i$ coefficients are coupling constants and are numerically computed as (in the unit of $\lambda^{-1/2} N_c^{-1} M_{KK}^{-1}$)

$$\begin{aligned}
c_1 &= \int dZ \frac{\bar{H}_E}{\pi K} = 62.6, \quad c_2 = 2\kappa \int dZ K \left(\psi_1'\right) \bar{H}_E = 7.1, \\
c_3 &= 2\kappa \int dZ K^{-1/3} \left(\psi_1\right)^2 \bar{H}_E = 69.7, \\
c_4 &= 2\kappa M_{KK}^2 \int dZ \frac{20ZK}{(5K-2)^2} \psi_1 \psi_1' H_E = 10.6 M_{KK}^2, \\
c_5 &= \int dZ \frac{\psi_1 \bar{H}_E}{\pi K} = 2019.6 N_c^{-1/2}, \\
\tilde{c}_1 &= \int dZ \frac{H_E}{4\pi K} = 16.4, \quad \tilde{c}_2 = \frac{1}{2}\kappa \int dZ K \left(\psi_1'\right)^2 H_E = 3.0, \\
\tilde{c}_3 &= \frac{1}{2}\kappa \int dZ K^{-1/3} \left(\psi_1\right)^2 H_E = 18.1, \quad \tilde{c}_5 = \int dZ \frac{\psi_1 H_E}{4\pi K} = 508.2 N_c^{-1/2}.
\end{aligned} \tag{187}$$

Then, the associated amplitude of glueball decay can be further evaluated by using the effective action $S_{G_E}^{\pi-\rho}$ with the coupling constants. One can also compute the effective action of meson involving other types of glueball by changing the formulas of the bulk gravitational polarization, as discussed in [29–32].

The current setup to obtain an effective action of meson and glueball interaction can also be generalized by including heavy flavor [107], which is to take into account the configuration in Figure 7b and the heavy–light meson field. The main idea is to pick up the gravitational polarization in bulk metric when we write down the D8-brane action with heavy flavor brane (i.e., with the replacement given in (170)). For example, by considering the gravitational polarization for the exotic glueball G_E in (97), the effective action of heavy–light meson and glueball provides such terms as

$$\begin{gathered}
\partial^2 G_E \partial_\mu Q_\nu^\dagger \partial^\mu Q^\nu, \partial^2 G_E Q_\mu^\dagger Q^\mu, \partial^2 G_E \partial_\mu Q^\dagger \partial^\mu Q, \partial^2 G_E Q^\dagger Q, \\
\partial^\mu \partial^\rho G_E \partial_\mu Q_\nu^\dagger \partial_\rho Q^\nu, \partial^\mu \partial^\nu G_E \partial_\mu Q^\dagger \partial_\nu Q, \partial^\mu \partial^\nu G_E Q_{\mu,}^\dagger Q_\nu, \\
G_E \partial_\mu Q_\nu^\dagger \partial^\mu Q^\nu, G_E Q_\mu^\dagger Q^\nu, G_E Q^\dagger Q, \\
\partial_\sigma G_E \partial^\rho Q^{\sigma\dagger} \partial_\rho Q, \partial_\sigma G_E \partial^\rho Q^{\sigma\dagger} Q_\rho, \partial^\mu G_E Q_\mu^\dagger Q,
\end{gathered} \tag{188}$$

which are the same types as the interaction given in (186). Here, we use Q_μ, Q to denote the vector and scalar heavy–light meson field, and the lowest heavy–light meson is identified to be D-meson with a charm quark. Accordingly, the effective action with heavy flavor and glueball may be useful to study the oscillation of D-meson pairs ($D - \bar{D}$) or B-meson pairs ($B - \bar{B}$) [108,109]. Note that since the heavy–light multiplet is created by the heavy–light string, even if the heavy flavor is taken into account, the interaction of heavy–light meson and glueball remains an open/closed string interaction through holography. Moreover, in the presence of the heavy–light meson and glueball, the effective action also mixes the interaction terms of glueball, light and heavy–light meson, which may describe the various interactions in hadron physics.

It is also possible to include the interaction of baryon (or baryonic meson) and glueball in a parallel way, that is, to consider the interaction of baryonic D4′-branes and bulk closed string [110]. Specifically, one can derive the Yang–Mills action presented in (32) with the gravitational polarization (97), then insert the BPST instanton configuration (82)–(85) as baryon under the large λ rescaling (77). Afterwards, by following the discussion in Section 2.5, we can obtain additional terms to the collective Hamiltonian (96) as follows:

$$\Delta H(t) \simeq \cos(\omega t)\left\{-\frac{27}{2}\pi^2+\left[-\frac{59049\pi^4}{20\rho^2}+\frac{27M_E^2+468}{16}\pi^2\left(2Z^2+\rho^2\right)\right]\lambda^{-1}+\mathcal{O}\left(\lambda^{-2}\right)\right\}. \tag{189}$$

Using the standard technique in quantum mechanics for the time-dependent perturbed Hamiltonian, it is possible to work out the decay rate of baryon involving glueball and its associated select rule. We note that when the heavy flavor is included, as in Section 2.3, the decay rate of heavy–light baryon or baryonic meson involving glueball can be achieved. For example, considering the exotic gravitational polarization (97), we can reach the time-dependent perturbed Hamiltonian, given as [111]:

$$\Delta H(t) \simeq \lambda^{-1/2}M_{KK}^{-1}\left(\frac{5}{216\pi}m_H^2+\frac{15m_H}{32\rho^2}\right)G_E\chi^\dagger\chi, \tag{190}$$

where we take the limit $m_H \to \infty$ followed $\lambda \to \infty$ to simplify the formula, and $\chi^\dagger\chi = N_Q$ refers to the number of heavy flavor quarks in the heavy–light meson. Then, the decay of heavy–light baryonic matter involving glueball can be evaluated using (190) to the quantum mechanical system (96) with heavy flavors. To close this section, we summarize the strings as various hadrons in the D4/D8 model in Figure 8, and we can see the various interactions of hadrons are interactions of strings through gauge–gravity duality in this model.

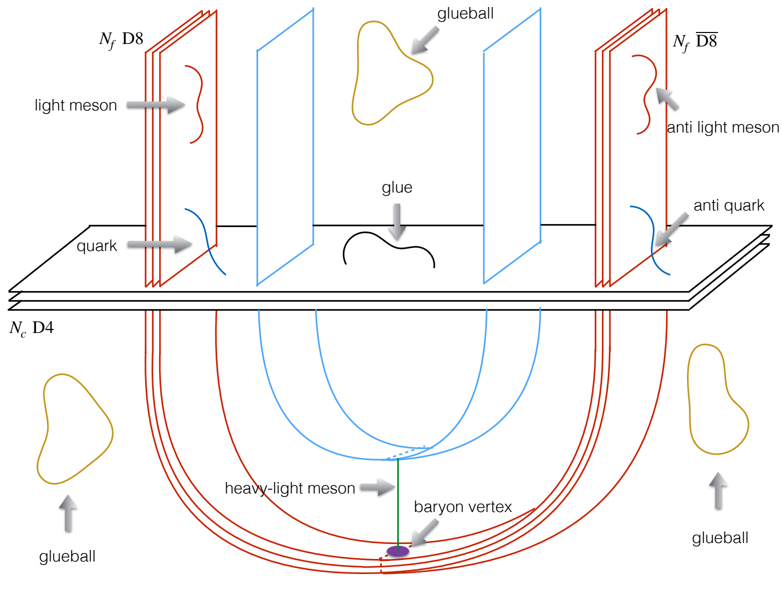

Figure 8. Strings as various hadrons in the D4/D8 model.

3.5. Theta Dependence in QCD

In Yang–Mills theory, there could be an topological term proportional to the θ angle [112]. In the large N_c limit, the full Lagrangian takes the following form:

$$S = \frac{N_c}{2\lambda}\mathrm{Tr}\int {}^\star F\wedge F - i\frac{\lambda}{8\pi^2}\frac{\theta}{N_c}\mathrm{Tr}\int F\wedge F. \tag{191}$$

While the value of angle θ may be experimentally small, it leads to many interesting effects, e.g., glueball spectrum [113], deconfinement transition [114,115], chiral magnetic effect [116,117], especially its large N_c limit [118]. Since the D4/D8 model is a holographic version of QCD, it is possible to introduce the θ term to the dual theory through the gauge–gravity duality.

The main goal of including a Yang–Mills θ term in holography is to introduce coincident N_0 D0-branes acting to the N_c D4-brane background (14). In this sense, we have to require N_0/N_c to be fixed when $N_c \to \infty$. For the SUGRA approach, the dynamics of the Ramond–Ramond 1-form C_1 must be picked up into the IIA SUGRA action (15) in order to include the charge in the D0-branes:

$$S_{\mathrm{IIA}}^{10\mathrm{d}} = \frac{1}{2\kappa_{10}^2}\int d^{10}x\sqrt{-G}e^{-2\phi}\left[\mathcal{R}^{(10)} + 4\partial_\mu\phi\partial\phi\right] - \frac{1}{4\kappa_{10}^2}\int d^{10}x\sqrt{-G}\left(|F_4|^2 + |F_2|^2\right), \tag{192}$$

where $F_2 = dC_1$. To obtain an analytical solution, we assume that the D0-branes are smeared homogeneously along x^4; hence, the associated equations of motion to (192) can be solved as follows:

$$\begin{aligned} ds^2 &= H_4^{-1/2}\left[-H_0^{-1/2}f_T(U)\left(dx^0\right)^2 + H_0^{1/2}dx_i dx^i\right] + H_4^{1/2}H_0^{1/2}\left[\frac{dU^2}{f_T(U)} + U^2 d\Omega_4^2\right], \\ H_4 &= 1 + \frac{R^3}{U^3}, H_0 = 1 - \frac{U_H^3}{U^3}\frac{\Theta^2}{1+\Theta^2}, e^\phi = H_4^{-1/4}H_0^{3/4}, C_1 = \frac{\Theta}{g_s}\frac{f_T}{H_0}dx^4, F_4 = 3R^3 g_s^{-1}, \end{aligned} \tag{193}$$

where Θ is a constant parameter. Taking the near-horizon limit so that $H_4 \to R^3/U^3$ and imposing the double Wick rotation, as discussed in Section 2.1, we can obtain a D0–D4 bubble background associated to (16), as follows:

$$\begin{aligned} ds^2 &= H_4^{-1/2}\left[H_0^{1/2}\eta_{\mu\nu}dx^\mu dx^\nu + H_0^{-1/2}f(U)\left(dx^4\right)^2\right] + H_4^{1/2}H_0^{1/2}\left[\frac{dU^2}{f_T(U)} + U^2 d\Omega_4^2\right], \\ H_4 &= \frac{R^3}{U^3}, H_0 = 1 - \frac{U_{KK}^3}{U^3}\frac{\Theta^2}{1+\Theta^2}, e^\phi = H_4^{-1/4}H_0^{3/4}, C_1 = -i\frac{\Theta}{g_s}\frac{f}{H_0}dx^4, F_4 = 3R^3 g_s^{-1}. \end{aligned} \tag{194}$$

Due to the presence of the D0-branes, we can see that the dual theory of (194) is pure Yang–Mills theory, with a θ term if a probe D4-brane located at the holographic boundary is taken into account:

$$\begin{aligned} S_{\mathrm{D4}} = &\left[-T_{\mathrm{D4}}\mathrm{STr}\int d^4x d\tau e^{-\phi}\sqrt{-\det(G + 2\pi\alpha' F)} + g_s T_{\mathrm{D4}}\int C_5 \right. \\ &\left. + \frac{1}{2}(2\pi\alpha')^2 g_s T_{\mathrm{D4}}\int C_1 \wedge F \wedge F\right]\Big|_{U\to\infty} \\ \simeq\ & -\frac{1}{2g_{\mathrm{YM}}^2}\mathrm{Tr}\int {}^*F \wedge F + i\frac{g_{\mathrm{YM}}^2}{8\pi^2}\theta\mathrm{Tr}\int F \wedge F + \mathcal{O}(F^4), \end{aligned} \tag{195}$$

which further implies that the bare θ angle relates to the Θ parameter in the solution (194) by

$$\Theta = \frac{\lambda}{8\pi^2}\left(\frac{\theta + 2k\pi}{N_c}\right), k \in \mathbb{Z} \tag{196}$$

as a fixed constant in the large N_c limit.

With the geometry background (194), it is possible to evaluate several properties of Yang–Mills theory with a θ term by following the discussions in previous sections; let us take a brief look at them for examples. First, we focus on the the ground state energy, which can be evaluated by using (104)–(108) as follows:

$$F(\Theta) = -\frac{2N_c^2\lambda}{3^7\pi^2}\frac{M_{KK}^4}{(1+\Theta^2)^3}. \tag{197}$$

In the expansion with respect to small Θ, (197) reduces to the minimized free energy difference,

$$\min_k[F(\Theta) - F(0)] \simeq \frac{1}{2}\chi_g\theta^2\left[1 + \bar{b}_2\frac{\theta^2}{N_c^2} + \bar{b}_4\frac{\theta^4}{N_c^4} + \mathcal{O}\left(\theta^6\right)\right], \tag{198}$$

as the energy of the θ vacuum, and the topological susceptibility reads as

$$\chi_g = \frac{\lambda^3 M_{KK}^4}{32(3\pi)^6}, \tag{199}$$

with

$$\bar{b}_2 = -\frac{\lambda^2}{32\pi^4}, \bar{b}_4 = -\frac{5\lambda^4}{3\times 2^{11}\pi^8}. \tag{200}$$

Moreover, one can consider a constant C_1 in the black D4-brane background (14), so that $F_2 = dC_1 = 0$. Hence, the ground state energy of deconfined Yang–Mills theory with a constant θ term can be identified as $F_{\mathrm{deconf.}}$, presented in (109).

Then, the QCD deconfinement phase transition can be obtained by comparing the free energy (197) with $F_{\mathrm{deconf.}}$ in (109) which leads to the critical temperature

$$T_c(\Theta) = \frac{M_{KK}}{2\pi}\frac{1}{\sqrt{1+\Theta^2}} \simeq \frac{M_{KK}}{2\pi}\left[1 - \frac{\lambda^2}{128\pi^4}\frac{\theta^2}{N_c^2} + \frac{3\lambda^4}{2^{15}\pi^8}\frac{\theta^4}{N_c^4} + \mathcal{O}\left(\frac{\theta^6}{N_c^6}\right)\right]. \tag{201}$$

Second, the QCD string tension also takes a correction due to the presence of θ term. Consider an open string stretched in the background (194) ending on a probe D4-brane at boundary. Using the AdS/CFT dictionary, the Wilson loop in the dual theory relates to the classical Nambu–Goto (NG) action S_{NG} of the open string corresponding to the tension T with quark potential V, as follows:

$$\langle W(\mathcal{C})\rangle \sim e^{-S_{NG}} \sim e^{-TV}. \tag{202}$$

In the static gauge, the relevant string embedding can be chosen as follows:

$$\tau = x^0 \in [0,T], \sigma = x \in [-l/2, l/2], U = U(x), \tag{203}$$

then the NG action is given as

$$S_{NG} = -\frac{1}{2\pi\alpha'}\int d\tau d\sigma\sqrt{-g_{\tau\tau}g_{\sigma\sigma}} = -\frac{1}{2\pi\alpha'}\int d\tau d\sigma\sqrt{-g_{00}\left[g_{xx} + g_{UU}U'(x)^2\right]}, \tag{204}$$

To quickly evaluate the QCD tension, let us consider the limit $l \to \infty$. In this limit, the open string must minimize its energy as much as possible; it forces the factor $\sqrt{-g_{00}g_{xx}}$ to become minimal to take the value at $U = U_{KK}$, since the size of x^4 shrinks at $U = U_{KK}$. Therefore, the QCD tension T_s is obtained from

$$S_{NG} \simeq -\frac{1}{2\pi\alpha'}Tl\sqrt{-g_{00}g_{xx}}|_{U=U_{KK}} = -T_sTl, \tag{205}$$

as

$$T_s = \frac{1}{2\pi\alpha'}\sqrt{-g_{00}g_{xx}}|_{U=U_{KK}} = \frac{\lambda}{27\pi}M_{KK}^2\frac{1}{\left(1+\Theta^2\right)^2}. \tag{206}$$

Next, let us investigate the glueball mass with the background (194). As the glueball corresponds to the gravitational fluctuation, by adding a perturbation to the metric presented in (194) as $g_{MN} \to g_{MN} + h_{MN}$, it reduces to an equation of motion for h_{MN}, given as

$$\frac{1}{2}\nabla_M\nabla_N h^K_K + \frac{1}{2}\nabla^2 h_{MN} - \left(\nabla^K\nabla_M h_{NK} + \nabla^K\nabla_N h_{MK}\right) - \frac{3}{2}h_{MN} = 0. \tag{207}$$

Here, since IIA SUGRA can be obtained by the dimension reduction from 11d M-theory, h_{MN} refers to the fluctuation on AdS$_7$, which means M, N runs over 0–6. Setting $h_{MN} = H_{MN}(U)e^{-ik\cdot x}$ with the ansatz

$$H_{MN}(U) = \frac{U}{R}H(U)\mathrm{diag}\left(0,1,1,1,0,-\frac{3}{1+\Theta^2},0\right), \tag{208}$$

it gives the eigen equation for $H(U)$ as

$$H''(U) + \frac{4U^3 - U_{KK}^3}{U(U^3 - U_{KK}^3)} H'(U) - \frac{M^2 R^2}{U^3 - U_{KK}^3} H(U) = 0, \tag{209}$$

which implies that the mass spectrum M with a correction due to Θ is

$$M \simeq \frac{M(0)}{\sqrt{1+\Theta^2}}. \tag{210}$$

The presence of θ also decreases the baryon mass m_B,

$$m_B = \frac{\lambda}{27\pi} N_c M_{KK} \frac{1}{\left(1+\Theta^2\right)^{3/2}}, \tag{211}$$

by imposing the metric presented in (194) into (76), which implies the evidence of metastable particles in QCD. By further analyzing the entanglement entropy on (194), it agrees consistently with the property of the possible metastable states in this model. Moreover, when we follow the discussion in Section 2.2, it is possible to introduce flavored meson in the D0–D4 background. The meson mass also acquires the correction by the θ angle, as in [41,42]. Further, following the instantonic description for baryon in Section 2.5, one can see the metastable baryonic spectrum in this model, as in [119]. In this sense, the Witten–Sakai–Sugimoto model in the D0-D4 brane background is recognized as a holographic version of QCD with a θ term.

4. Summary and Outlook

In this review, we look back to the fundamental properties of the D4/D8 model, which include the D4-brane background, the embedding of the D8/$\overline{\text{D8}}$-branes, and how to identify mesons, baryons and glueballs in this model. Moreover, we revisit some interesting topics about QCD by using this model, which relate to the deconfinement transition, chiral phase, heavy flavor, various interactions of hadrons and the θ term in QCD. This review illustrates that string theory can provide a powerful method for studying the strongly coupled regime of QCD, which is out of the reach of the traditional methods of perturbative QFT. We particularly note here that there are additional interesting approaches based on this model that are absent in the main text of this review; they relate to the holographic Schwinger effect [120–123], the fluid/gravity correspondence [124–128], corrections to the instanton as baryon [129,130], the approaches to the D3/D7 model [131,132] and applications in studying neutron stars [133,134]. With all of these achievements, it may be possible to work out an exact holographic version of QCD based on the D4/D8 model in future work, to reinterpret the fundamental element of strong interactions according to gauge–gravity duality.

Author Contributions: Conceptualization, S.-W.L.; methodology, S.-W.L.; software, X.-T.Z.; validation, X.-T.Z.; formal analysis, X.-T.Z.; investigation, S.-W.L.; writing—original draft preparation, S.-W.L.; writing—review and editing, S.-W.L. and X.-T.Z.; supervision, S.-W.L. and X.-T.Z.; project administration, S.-W.L.; funding acquisition, S.-W.L. and X.-T.Z. All authors have read and agreed to the published version of the manuscript.

Funding: This work is supported by the National Natural Science Foundation of China (NSFC) under Grant No. 12005033 and the Fundamental Research Funds for the Central Universities under Grant No. 3132023198.

Data Availability Statement: Not applicable.

Conflicts of Interest: The authors declare no conflict of interest.

Appendix A. The Type II Supergravity Solution

In this appendix, let us collect the D_p-brane solution in the type II SUGRA. We note that all the discussion in this appendix is valid to the gravity solution presented in the main text if we set $p = 4$. In the string frame, the action for type II SUGRA sourced by a stack of N_p coincident D_p-branes can be written as

$$S_{\mathrm{II}} = \frac{1}{2\kappa_{10}^2} \int d^{10}x \sqrt{-g} \Big[e^{-2\phi} \Big(\mathcal{R} + 4\partial_M \phi \partial^M \phi \Big) - \frac{g_s^2}{2} \big| F_{p+2} \big|^2 \Big], \tag{A1}$$

where $2\kappa_{10}^2 = 16\pi G_{10} = (2\pi)^7 l_s^8 g_s^2$ is the 10d gravity coupling constant, $\mathcal{R}, \phi, C_{p+1}$ are, respectively the 10d curvature, dilaton and Ramond–Ramond $p+1$-form field with $F_{p+2} = dC_{p+1}$. Note that in string theory, the dilaton field may also be defined as Φ by

$$\Phi - \Phi_0 = \phi, e^{\Phi_0} = g_s. \tag{A2}$$

Since a D_p-brane for $p = 4, 5, 6$ is magnetically dual to the D_p-brane for $p = 2, 1, 0$ and the D3-brane is self-dual, we only consider the case for $p < 7$ in (A1). Varying action (A1) with respect to g_{MN}, ϕ, C_{p+1}, the associated equations of motion are collected as follows:

$$\begin{aligned} 0 &= \mathcal{R} + 4\nabla^2\phi - 4(\nabla\phi)^2, \\ 0 &= \partial_N \Big(\sqrt{-g} F^{NM_1 \ldots M_{p+1}} \Big), \\ 0 &= \mathcal{R}_{MN} - \tfrac{1}{2} g_{MN} \mathcal{R} + 2\nabla_M \nabla_N \phi + 2 g_{MN} (\nabla\phi)^2 - 2 g_{MN} \nabla^2 \phi \\ &= \tfrac{g_s^2}{2(p+1)!} e^{2\phi} \Big[F_M^{\ K_1 \ldots K_{p+1}} F_{NK_1 \ldots K_{p+1}} - \tfrac{(p+1)!}{2} g_{MN} \big| F_{p+2} \big|^2 \Big]. \end{aligned} \tag{A3}$$

The solution for (A3) can be obtained by using the simply homogeneous ansatz,

$$\begin{aligned} ds^2 &= H_p^{-\frac{1}{2}} \eta_{ab} dx^a dx^b + H_p^{\frac{1}{2}} \Big(dr^2 + r^2 d\Omega_{8-p}^2 \Big),\ a, b = 0, 1 \ldots p \\ e^\phi &= H_p^{-\frac{p-3}{4}}, C_{01\ldots p} = g_s^{-1} H_p^{-1}, F_{r01\ldots p} = \tfrac{(7-p) g_s^{-1} h_p^{7-p}}{r^{8-p} H_p^2}, \end{aligned} \tag{A4}$$

where the harmonic function H_p is solved through (A3) as follows:

$$H_p(r) = 1 + \frac{h_p^{7-p}}{r^{7-p}}. \tag{A5}$$

Here, r refers to the radial coordinate vertical to the D_p-brane; Ω_{8-p} is the associated angle coordinate in the transverse space. The constant h_p relates to the charge of the D_p-brane, computed as follows:

$$h_p^{7-p} = \big(2\sqrt{\pi} \big)^{5-p} g_s N_p \Gamma \Big(\frac{7-p}{2} \Big) l_s^{7-p}. \tag{A6}$$

Solution (A4), representing extremal black D_p-branes, reduces to the BPS condition as follows:

$$2\kappa_{10}^2 g_s T_{\mathrm{D}_p} N_p = \int_{S^{8-p}} {}^\star F_{p+2}, \tag{A7}$$

due to the action for the Ramond–Ramond (R-R) field C_{p+1} with a source of N_p coincident D_p-branes,

$$S_{\mathrm{R-R}} = -\frac{1}{4\kappa_{10}^2} \int F_{p+2} \wedge {}^\star F_{p+2} + g_s T_{\mathrm{D}_p} \int_{p+1} C_{p+1}. \tag{A8}$$

The equations of motion (A3) also allow for the near-extremal solution, as follows:

$$\begin{aligned} ds^2 &= H_p^{-\frac{1}{2}} \big[f(r) dt^2 + \delta_{ij} dx^i dx^j \big] + H_p^{\frac{1}{2}} \Big[\tfrac{dr^2}{f(r)} + r^2 d\Omega_{8-p}^2 \Big], \\ e^\phi &= H_p^{-\frac{p-3}{4}}, C_{01\ldots p} = g_s^{-1} H_p^{-1}, F_{r01\ldots p} = \tfrac{(7-p) g_s^{-1} h_p^{7-p}}{r^{8-p} H_p^2}, \end{aligned} \tag{A9}$$

where i, j run over the spacial index of the D_p-branes. The functions $f(r), H_p(r)$ are solved, respectively, as follows:

$$f(r) = 1 - \frac{r_H^{7-p}}{r^{7-p}}, H_p(r) = 1 + \frac{r_p^{7-p}}{r^{7-p}}, \tag{A10}$$

where r_H refers to the horizon of the D_p-branes. Notice that the equation of motion (A3) reduces to a constraint,

$$4\nabla_M\phi\nabla^M\phi - 2\nabla^2\phi = \frac{p-3}{2} g_s^2 e^{2\phi} |F_{p+2}|^2, \tag{A11}$$

which implies that

$$r_p^{7-p} = \sqrt{h_p^{2(7-p)} + \left(\frac{r_H^{7-p}}{2}\right)^2} - \frac{r_H^{7-p}}{2}. \tag{A12}$$

So, we have $r_p \to h_p$ if $r_H \to 0$; thus, the near-extremal solution will return to the extremal solution in this limit.

Appendix B. Dimensional Reduction for Spinors

In this section, we collect the dimensional reduction for spinors, and one can see that various boundary conditions determine the associated mass of fermion in the lower dimension. Consider a complex massless spinor Ψ in $\mathbb{R}^{d+1}$ satisfying the Dirac equation

$$\gamma^M\partial_M\Psi = 0, \tag{A13}$$

where M runs over $\mathbb{R}^{d+1}$. When one of the spatial directions is compactified on a circle S^1, $\mathbb{R}^{d+1}$ becomes $\mathbb{R}^d \times S^1$. Let us denote the coordinates on $\mathbb{R}^d, S^1$ as x^μ, y, respectively. Then Fourier series of Ψ can be written as the summary of its modes on S^1 as

$$\Psi(x^\mu, y) = \sum_k e^{\frac{iky}{L}} \psi_k(x^\mu), \tag{A14}$$

where L refers to the radius of S^1 and k is integer or half-integer. Thus, the boundary of the spinor Ψ can be periodic or antiperiodic:

$$\Psi(x^\mu, y) = \pm\Psi(x^\mu, y + 2\pi L), \tag{A15}$$

where k is integer and half-integer, respectively. Mostly, the antiperiodic boundary condition for fermion is permitted, since observables are usually the combination of an even power of spinors. Inserting (A14) into (A13), it leads to

$$\left(\gamma^\mu\partial_\mu - i\gamma_*\frac{k}{L}\right)\psi_k(x^\mu) = 0, \tag{A16}$$

where $\gamma_* = \gamma^y$. So, we can see that $\psi_k(x^\mu)$ is massive spinor in $\mathbb{R}^d$ with an effective mass $i\gamma_*\frac{k}{L}$, unless $k = 0$. This implies that under the dimension reduction, the spinor in the lower dimension is always massive if the antiperiodic boundary condition is imposed. Note that in the low-energy theory, only the mode with minimal k is of concern; thus, it means that the fermion is massless/massive with periodic and antiperiodic boundary conditions, respectively, in the low-energy theory.

Appendix C. Supersymmetric Meson on the Flavor Brane

While the D4/D8 model achieves great success, it contains issues. The most important issue is that due to the remaining supersymmetry on the D8-branes, the D4/D8 model contains supersymmetrically fermionic mesons (mesino) on the flavor N_f D8/$\overline{\text{D8}}$-branes, which should not be presented in QCD [135]. As we specified in Section 2.1, the supersymmetry on N_c D4-branes breaks down due to its compactified direction x^4; however, there is no mechanism to break down the supersymmetry on the flavor branes, since the N_f D8/$\overline{\text{D8}}$-branes are perpendicular to the compactified direction x^4. Therefore, in principle, there is no reason to neglect the supersymmetric fermions in this model. So, let us pick up the fermionic action for the D8-branes in addition to their bosonic action (22). Up to the quadratic order, the fermionic action for the D8-brane reads as follows [136–138]:

$$S_{\mathrm{D8}}^{(f)}=i\frac{T_{\mathrm{D8}}}{2}\int d^9xe^{-\phi}\mathrm{STr}\sqrt{-\det[g_{ab}+(2\pi\alpha')\mathcal{F}_{ab}]}\bar{\Psi}(1-\Gamma_{\mathrm{D8}})\left(\Gamma^c\hat{D}_c-\Delta+\hat{L}_{D8}\right)\Psi, \tag{A17}$$

where Ψ refers to 32-component Majorana spinor in 10d spacetime, and

$$\begin{aligned}
\Gamma_{\mathrm{D8}} &= \frac{\sqrt{-\det[g_{ab}]}}{\sqrt{-\det[g_{ab}+(2\pi\alpha')\mathcal{F}_{ab}]}}\Gamma_{\mathrm{D8}}^{(0)}\Gamma^{11}\sum_q\frac{(-\Gamma^{11})^q}{q!2^q}\Gamma^{a_1\ldots a_{2q}}\mathcal{F}_{a_1a_2}\ldots\mathcal{F}_{a_{2q-1}a_{2q}},\\
\hat{L}_{D8} &= -\frac{\sqrt{-\det[g_{ab}]}}{\sqrt{-\det[g_{ab}+(2\pi\alpha')\mathcal{F}_{ab}]}}\Gamma_{\mathrm{D8}}^{(0)}\sum_{q\geq1}\frac{(-\Gamma^{11})^{q-1}}{(q-1)!2^{q-1}}\Gamma^{a_1\ldots a_{2q-1}}\mathcal{F}_{a_1a_2}\ldots\mathcal{F}_{a_{2q-1}c}g^{bc}\hat{D}_b,\\
\Gamma_{\mathrm{D8}}^{(0)} &= \frac{\epsilon^{a_1\ldots a_9}}{9!\sqrt{-\det[g_{ab}]}}\Gamma_{a_1\ldots a_9}=-\Gamma^{11}\Gamma^{\underline{5}},\\
\Delta &= \frac{1}{2}\Gamma^M\partial_M\phi-\frac{1}{8}\frac{1}{4!}g_se^{\phi}F_{MNPQ}\Gamma^{MNPQ},\\
\hat{D}_M &= \nabla_M-\frac{1}{8}\frac{1}{4!}g_se^{\phi}F_{MNPQ}\Gamma^{MNPQ}\Gamma_M,\\
\nabla_M &= \partial_M+\frac{1}{4}\omega_M^{\underline{NP}}\Gamma_{\underline{NP}}.
\end{aligned} \tag{A18}$$

Action (A17) is the fermionic action for D8-brane obtained under T-duality. The notation in (A17) and (A18) is given as follows. The index labeled by capital letters M,N,P,Q runs over 10d spacetime, and that labeled by lowercase letters runs over D8-brane. The index with underline corresponds to index in the flat tangent space used by elfbein, e.g., $g_{MN}=e_M^{\underline{M}}\eta_{\underline{MN}}e_N^{\underline{N}}$; so, we have, e.g., $\Gamma^a=g^{ab}\partial_bX^Me_M^{\underline{N}}\Gamma_{\underline{N}}$. Γ^M refers to the Dirac matrix, satisfying $\left\{\Gamma^M,\Gamma^N\right\}=2g^{MN}$, and $\omega_M^{\underline{NP}}$ refers to the spin connection. F_{MNPQ} refers to the components of the Ramond–Ramond F_4 and ϕ is the dilaton field, which are all given in Section 2. The gamma matrix Γ^{MNPQ} is given by $\Gamma^{MNPQ}=\Gamma^{[M}\Gamma^N\Gamma^P\Gamma^{Q]}$. Here, $\mathcal{F}_{ab}=F_{ab}+B_{ab}$, where F_{ab} is the gauge field strength on the flavor brane and B_{ab} is the antisymmetric tensor B_{MN} induced on the flavor brane, which can be set to zero.

Imposing the bubble solution given in (16) and supergravity solutions for the dilaton ϕ and Ramond–Ramond F_4 to (A17), after some calculations, it becomes

$$S_{\mathrm{D8}}^{(f)}=\frac{iT}{(2\pi\alpha')^2\Omega_4}\int d^4xdZd\Omega_4\tilde{\Psi}P_-\left[\frac{2}{3}M_{KK}K^{-\frac{1}{2}}\Gamma^{\underline{m}}\nabla_m^{S^4}+K^{-2/3}\Gamma^{\underline{\mu}}\partial_\mu+M_{KK}\Gamma_{\underline{4}}\partial_Z\right]\Psi, \tag{A19}$$

where $\Gamma^{\underline{m}}\nabla_m^{S^4}$ is the Dirac operator on S^4, i.e., the index m runs over S^4, and

$$\tilde{\Psi}=K^{-13/24}\Psi, K(Z)=1+Z^2, T=\left(\frac{3}{2}\right)^4T_{\mathrm{D8}}\Omega_4(2\pi\alpha')^2\frac{\left(\frac{2}{3}M_{KK}R\right)^{21/2}}{M_{KK}^5}, P_-=\frac{1}{2}(1-\Gamma_{\mathrm{D8}}). \tag{A20}$$

Since we are interested in the fermionic part, the gauge field included by $\mathcal{F}_{ab}$ is turned off, i.e., $\mathcal{F}_{ab}=0$. Afterwards, in order to obtain a 5d effective action, such as the mesonic action given in (33), we can decompose the spinor Ψ into a 3+1-dimensional part $\psi(x,Z)$ as mesino, an S^4 part χ and a remaining 2d part λ, as follows:

$$\Psi=\psi\otimes\chi\left(S^4\right)\otimes\lambda. \tag{A21}$$

The associated gamma matrices can be chosen as

$$\begin{aligned}\Gamma^{\underline{\mu}} &= \sigma_1 \otimes \gamma^{\underline{\mu}} \otimes \mathbf{1}, \mu = 0,1,2,3\\ \Gamma^{\underline{4}} &= \sigma_1 \otimes \gamma \otimes \mathbf{1},\\ \Gamma^{\underline{5}} &= \sigma_2 \otimes \mathbf{1} \otimes \tilde{\gamma},\\ \Gamma^{\underline{m}} &= \sigma_2 \otimes \mathbf{1} \otimes \tilde{\gamma}^{\underline{m}}, m = 6,7,8,9,\\ \gamma &= i\gamma^{\underline{0}}\gamma^{\underline{1}}\gamma^{\underline{2}}\gamma^{\underline{3}},\\ \tilde{\gamma} &= i\gamma^{\underline{6}}\gamma^{\underline{7}}\gamma^{\underline{8}}\gamma^{\underline{9}},\end{aligned} \tag{A22}$$

where $\sigma_{1,2,3}$ refer to the Pauli matrices. In this decomposition, the 10d chirality matrix takes a very simple form as $\Gamma^{11} = \sigma_3 \otimes \mathbf{1} \otimes \mathbf{1}$. If we chose the σ_3 representation, λ can be decomposed by the eigenstates of σ_3 with

$$\sigma_3\lambda_\pm = \lambda_\pm, \sigma_1\lambda_\pm = \lambda_\mp, \sigma_2\lambda_\pm = \pm i\lambda_\mp, \tag{A23}$$

where $\lambda_\pm$ refers to the two eigenstates of σ_3. Since the kappa symmetry fixes the condition $\Gamma^{11}\Psi = \Psi$, we have to chose $\lambda = \lambda_+$. Moreover, as χ must satisfy the Dirac equation on S^4, it can be decomposed by the spherical harmonic function. So, the eigenstates of $\Gamma^{\underline{m}}\nabla_m^{S^4}$ can be chosen as [139],

$$\Gamma^{\underline{m}}\nabla_m^{S^4}\chi^{\pm l,s} = i\Lambda_l^\pm\chi^{\pm l,s}; \Lambda_l^\pm = \pm(2+l), l = 0,1... \tag{A24}$$

where s, l are angular quantum numbers carried by spherical harmonic function.

Putting (A21) into (A19) with the decomposition (A22)–(A24) for χ and λ, we finally reach a 5d effective action for then mesino field:

$$S = iT\int d^4x dZ\bar{\psi}\left(-\frac{2}{3}M_{KK}\lambda K^{-1/2} + K^{-2/3}\gamma^{\underline{\mu}}\partial_\mu + M_{KK}\gamma\partial_Z\right)\psi. \tag{A25}$$

The 5d mesino ψ can be further decomposed by working with

$$\psi(x,Z) = \begin{pmatrix}\psi_+\\ \psi_-\end{pmatrix} = \sum_n\begin{bmatrix}\psi_+^{(n)}(x)f_+^{(n)}(Z)\\ \psi_-^{(n)}(x)f_-^{(n)}(Z)\end{bmatrix}, \tag{A26}$$

where $f_\pm^{(n)}(Z)$ are real eigenfunctions of the coupled equations

$$\begin{aligned}-\tfrac{2\lambda}{3}K^{-1/2}f_+^{(n)} + \partial_Z f_+^{(n)} &= \Lambda_n M_{KK}K^{-2/3}f_-^{(n)},\\ -\tfrac{2\lambda}{3}K^{-1/2}f_-^{(n)} - \partial_Z f_-^{(n)} &= \Lambda_n M_{KK}K^{-2/3}f_+^{(n)},\end{aligned} \tag{A27}$$

with the normalizations

$$T\int dZK^{-2/3}f_i^{(n)}f_j^{(m)} = \delta^{mn}\delta_{ij},\ i,j = +,-, \tag{A28}$$

Plugging (A26)–(A28) into (A25), the action takes the canonical form of ($M_n = \Lambda_n M_{KK}$)

$$S = -\int d^4x\sum_n\left\{\psi_-^{(n)\dagger}i\sigma^\mu\partial_\mu\psi_-^{(n)} + \psi_+^{(n)\dagger}i\bar{\sigma}^\mu\partial_\mu\psi_+^{(n)} + M_n\left[\psi_-^{(n)\dagger}\psi_+^{(n)} + \psi_+^{(n)\dagger}\psi_-^{(n)}\right]\right\}. \tag{A29}$$

Defining the Dirac spinor written in the Wely basis as

$$\psi^{(n)} = \begin{pmatrix}\psi_+^{(n)}(x)\\ \psi_-^{(n)}(x)\end{pmatrix}, \tag{A30}$$

action (A29) can be rewritten as ($\{\gamma^\mu, \gamma^\nu\} = 2\eta^{\mu\nu}$)

$$S = i\int d^4x\sum_n\left[\bar{\psi}^{(n)}\gamma^\mu\partial_\mu\psi^{(n)} + M_n\bar{\psi}^{(n)}\psi^{(n)}\right], \tag{A31}$$

leading to a standard action for fermion. As we can see, the fermionic action illustrates that the mesino mass takes the same order of meson mass; hence, it should be not neglected in principle, and the authors of [140] also confirm this conclusion, which is consistent with the remaining supersymmetry on D8-branes.

Moreover, when the bosonic gauge field is turned on, action (A17) reduces to interaction terms of meson and mesino up to $\mathcal{O}(\mathcal{F},\Psi^2)$, as follows:

$$\begin{aligned} S_{int} = \; & i\frac{T_{D8}}{4}\int d^9x\sqrt{-g}e^{-\phi}\bar{\Psi}\Gamma_{\underline{5}}\Gamma^{11}\Gamma^{ab}\mathcal{F}_{ab}\left(\Gamma^c\hat{D}_c-\Delta\right)\Psi \\ & -i\frac{T_{D8}}{2}\int d^9x\sqrt{-g}e^{-\phi}\bar{\Psi}\left(1-\Gamma_{\underline{5}}\right)\Gamma^{\underline{5}}\Gamma^{11}\Gamma^a\mathcal{F}_a{}^b\hat{D}_b\Psi. \end{aligned} \tag{A32}$$

Using decomposition (46) for A_a and (A22)–(A24) for Ψ, action (A32) includes interaction of π meson and mesino as follows:

$$\begin{aligned} S_{int} = \; & \frac{M_{KK}}{f_\pi M_{int}^2}\sum_{n,p}\int d^4x\partial_\mu\pi\left[M_{KK}t_{\pi,n,p}\bar{\psi}^{(n)}i\gamma^\mu\gamma^{n+p+1}\psi^{(p)}\right] \\ & +l_{\pi,n,p}\bar{\psi}^{(n)}(-\gamma)^{n+p+1}\partial^\mu\psi^{(p)}, \end{aligned} \tag{A33}$$

where the coupling constant is evaluated numerically as

$$\begin{aligned} t_{\pi,n,p} &= \frac{1}{2}\int dZK^{-5/6}\left[f_+^{(n)}f_+^{(p)\prime}-f_+^{(p)}f_+^{(n)\prime}+iK^{-1/2}f_+^{(n)}f_+^{(p)}\right], \\ l_{\pi,n,p} &= \int dZK^{-3/2}f_+^{(n)}f_-^{(p)}. \end{aligned} \tag{A34}$$

One can further work out the interaction terms of ρ meson and mesino similarly. Since there is no mechanism to suppress the interaction of meson and mesino or break down the supersymmetry on the D8-brane, we have to take into account these interactions in this model in principle while they are absent in realistic QCD.

Although we do not attempt to figure out this issue completely in this review, we give some comments that may be suggestive. The way to break down the supersymmetry on D8-branes may follow the discussion in [23], that is, to compactify one of the directions of the D8-brane (which is vertical to the N_c D4-branes) on another circle, then impose the periodic and antiperiodic boundary condition to the meson and mesino, respectively. Afterwards, the supersymmetry on the D8-branes breaks down, then the spectrum of meson and mesino is separated by a energy scale $1/\beta_s$, where β_s refers to the size of the compactified direction of the D8-brane. Another alternative scheme is to consider that the bubble solution (16) has a period β_T with $\beta_T \gg 1$; hence, the dual theory is nonsupersymmetric above the size β_T if we perform the same dimension reduction as [23]. Therefore, it means that the supersymmetry gets to rise only at a temperature of exactly zero due to $\beta_T = 1/T$, which is the ideal case, out of reach physically. So, the dual theory on the D8-brane would be nonsupersymmetrical at any finite temperature.

References

1. Witten, E. Anti-de Sitter space and holography. *Adv. Theor. Math. Phys.* **1998**, *2*, 253–291. [CrossRef]
2. Maldacena, J.M. The Large N limit of superconformal field theories and supergravity. *Adv. Theor. Math. Phys.* **1998**, *2*, 231–252. [CrossRef]
3. Aharony, O.; Gubser, S.S.; Maldacena, J.M.; Ooguri, H. Large N field theories, string theory and gravity. *Phys. Rept.* **2000**, *323*, 183. [CrossRef]
4. Maldacena, J. Wilson loops in large N field theories. *Phys. Rev. Lett.* **1998**, *80*, 4859–4862. [CrossRef]
5. Rey, S.; Theisen, S.; Yee, J. Wilson-Polyakov loop at finite temperature in large N gauge theory and anti-de Sitter supergravity. *Nucl. Phys. B* **1998**, *527*, 171–186. [CrossRef]
6. Brandhuber, A.; Itzhaki, N.; Sonnenschein, J.; Yankielowicz, S. Wilson loops in the large N limit at finite temperature. *Phys. Lett. B* **1998**, *434*, 36–40. [CrossRef]
7. Policastro, G.; Son, D.T.; Starinets, A.O. From AdS/CFT correspondence to hydrodynamics. *J. High Energy Phys.* **2002**, *9*, 43. [CrossRef]
8. Son, D.T.; Starinets, A.O. Minkowski space correlators in AdS/CFT correspondence: Recipe and applications. *J. High Energy Phys.* **2002**, *9*, 42. [CrossRef]
9. Kovtun, P.; Son, D.T.; Starinets, A.O. Viscosity in strongly interacting quantum field theories from black hole physics. *Phys. Rev. Lett.* **2005**, *94*, 111601. [CrossRef]
10. Iqbal, N.; Liu, H. Real-time response in AdS/CFT with application to spinors. *Fortsch. Phys.* **2009**, *57*, 367–384. [CrossRef]

11. Liu, H.; McGreevy, J.; Vegh, D. Non-Fermi liquids from holography. *Phys. Rev. D* **2011**, *83*, 065029. [CrossRef]
12. Semenoff, G.W.; Zarembo, K. Holographic Schwinger Effect. *Phys. Rev. Lett.* **2011**, *107*, 171601. [CrossRef] [PubMed]
13. Ryu, S.; Takayanagi, T. Holographic derivation of entanglement entropy from AdS/CFT. *Phys. Rev. Lett.* **2006**, *96*, 181602. [CrossRef] [PubMed]
14. Klebanov, I.R.; Kutasov, D.; Murugan, A. Entanglement as a probe of confinement. *Nucl. Phys. B* **2008**, *796*, 274–293. [CrossRef]
15. Harlow, D. Jerusalem Lectures on Black Holes and Quantum Information. *Rev. Mod. Phys.* **2016**, *88*, 015002. [CrossRef]
16. Gross, D.J.; Wilczek, F. Ultraviolet Behavior of Nonabelian Gauge Theories. *Phys. Rev. Lett.* **1973**, *30*, 1343–1346. [CrossRef]
17. Politzer, H.D. Reliable Perturbative Results for Strong Interactions? *Phys. Rev. Lett.* **1973**, *30*, 1346–1349. [CrossRef]
18. Erlich, J.; Katz, E.; Son, D.T.; Stephanov, M.A. QCD and a holographic model of hadrons. *Phys. Rev. Lett.* **2005**, *95*, 261602. [CrossRef]
19. Karch, A.; Katz, E.; Son, D.T.; Stephanov, M.A. Linear Confinement and AdS/QCD. *arXiv* **2006**, arXiv:hep-ph/0602229.
20. Rold, L.; Pomarol, A. Chiral symmetry breaking from five dimensional spaces. *Nucl. Phys. B* **2005**, *721*, 79–97. [CrossRef]
21. Casalderrey-Solana, J.; Liu, H.; Mateos, D.; Rajagopal, K.; Wiedemann, U.A. *Gauge/Gravity Duality, Hot QCD and Heavy Ion Collisions*; Cambridge University Press: Cambridge, UK, 2011.
22. Kruczenski, M.; Mateos, D.; Myers, R.C.; Winters, D.J. Towards a holographic dual of large N(c) QCD. *J. High Energy Phys.* **2004**, *5*, 41. [CrossRef]
23. Witten, E. Anti-de Sitter space, thermal phase transition, and confinement in gauge theories. *Adv. Theor. Math. Phys.* **1998**, *2*, 505–532. [CrossRef]
24. Sakai, T.; Sugimoto, S. Low energy hadron physics in holographic QCD. *Prog. Theor. Phys.* **2005**, *113*, 843–882. [CrossRef]
25. Sakai, T.; Sugimoto, S. More on a holographic dual of QCD. *Prog. Theor. Phys.* **2005**, *114*, 1083–1118. [CrossRef]
26. Witten, E. Baryons and branes in anti-de Sitter space. *J. High Energy Phys.* **1998**, *7*, 6. [CrossRef]
27. Hata, H.; Sakai, T.; Sugimoto, S.; Yamato, S. Baryons from instantons in holographic QCD. *Prog. Theor. Phys.* **2007**, *117*, 1157. [CrossRef]
28. Hata, H.; Murata, M. Baryons and the Chern-Simons term in holographic QCD with three flavors. *Prog. Theor. Phys.* **2008**, *119*, 461–490. [CrossRef]
29. Constable, N.R.; Myers, R.C. Spin-two glueballs, positive energy theorems and the AdS/CFT correspondence. *J. High Energy Phys.* **1999**, *9910*, 37. [CrossRef]
30. Brower, R.C.; Mathur, S.D.; Tan, C.-I. Glueball spectrum for QCD from AdS supergravity duality. *Nucl. Phys. B* **2000**, *587*, 249–276. [CrossRef]
31. Hashimoto, K.; Tan, C.-I.; Terashima, S. Glueball Decay in Holographic QCD. *Phys. Rev.* **2008**, *D77*, 086001. [CrossRef]
32. Brünner, F.; Parganlija, D. Rebhan Glueball Decay Rates in the Witten-Sakai-Sugimoto Model. *Phys. Rev.* **2015**, *D91*, 106002; Erratum in *Phys. Rev.* **2016**, *D93*, 109903.
33. Aharony, O.; Sonnenschein, J.; Yankielowicz, S. A Holographic model of deconfinement and chiral symmetry restoration. *Ann. Phys.* **2007**, *322*, 1420–1443. [CrossRef]
34. Bigazzi, F.; Cotrone, A.L. Holographic QCD with Dynamical Flavors. *J. High Energy Phys.* **2015**, *1501*, 104. [CrossRef]
35. Li, S.; Jia, T. Dynamically flavored description of holographic QCD in the presence of a magnetic field. *Phys. Rev. D* **2017**, *96*, 066032. [CrossRef]
36. Bergman, O.; Lifschytz, G.; Lippert, M. Holographic Nuclear Physics. *J. High Energy Phys.* **2007**, *11*, 56. [CrossRef]
37. Li, S.; Schmitt, A.; Wang, Q. From holography towards real-world nuclear matter. *Phys. Rev. D* **2015**, *92*, 026006. [CrossRef]
38. Liu, Y.; Zahed, I. Heavy-light mesons in chiral AdS/QCD. *Phys. Lett. B* **2017**, *769*, 314–321. [CrossRef]
39. Liu, Y.; Zahed, I. Holographic Heavy-Light Chiral Effective Action. *Phys. Rev. D* **2017**, *95*, 056022. [CrossRef]
40. Kovensky, N.; Schmitt, A. Heavy Holographic QCD. *J. High Energy Phys.* **2020**, *2*, 96. [CrossRef]
41. Wu, C.; Xiao, Z.; Zhou, D. Sakai-Sugimoto model in D0–D4 background. *Phys. Rev. D* **2013**, *88*, 026016. [CrossRef]
42. Seki, S.; Sin, S. A New Model of Holographic QCD and Chiral Condensate in Dense Matter. *J. High Energy Phys.* **2013**, *10*, 223. [CrossRef]
43. Bartolini, L.; Bigazzi, F.; Bolognesi, S.; Cotrone, A.L.; Manenti, A. Theta dependence in Holographic QCD. *J. High Energy Phys.* **2017**, *2*, 29. [CrossRef]
44. Bigazzi, F.; Cotrone, A.L.; Sisca, R. Notes on Theta Dependence in Holographic Yang-Mills. *J. High Energy Phys.* **2015**, *8*, 90. [CrossRef]
45. Bigazzi, F.; Caddeo, A.; Cotrone, A.L.; Vecchia, P.D.; Marzolla, A. The Holographic QCD Axion. *J. High Energy Phys.* **2019**, *12*, 56. [CrossRef]
46. Hashimoto, K.; Sakai, T.; Sugimoto, S. Nuclear Force from String Theory. *Prog. Theor. Phys.* **2009**, *122*, 427–476. [CrossRef]
47. Hashimoto, K.; Iizuka, N.; Yi, P. A Matrix Model for Baryons and Nuclear Forces. *J. High Energy Phys.* **2010**, *10*, 3. [CrossRef]
48. Hashimoto, K.; Iizuka, N. Three-Body Nuclear Forces from a Matrix Model. *J. High Energy Phys.* **2010**, *11*, 58. [CrossRef]
49. Hashimoto, K.; Matsuo, Y. Nuclear binding energy in holographic QCD. *Phys. Rev. D* **2021**, *104*, 026006. [CrossRef]
50. Li, S.; Jia, T. Matrix model and Holographic Baryons in the D0–D4 background. *Phys. Rev. D* **2015**, *92*, 046007. [CrossRef]
51. Li, S.; Jia, T. Three-body force for baryons from the D0–D4/D8 brane matrix model. *Phys. Rev. D* **2016**, *93*, 065051. [CrossRef]
52. Kaplunovsky, V.; Sonnenschein, J. Searching for an Attractive Force in Holographic Nuclear Physics. *J. High Energy Phys.* **2011**, *5*, 58. [CrossRef]

53. Becker, K.; Becker, M.; Schwarz, J.H. *String Theory and M-Theory, A Modern Introduction*; Cambridge University Press: Cambridge, UK, 2007.
54. Witten, E. String Theory Dynamics in Various Dimensions. *Nucl. Phys. B* **1995**, *443*, 197. [CrossRef]
55. Sugimoto, S.; Takahashi, K. QED and string theory. *J. High Energy Phys.* **2004**, *4*, 51. [CrossRef]
56. Antonyan, E.; Harvey, J.A.; Jensen, S.; Kutasov, D. NJL and QCD from String Theory. *arXiv* **2006**, arXiv:hep-th/0604017.
57. Freedman, D.Z.; Proeyen, A.V. *Supergravity*; Cambridge University Press: Cambridge, UK, 2012.
58. Mandal, G.; Morita, T. Gregory-Laflamme as the confinement/deconfinement transition in holographic QCD. *J. High Energy Phys.* **2011**, *9*, 73. [CrossRef]
59. Mandal, G.; Morita, T. What is the gravity dual of the confinement/deconfinement transition in holographic QCD? *J. Phys. Conf. Ser.* **2012**, *343*, 012079.
60. Johnson, C.V. *D-Branes*; Cambridge University Press: Cambridge, UK, 2006.
61. Zahed, I.; Brown, G.E. The Skyrme Model. *Phys. Rept.* **1986**, *142*, 1–102. [CrossRef]
62. Witten, E. Global Aspects of Current Algebra. *Nucl. Phys. B* **1983**, *223*, 422. [CrossRef]
63. Kaymakcalan, O.; Rajeev, S.; Schechter, J. Nonabelian Anomaly and Vector Meson Decays. *Phys. Rev. D* **1984**, *30*, 594. [CrossRef]
64. Rey, S.-J.; Yee, J.-T. Macroscopic strings as heavy quarks in large N gauge theory and anti-de Sitter supergravity. *Eur. Phys. J. C* **2001**, *22*, 379–394. [CrossRef]
65. Gross, D.J.; Ooguri, H. Aspects of large N gauge theory dynamics as seen by string theory. *Phys. Rev. D* **1998**, *58*, 106002. [CrossRef]
66. Tong, D. TASI lectures on solitons: Instantons, monopoles, vortices and kinks. *arXiv* **2005**, arXiv: hep-th/0509216.
67. Witten, E. Current Algebra, Baryons, and Quark Confinement. *Nucl. Phys. B* **1983**, *223*, 433–444. [CrossRef]
68. Seo, Y.; Sin, S.-J. Baryon Mass in medium with Holographic QCD. *J. High Energy Phys.* **2008**, *4*, 10. [CrossRef]
69. Adkins, G.; Nappi, C.; Witten, E. Static Properties of Nucleons in the Skyrme Model. *Nucl. Phys. B* **1983**, *228*, 552. [CrossRef]
70. Lau, P.; Sugimoto, S. Chern-Simons 5-form and Holographic Baryons. *Phys. Rev. D* **2017**, *95*, 126007. [CrossRef]
71. Mateos, D.; Myers, R.C.; Thomson, R.M. Thermodynamics of the brane. *J. High Energy Phys.* **2007**, *705*, 67. [CrossRef]
72. Bayona, A.B. Holographic deconfinement transition in the presence of a magnetic field. *J. High Energy Phys.* **2013**, *1311*, 168. [CrossRef]
73. Bigazzi, F.; Cotrone, A.L.; Mas, J.; Mayerson, D.; Tarrio, J. D3–D7 Quark-Gluon Plasmas at Finite Baryon Density. *J. High Energy Phys.* **2011**, *1104*, 60. [CrossRef]
74. Cotrone, A.L.; Tarrio, J. Consistent reduction of charged D3–D7 systems. *J. High Energy Phys.* **2012**, *164*, 1210. [CrossRef]
75. Bigazzi, F.; Cotrone, A.L.; Tarrio, J. Charged D3–D7 plasmas: Novel solutions, extremality and stability issues. *J. High Energy Phys.* **2013**, *1307*, 74. [CrossRef]
76. Benincasa, P. A note on Holographic Renormalization of Probe D-Branes. *arXiv* **2009**, arXiv:0903.4356.
77. Papadimitriou, I. Holographic renormalization as a canonical transformation. *J. High Energy Phys.* **2010**, *1011*, 14. [CrossRef]
78. Papadimitriou, I. Holographic Renormalization of general dilaton-axion gravity. *J. High Energy Phys.* **2011**, *1108*, 119. [CrossRef]
79. Giataganas, D.; Irges, N. Flavor Corrections in the Static Potential in Holographic QCD. *Phys. Rev. D* **2012**, *85*, 046001. [CrossRef]
80. Deuzeman, A.; Lombardo, M.P.; Miura, K.; da Silva, T.N.; Pallante, E. Phases of many flavors QCD: Lattice results. *arXiv* **2012**, arXiv:1304.3245.
81. Braun, J.; Gies, H. Scaling laws near the conformal window of many-flavor QCD. *J. High Energy Phys.* **2010**, *1005*, 60. [CrossRef]
82. Liao, J.; Shuryak, E. Effect of Light Fermions on the Confinement Transition in QCD-like Theories. *Phys. Rev. Lett.* **2012**, *109*, 152001. [CrossRef]
83. Bali, G.S.; Bruckmann, F.; Endrodi, G.; Fodor, Z.; Katz, S.D.; Krieg, S.; Schafer, A.; Szabo, K.K. The QCD phase diagram for external magnetic fields. *J. High Energy Phys.* **2012**, *2*, 44. [CrossRef]
84. Bali, G.S.; Bruckmann, F.; Endrődi, G.; Katz, S.D.; Schäfer, A. The QCD equation of state in background magnetic fields. *J. High Energy Phys.* **2014**, *8*, 177. [CrossRef]
85. Fukushima, K.; Hidaka, Y. Magnetic Catalysis Versus Magnetic Inhibition. *Phys. Rev. Lett.* **2013**, *110*, 031601. [CrossRef] [PubMed]
86. Fraga, E.S.; Palhares, L.F. Deconfinement in the presence of a strong magnetic background: An exercise within the MIT bag model. *Phys. Rev. D* **2012**, *86*, 016008. [CrossRef]
87. Sachan, S.; Siwach, S. Thermodynamics of soft wall AdS/QCD at finite chemical potential. *Mod. Phys. Lett. A* **2012**, *27*, 1250163. [CrossRef]
88. Sachan, S. Study of confinement/deconfinement transition in AdS/QCD with generalized warp factors. *Adv. High Energy Phys.* **2014**, *2014*, 543526. [CrossRef]
89. Sevrin, A.; Troost, J.; Troost, W. The non-Abelian Born-Infeld action at order F^6. *Nucl. Phys. B* **2001**, *603*, 389–412. [CrossRef]
90. Rozali, M.; Shieh, H.-H.; Raamsdonk, M.V.; Wu, J. Cold Nuclear Matter in Holographic QCD. *J. High Energy Phys.* **2008**, *1*, 53. [CrossRef]
91. Ghoroku, K.; Kubo, K.; Tachibana, M.; Taminato, T.; Toyoda, F. Holographic cold nuclear matter as dilute instanton gas. *Phys. Rev. D* **2013**, *87*, 066006. [CrossRef]
92. Schaefer, B.-J.; Pawlowski, J.M.; Wambach, J. The Phase Structure of the Polyakov–Quark–Meson Model. *Phys. Rev. D* **2007**, *76*, 074023. [CrossRef]

93. Schaefer, B.-J.; Wagner, M.; Wambach, J. Thermodynamics of (2 + 1)-flavor QCD: Confronting Models with Lattice Studies. *Phys. Rev. D* **2010**, *81*, 074013. [CrossRef]
94. Nambu, Y.; Lasinio, G.J. Dynamical Model of Elementary Particles Based on an Analogy with Superconductivity. I. *Phys. Rev.* **1961**, *122*, 345–358. [CrossRef]
95. Nambu, Y.; Lasinio, G.J. Dynamical model of elementary particles based on an analogy with superconductivity. II. *Phys. Rev.* **1961**, *124*, 246–254. [CrossRef]
96. Fukushima, K. Chiral effective model with the Polyakov loop. *Phys. Lett. B* **2004**, *591*, 277–284. [CrossRef]
97. Buballa, M. NJL model analysis of quark matter at large density. *Phys. Rept.* **2005**, *407*, 205–376. [CrossRef]
98. Ruester, S.B.; Werth, V.; Buballa, M.; Shovkovy, I.A.; Rischke, D.H. The Phase diagram of neutral quark matter: Self-consistent treatment of quark masses. *Phys. Rev. D* **2005**, *72*, 034004. [CrossRef]
99. Walecka, J.D. A Theory of highly condensed matter. *Ann. Phys.* **1974**, *83*, 491–529. [CrossRef]
100. Boguta, J.; Bodmer, A.R. Relativistic Calculation of Nuclear Matter and the Nuclear Surface. *Nucl. Phys. A* **1977**, *292*, 413–428. [CrossRef]
101. Gallas, S.; Giacosa, F.; Pagliara, G. Nuclear matter within a dilatation-invariant parity doublet model: The role of the tetraquark at nonzero density. *Nucl. Phys. A* **2011**, *872*, 13–24. [CrossRef]
102. Floerchinger, S.; Wetterich, C. Chemical freeze-out in heavy ion collisions at large baryon densities. *Nucl. Phys. A* **2012**, *891*, 11–24. [CrossRef]
103. Myers, R.C. Dielectric-Branes. *J. High Energy Phys.* **1999**, *22*, 9912. [CrossRef]
104. Liu, Y.; Nowak, M.A. Hyperons and θ s + in holographic QCD. *Phys. Rev. D* **2022**, *105*, 114021. [CrossRef]
105. Liu, Y.; Zahed, I. Heavy Baryons and their Exotics from Instantons in Holographic QCD. *Phys. Rev. D* **2017**, *95*, 116012. [CrossRef]
106. Liu, Y.; Zahed, I. Heavy and Strange Holographic Baryons. *Phys. Rev. D* **2017**, *96*, 056027. [CrossRef]
107. Li, S. The interaction of glueball and heavy-light flavoured meson in holographic QCD. *Eur. Phys. J. C* **2020**, *80*, 881. [CrossRef]
108. BESIII Collaboration. Measurement of yCP in $D^0 - \bar{D}^0$ oscillation using quantum correlations in $e^-e^+ \to D^0\bar{D}^0$ at √s = 3.773 GeV. *Phys. Lett. B* **2015**, *774*, 339–346.
109. CDF Collaboration. Observation of Bs-Bsbar Oscillations. *Phys. Rev. Lett.* **2006**, *97*, 242003. [CrossRef] [PubMed]
110. Li, S.-W. Glueball–baryon interactions in holographic QCD. *Phys. Lett. B* **2017**, *773*, 142–149. [CrossRef]
111. Li, S.-W. Holographic description of heavy-flavored baryonic matter decay involving glueball. *Phys. Rev. D* **2019**, *99*, 046013. [CrossRef]
112. Vicari, E.; Panagopoulos, H. Theta dependence of SU(N) gauge theories in the presence of a topological term. *Phys. Rept.* **2009**, *470*, 93–150. [CrossRef]
113. Debbio, L.D.; Manca, G.M.; Panagopoulos, H.; Skouroupathis, A.; Vicari, E. Theta-dependence of the spectrum of SU(N) gauge theories. *J. High Energy Phys.* **2006**, *6*, 5. [CrossRef]
114. D'Elia, M.; Negro, F. Phase diagram of Yang-Mills theories in the presence of a θ term. *Phys. Rev. D* **2013**, *88*, 034503. [CrossRef]
115. D'Elia, M.; Negro, F. θ dependence of the deconfinement temperature in Yang-Mills theories. *Phys. Rev. Lett.* **2012**, *109*, 072001. [CrossRef] [PubMed]
116. Fukushima, K.; Kharzeev, D.E.; Warringa, H.J. The Chiral Magnetic Effect. *Phys. Rev. D* **2008**, *78*, 074033. [CrossRef]
117. Kharzeev, D.E. The Chiral Magnetic Effect and Anomaly-Induced Transport. *Prog. Part. Nucl. Phys.* **2014**, *75*, 133–151. [CrossRef]
118. Witten, E. Theta dependence in the large N limit of four-dimensional gauge theories. *Phys. Rev. Lett.* **1998**, *81*, 2862–2865. [CrossRef]
119. Cai, W.; Wu, C.; Xiao, Z. Baryons in the Sakai-Sugimoto model in the D0–D4 background. *Phys. Rev. D* **2014**, *90*, 106001. [CrossRef]
120. Cai, W.; Li, K.; Li, S. Electromagnetic instability and Schwinger effect in the Witten–Sakai–Sugimoto model with D0–D4 background. *Eur. Phys. J. C* **2019**, *79*, 904. [CrossRef]
121. Hashimoto, K.; Oka, T.; Sonoda, A. Electromagnetic instability in holographic QCD. *J. High Energy Phys.* **2015**, *6*, 1. [CrossRef]
122. Li, S.; Luo, S.; Li, H. Holographic Schwinger effect and electric instability with anisotropy. *J. High Energy Phys.* **2022**, *8*, 206. [CrossRef]
123. Li, S. Holographic Schwinger effect in the confining background with D-instanton. *Eur. Phys. J. C* **2021**, *81*, 797. [CrossRef]
124. Wu, C.; Chen, Y.; Huang, M. Fluid/gravity correspondence: A nonconformal realization in compactified D4 branes. *Phys. Rev. D* **2016**, *93*, 066005. [CrossRef]
125. Wu, C.; Chen, Y.; Huang, M. Fluid/gravity correspondence: Second order transport coefficients in compactified D4-branes. *J. High Energy Phys.* **2017**, *1*, 118. [CrossRef]
126. Wu, C.; Chen, Y.; Huang, M. Chiral vortical effect from the compactified D4-branes with smeared D0-brane charge. *J. High Energy Phys.* **2017**, *3*, 82. [CrossRef]
127. Cai, W.; Li, S. Sound waves in the compactified D0–D4 brane system. *Phys. Rev. D* **2016**, *94*, 066012. [CrossRef]
128. Benincasa, P.; Buchel, A. Hydrodynamics of Sakai-Sugimoto model in the quenched approximation. *Phys. Lett. B* **2006**, *640*, 108–115. [CrossRef]
129. Imaanpur, A. Correction to baryon spectrum in holographic QCD. *Phys. Lett. B* **2022**, *832*, 137233. [CrossRef]
130. Li, S.; Li, H.; Luo, S. Corrections to the instanton configuration as baryon in holographic QCD. *Phys. Rev. D* **2022**, *106*, 126027. [CrossRef]

131. Li, S.; Luo, S.; Hu, Y. Holographic QCD_3 and Chern-Simons theory from anisotropic supergravity. *J. High Energy Phys.* **2022**, *6*, 40. [CrossRef]
132. Li, S.; Luo, S.; Tan, M. Three-dimensional Yang-Mills-Chern-Simons theory from a D3-brane background with D-instantons. *Phys. Rev. D* **2021**, *104*, 066008. [CrossRef]
133. Schmitt, A.; Shternin, P. Reaction rates and transport in neutron stars. *Astrophys. Space Sci. Libr.* **2018**, *457*, 455–574.
134. Kovensky, N.; Poole, A.; Schmitt, A. Building a realistic neutron star from holography. *Phys. Rev. D* **2022**, *105*, 034022. [CrossRef]
135. Heise, R.; Svendsen, H. A Note on fermions in holographic QCD. *J. High Energy Phys.* **2007**, *8*, 65. [CrossRef]
136. Marolf, D.; Martucci, L.; Silva, P.J. Fermions, T-duality and effective actions for D-branes in bosonic backgrounds. *J. High Energy Phys.* **2003**, *4*, 51. [CrossRef]
137. Marolf, D.; Martucci, L.; Silva, P.J. Actions and fermionic symmetries for D-branes in bosonic backgrounds. *J. High Energy Phys.* **2003**, *7*, 19. [CrossRef]
138. Martucci, L.; Rosseel, J.; Van den Bleeken, D.; Van Proeyen, A. Dirac actions for D-branes on backgrounds with fluxes. *Class. Quant. Grav.* **2005**, *22*, 2745–2764. [CrossRef]
139. Camporesi, R.; Higuchi, A. On the eigenfunctions of the Dirac operator on spheres and real hyperbolic spaces. *J. Geom. Phys.* **1996**, *20*, 1–18. [CrossRef]
140. Nakas, T.; Rigatos, K.S. Fermions and baryons as open-string states from brane junctions. *J. High Energy Phys.* **2020**, *12*, 157. [CrossRef]